RESILIENT ECOSYSTEMS, RESILIENT COMMUNITIES – SITUATIONAL ANALYSIS OF THE MOATA'A COMMUNITY AND MANGROVE ENVIRONMENT

FINAL MOATA'A MANGROVE ECOSYSTEM ANALYSIS REPORT

Irish Aid
Rialtas na hÉireann
Government of Ireland

Centre for Water Security and Environmental Sustainability and School of Engineering.

THE UNIVERSITY OF NEWCASTLE AUSTRALIA

SPREP PROE

Secretariat of the Pacific Regional Environment Programme (SPREP)

Eliana Jorquera, Juan Quijano-Baron, Jose Rodriguez and Patricia Saco

Citation: Jorquera, E., Quijano-Baron, J. P., Rodriguez, J and Saco, P. 2022. *Final Moata'a mangrove ecosystem analysis report*. SPREP, Apia, Samoa.

ACKNOWLEDGEMENTS

The project was funded by Irish Aid through the Secretariat of the Regional Environment Programme. It has been developed in consultation with the Moata'a Village Council, the Ministry of Natural Resources and Environment (Climate Change Division; Division of Environment and Conservation; Water Resources Division); Ministry of Agriculture and Fisheries, Ministry of Women, Community and Social Development, and the Samoan Tourism Authority. We are very grateful to Filomena Nelson and Peter Davies from Secretariat of the Regional Environment Programme and Emarosa Romeo and Asuao Malaki Iakopo from the Ministry of Natural Resources and Environment for the information provided. We also acknowledge the support of Angelo Breda and Steven Sandi from the University of Newcastle.

CONTENTS

LIST OF FIGURES

LIST OF TABLES

ABBREVIATIONS

AR6 - Sixth Assessment Report of the IPCC

C2RCC - Case-2 Regional CoastColour

D - mean depth below high tide

DEM – Digital Elevation Model

EGM - Eco-geomorphological Model

EROS - Earth Resources Observation and Science

FAO – Food and Agriculture Organization

H – Hydroperiod

HSM - Hydro-sedimentological model

HRU – Hydrologic Response Unit

HWSD – Harmonized World Soil Database

IPCC - Intergovernmental Panel on Climate Change

MNRE – Ministry of Natural Resources and Environment

NSE - Nash–Sutcliffe efficiency

PBIAS - Percent bias

PUMA - Planning and Urban Management Agency

R2 - Correlation coefficient

RCP8.5 - Representative Concentration Pathway high-emissions scenario

RSR - Root mean square error to the standard deviation of measured data

SLR - Sea level rise

SWAT - Soil and Water Assessment Tool

SPREP - Pacific Regional Environment Programme

SRTM - Shuttle Radar Topography Mission

TCs - Tropical cyclones and tropical depressions

UN – United Nations

UNESCO – United Nations Educational, Scientific and Cultural Organization

USGS - United States Geological Service

SUMMARY

Mangrove ecosystems are under pressure due to anthropogenic stressors and sea level rise. The resilience of mangroves will depend on the rate of accretion of sediments compared to the rate of sea-level rise and their capability to colonise higher elevation areas or buffer zones. This will also be affected by the measures to protect the existing mangroves against anthropogenic pressures.

The Secretariat of the Pacific Regional Environment Programme (SPREP) and the University of Newcastle signed a partnership agreement to analyse the ecosystem sustainably and determine possible adaptation interventions against climate change of the Moata'a mangroves, Samoa. This report presents the Output 4, "Final Moata'a Mangrove Ecosystem Analysis Report" from the project: "Mangrove, catchment and climate change impacts assessment and mangrove ecosystem analysis".

The report comprises an analysis of background studies relevant for the project and the available information, including data quality assessment and gap filling, a description of the modelling tools and assumptions, results from hydro-sedimentological and ecosystem assessments, and resilience analysis of the Moata'a mangrove ecosystem considering future changes in climate, land use and infrastructure construction.

The data and background information were used to develop hydrosedimentological models of the Moata'a catchment and also of the Vaisigano catchment using the freely available software SWAT. The Vaisigano catchment was included in the analysis because it contributes important amounts of sediment and water to the Moata'a mangrove ecosystem during large floods, The results from the hydrosedimentological analysis were used in conjunction with tidal flows and sediments to analyse the response of the mangrove ecosystem to sea level rise using an ecogeomorphological model.

The ecosystem response assessment indicated that approximately 40% of the mangrove area can be lost over the next 100 years due to the sea level rise that corresponds to a high emission pathway (RCP8.5 of AR6 IPCC report). Mangroves can respond to sea level rise by increasing their elevation when capturing sediments and organic material in the soil or by migrating to higher ground, but the high values of

sea level rise limit the effectiveness of these mechanisms. Analysis of uncertainties in the model topographic data indicated that the loss of mangroves can be between approximately 30% and 60% over the next 100 years.

The resilience of the Moata'a mangrove was studied by analysing the response of the ecosystem under different scenarios of climatic and man-made alterations at the catchment scale, in conjunction with sea level rise. A scenario that considered the construction of levees and a dam for flood protection resulted in a reduced resilience of the ecosystem due to a reduced delivery of sediment to the wetland. Conversely, a scenario that considered an increase in rainfall intensity due to a 4°C temperature rise greatly improved the resilience of the ecosystem because of a higher production of sediment due to erosion. A scenario that considered land use changes due to replacement of forest by agriculture in areas of the Vaisigano catchment had little effect on the mangroves resilience as the sediment inputs increased only marginally and water quality effects were not accounted for.

The results indicate that the mangrove ecosystem resilience is very sensitive to reductions in sediment availability. Maintaining the connectivity of flow and sediment within the mangrove wetland and with the Vaisigano river and the coastal areas is vital for the resilience of the mangrove ecosystem. In addition, implementation of buffer zones at elevations that can promote migration are recommended to accommodate future mangrove colonization. Regular monitoring is required to assess the effectiveness of any preventive measures and to be able to implement adaptive management strategies.

INTRODUCTION

Mangroves act as a natural protection against storms and coastal erosion by reducing the energy of waves and wind. Mangroves are home to rich marine and terrestrial ecosystems, they can filter and purify water and play an essential role in sequestering carbon. Urban coastal developments have altered mangrove areas by clearing and filling. Modifications of the inputs of water and sediments and the hardening of shorelines have put pressure on the mangrove's survival. Additionally, climate change is exerting further stress on mangroves when these ecosystems increase their vertical position at a slower pace than sea level rise, which leads to mangrove drowning.

The resilience of the mangrove area depends on different factors. First, the rate of accretion of sediments creates additional layers of soil in the mangrove area and can attenuate the effects of sea-level rise. This effect is linked to the sediments produced in the catchment area, the rainfall intensity, the frequency of rainfall events, and the land use. Second, measures to protect the existing mangroves against anthropogenic pressures (e.g. avoid over exploitation of resources, land reclamation and filling) can conserve existing areas and promote new areas for colonisation.

Moata'a is an urban village of around 300 – 500 households located in the Upolu Island of Samoa (see Figure 1). The Moata'a catchment has an area of approximately 3.5 km^2, including a mangrove wetland. Historically, this wetland has been affected by anthropogenic pressures (urban expansion, uncontrolled extraction of natural resources, pollution and modification of input flows and tidal regime). Moata'a is also an area affected by extreme weather conditions (e.g., tropical cyclones, floods) that can be intensified due to climate change.

Moata'a is in the flood plain area of the Vaisigano river, which is one of the main rivers in the Upolu Island. The inputs of water and sediments to the Moata'a mangroves are affected by the Vaisigano river. The Vaisigano river catchment is characterised by a mountainous topography covered with forest, and a narrow coastline. During large flood events, a transfer of water occurs from the Vaisigano to the Moata'a catchment, as shown in Figure 2. In these extreme events, important amounts of sediments can be discharged into the mangrove areas.

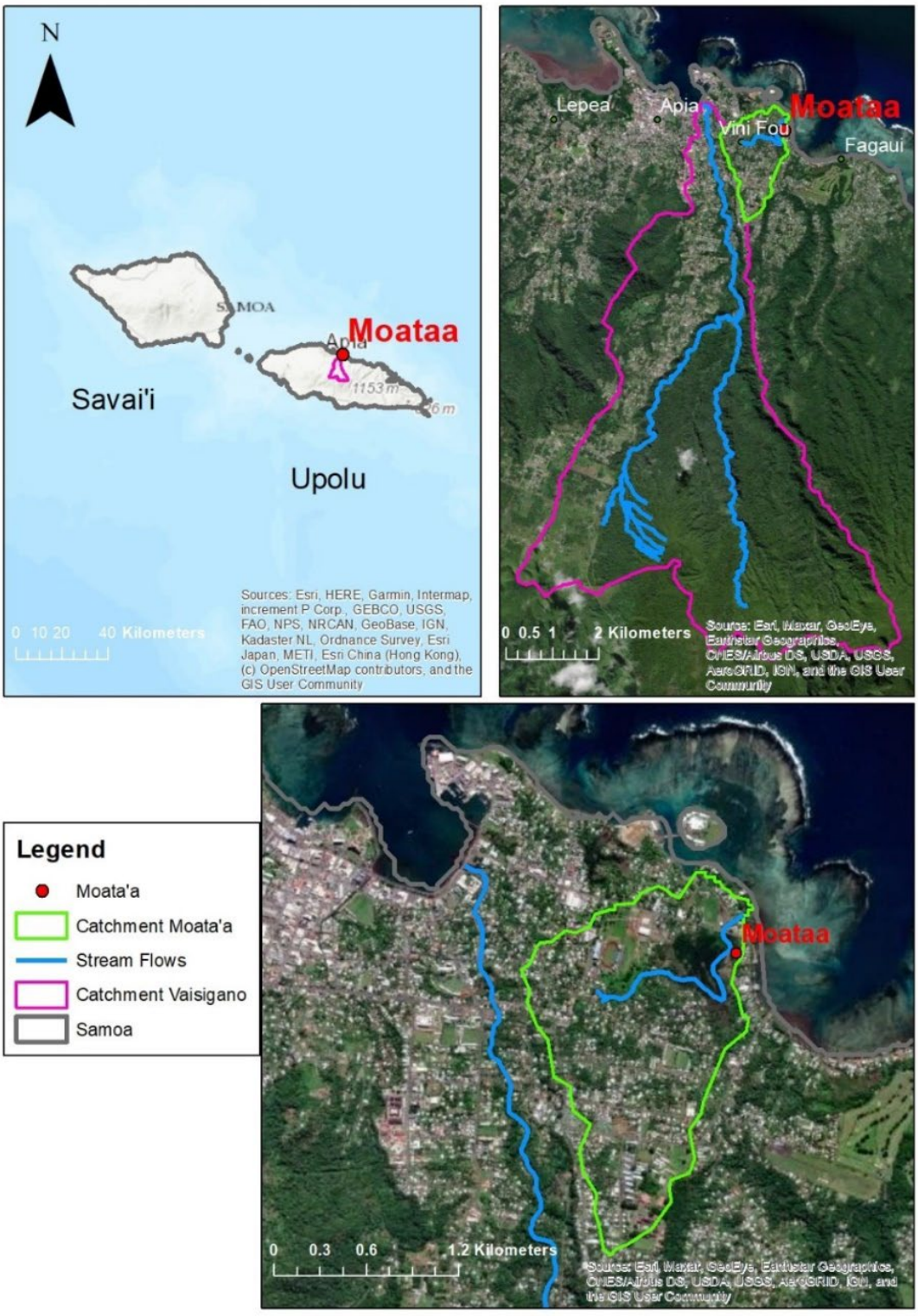

Figure 1. Moata'a location and catchment.

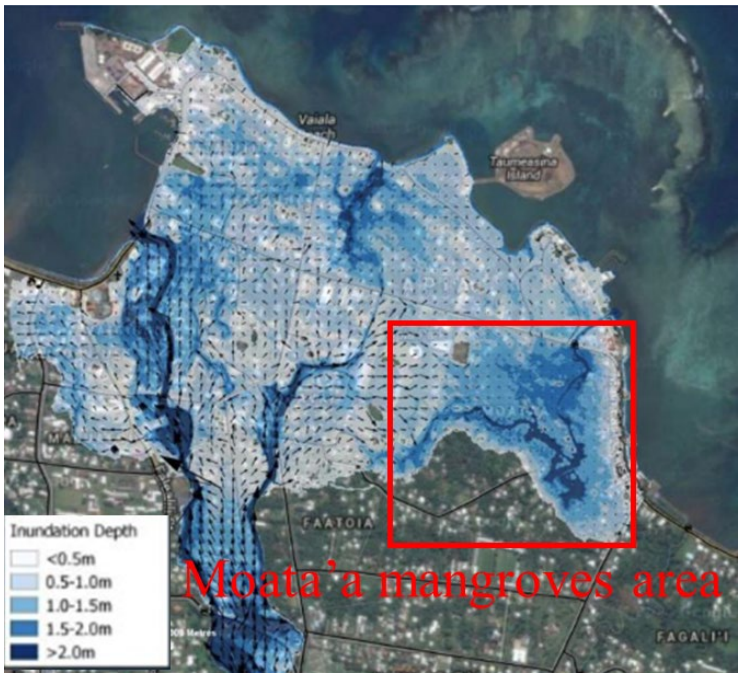

Figure 2. Flooding in Apia and Moata'a Left: Flash flooding (Yeo, 2001), Right: Flood Map extent from a hydrodynamic model (Green Climate Fund, 2016).

This report presents the analysis of the hydro-sedimentological and eco-geomorphological assessment of the Moata'a catchment and wetland, as well as the ecosystem resilience assessment of the wetland to changes in climate, land use and infrastructure construction. The hydro-sedimentological assessment of the Moata'a and Vaisigano catchments was performed using the Soil & Water Assessment Tool (SWAT). With SWAT, the water and sediments produced by the catchments entering the Moata'a mangroves were determined. Then, the eco-geomorphological model was implemented to evaluate the response of Moata'a mangroves to sea-level rise and climate change. Finally, the ecosystem resilience was assessed, identifying conditions that will enhance or weaken the mangrove's long-term persistence.

This report presents the Output 4 "Final Moata'a Mangrove Ecosystem Analysis Report" from the project "Mangrove, catchment and climate change impacts assessment and mangrove ecosystem analysis". The report is organized as follows: section 2 presents a summary of the principal background studies and the available information, including data quality assessment and gap filling; section 3 describes the methodology adopted in this study and the assumptions made; sections 4 and 5 present results of the hydro-sedimentological assessment of the catchments and the ecosystem analysis of the wetland, respectively; section 6 deals with the resilience

analysis of the mangroves, and section 7 provides final comments and recommendations.

BACKGROUND STUDIES AND AVAILABLE INFORMATION

BACKGROUND STUDIES

MANGROVES

Mangroves are vital to preserve the biodiversity of freshwater and marine ecosystems and provide protection against natural disasters (tsunamis, cyclones and storms). They protect the land from erosion and have important cultural values for the surrounding communities, which use the mangrove's natural resources for medicines, ornamentation, building materials, recreation and as source of food (SPREP and PROE, 2011).

Moata'a mangroves currently cover around 5 hectares; however, they used to cover tree times this area. In 1974, Moata'a mangrove coverage was around 20 hectares, but by 1990 this was reduced to 10 hectares due the land reclamation. In Figure 3, it can be noticed that the north and south part of the mangrove area was significantly reduced from 1970 to 1990 and that the river direction and water outlet was modified from northward to eastward. In 2013, it was reported that around 50% of Moata'a mangroves had been destroyed due land reclamation, decreasing the biodiversity and affecting ecosystem services (Saifaleupolu and Elisara, 2013). One of the main issues was the use of mangrove wood as firewood or for building purposes, which has subsequently been banned by the matai council.

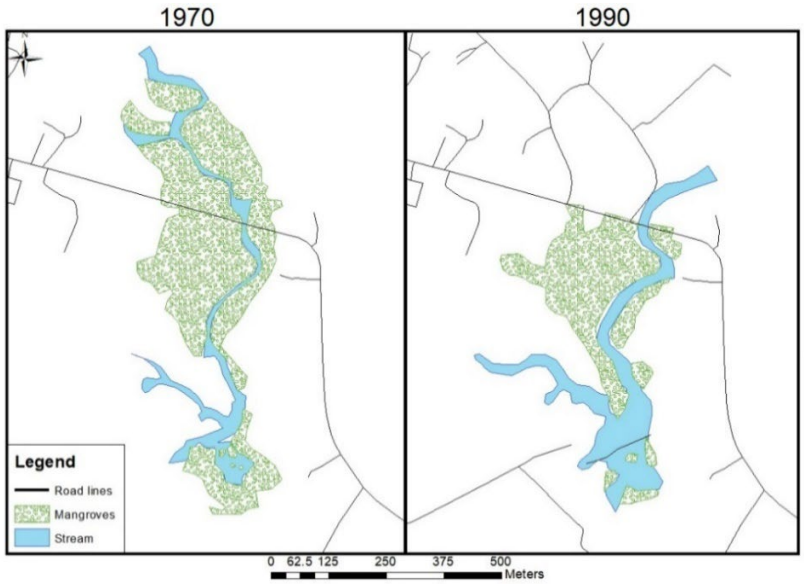

Figure 3. Mangrove extent in 1970 and 1990 (Based on (Suluvale, 2001)

Since 1990, land reclamation on mangroves has decreased considerably. Comparing the mangrove extension in 1990 (Figure 3), 2002 (Figure 4) and 2019 (Figure 5), it can be seen that mangroves expanded to the northwest by 2002 and stayed relatively unmodified until 2019. This illustrates that mangroves are resilient when not affected by excessive anthropogenic pressures.

Figure 4. Mangrove extent in 2002.

Figure 5. Mangrove extent in 2019.

ECOLOGY - FLORA AND FAUNA

The Moata'a mangroves constitute a rich and diverse ecosystem. The main mangrove species in the study site is the Samoan mangrove (*Rhizophora samoensis*), with a small population of Orange mangrove (*Bruguiera gymnorrhiza*). Other species that can be found in the area are Sea hibiscus (*Hibiscus tiliaceus*), Lala (*Dendrolobium umbellatum*), Mangrove grass (*Paspalum vaginatum*), Swamp fern (*Acrostichum aureum*), Aloalo ta (*Clerodendum inerme*), Fetau (*Calophyllum inophyllum*), Kuava (*Pueraria Montana var. lobata.*), Laufala (*Pandanus spurius*), Milo (*Thespesia populnea*), Niu (*Cocos nucifera*), Nonu (*Morinda citrifolia*), Pu'a (*Hernandia nymphaeifolia*), Talie (*Terminalia catappa*). (Saifaleupolu and Elisara, 2013). There are also invasive species in the Moata'a mangroves: tamaligi pa'epa'e (*Albizia falcataria*) and the tamaligi uliuli (*Albizia chinesis*). Regarding fauna, many species of crabs (mangrove crab, red-claw crab and land crab), birds (bulbul, mina, starling, honeyeater, heron, fantail, among others), fish (mud skipper, tamala, mullet, sword fish, eel, among others), reptiles and mammals are found in the Moata'a mangroves (Saifaleupolu and Elisara, 2013). However, there is evidence of declining numbers in fisheries due the anthropogenic pressures (Saifaleupolu and Elisara, 2013).

LAND USE

Samoa is mainly composed of mountainous rain forest and small areas of riverine, swamp, mangrove, and beach forest. The land use of the island has changed due to anthropogenic pressure including deforestation for timber use, extension of agricultural lands, growth of urban areas and unsustainable use of natural resources (Green Climate Fund, 2016).

As seen in Figure 6, coconut crops are one of the main agricultural products in Samoa and its derivates (coconut cream, coconut oil and copra) are important Samoan exports. Few forests remain in the coastal areas, which have been converted to agriculture and urban settlements.

Figure 7 presents the land use map for Apia, generated in 2015 by the Planning and Urban Management Agency (PUMA) and Ministry of Natural Resources and Environment (MNRE) (PUMA & MNRE, 2015). The land uses identified in the area are

agriculture, forestry, rural residential, residential, office/commercial, industrial, and open space/recreation.

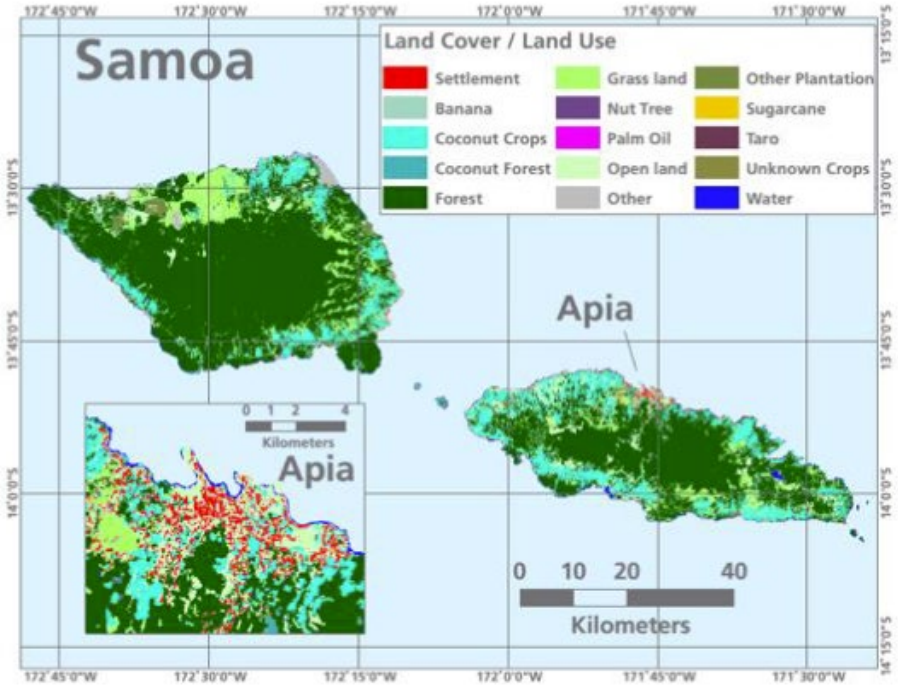

Figure 6. Samoan Land uses (Green Climate Fund, 2016).

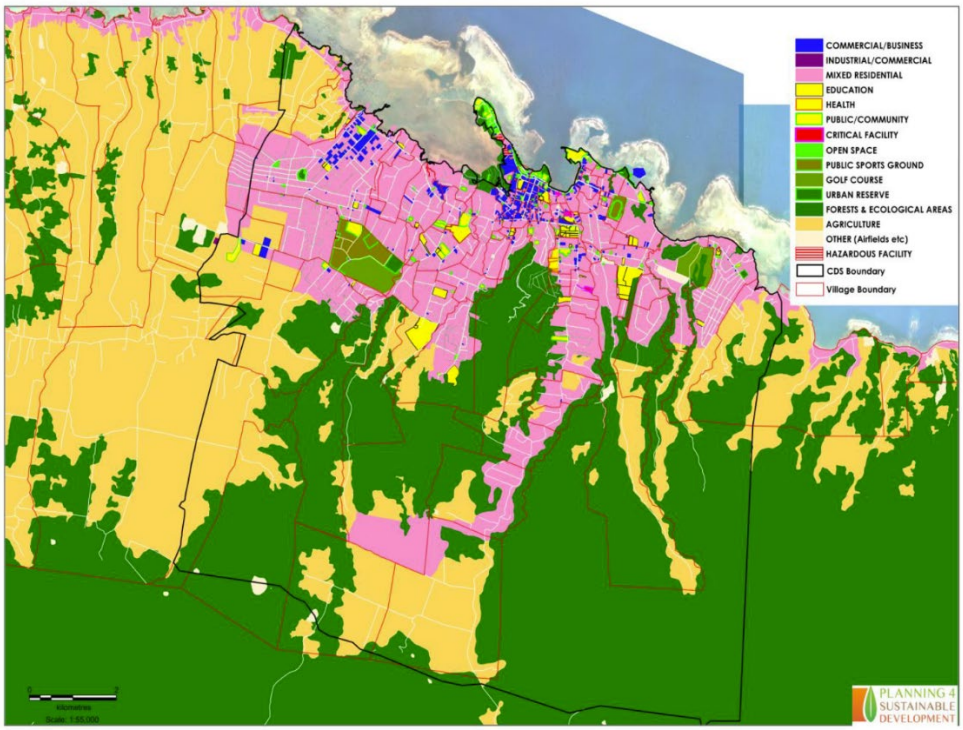

Figure 7. Apia land use map (PUMA & MNRE, 2015).

Moata'a catchment is mainly composed of urban settlements that have been displacing the mangrove forest areas. In Figure 8 it can be seen that the urban density has increased from 2002 to 2019. Moata'a mangroves constitute the main refuge for fauna and flora within the catchment (the catchment is delineated in red).

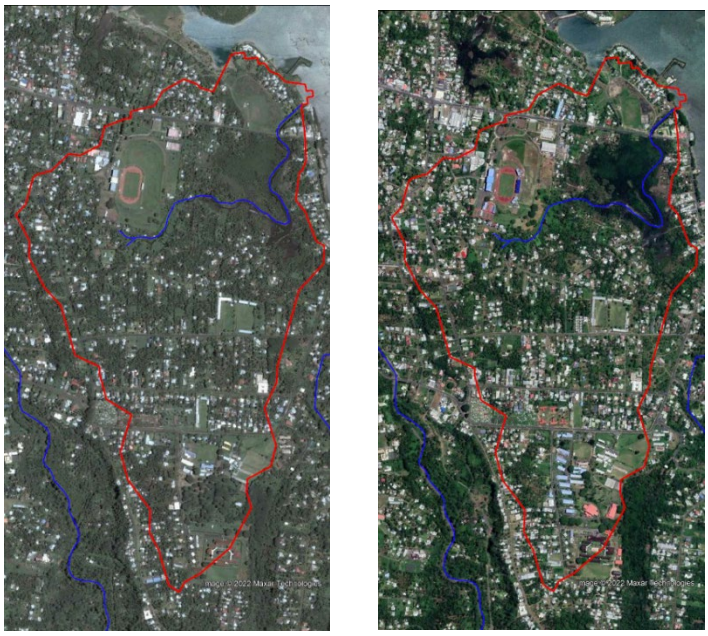

Figure 8. Moata'a catchment land use comparison 2002 and 2019.

CONTAMINATION

Moata'a mangrove main contamination problem is the wastewater disposal and sewage leachate from urban areas, which results in high bacterial levels that can generate water-borne diseases. Additionally, runoff can drag contaminants from the urban areas, which could contain heavy metals. Agricultural lands nearby could be also contributing to high nutrient levels (phosphorous and nitrogen) in the water. Records of water contaminants measurement (Table 1), indicate high levels of Mercury, Total coliform and E.coli.

Table 1. Water contaminants measurement (Saifaleupolu and Elisara, 2013).

Pollutant	Value
Mercury	10.61 µg/kg
Total coliform	2,100 cfu/100ml
E.coli	1,850 cfu/100ml

HYDROLOGY AND FLOODING

Samoa has a wet tropical climate, composed of a wet summer (December-May) and a drier winter season (June-November). There are different factors that affect rainfall distribution in the island. First, the presence of high mountains promotes orographic rainfall. Second, the island is affected by the South Pacific Convergence Zone, which is a climatic phenomenon that brings a band of low-level convergence, cloudiness, and precipitation. Additionally, Samoa is affected by tropical storms and cyclones, which generate intense rainfalls that are associated with the largest floods (Terry et al., 2006). From 1970 until 2003, 17 cyclones were recorded, most of them associated with flooding in Apia and surrounding areas. Table 2 reports the main flooding events recorded in Apia.

Table 2. Historic Flooding records in Apia adapted from Yeo (2001).

#	Date
1	March - 1923
2	January - 1931
3	January - 1935
4	January - 1939
5	November - 1974
6	January - 1975
7	February - 1982
8	January - 1989
9	February - 1990
10	January - 1991
11	December - 1991
12	January - 2000
13	December - 2003
14	January - 2011
15	December - 2012
16	March - 2016
17	February - 2018
18	December - 2020
19	January - 2021

Flooding in Samoa is mainly caused by tropical cyclones and the short and steep hills that promote a rapid water transport to a densely populated plain area. Furthermore, flooding could be the result of Tsunamis. For example, in September 2009, an 8.1 magnitude earthquake (190 km southwest of Samoa) triggered a

Tsunami (14-meter waves) that generated damage as far as 400 meters inland (Jaffe et al., 2011).

Flooding greatly affects Samoa and produces extensive damage. In 1990, flooding produced by tropical Cyclone Ofa destroyed the gauging station as well as the buildings of the Samoan Meteorological Office in Apia (Terry et al., 2006). In April of 2001, a flash flood resulting from 200 mm rainfall in less than two hours affected about 5000 residents in Apia (Yeo, 2001). In 2012, Cyclone Evans generated damages in Samoa of approximately US$200 million (Green Climate Fund, 2016).

Regarding Moata'a village, the area is prone to flooding due the 10 freshwater springs that discharge into the mangroves, but also due to its proximity to the coast and to the Vaisigano River. Figure 9 shows the flood frequency curve for the Alaoa East gauging station on the Vaisigano River, where it can be observed that for a measured return period of 17 years, up to 70 m^3/s can be expected (Terry et al., 2006). For high return periods, the Vaisigano River cannot contain the flows, generating flooding that can affect Moata'a village. For instance, in December 2012, the Vaisigano River flooded during Tropical Cyclone Evans, affecting Moata'a mangroves (Saifaleupolu and Elisara, 2013). Figure 10 shows that the flash flood of April 2001 also affected a great part of the village. Results from a hydrodynamic models applied to the Vaisigano River (Figure 11) indicated that for extreme rainfall scenarios most of Apia and Moata'a would be affected by flooding (Green Climate Fund, 2016).

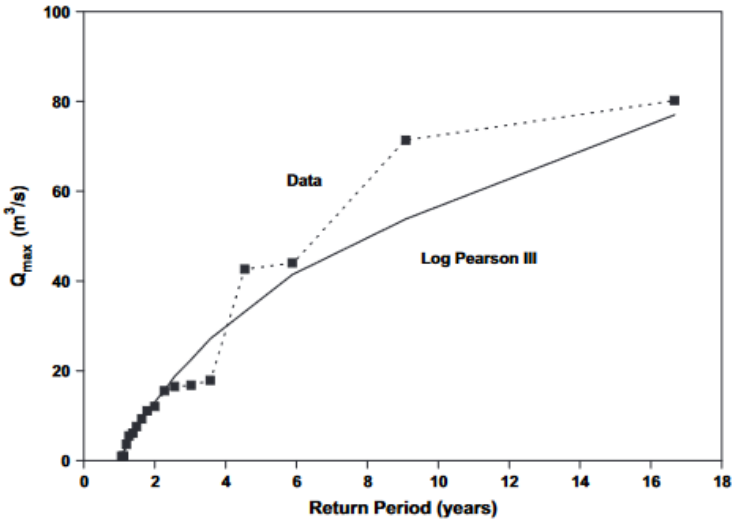

Figure 9. Flood frequency curve for the Vaisigano River near Apia (Terry et al., 2006).

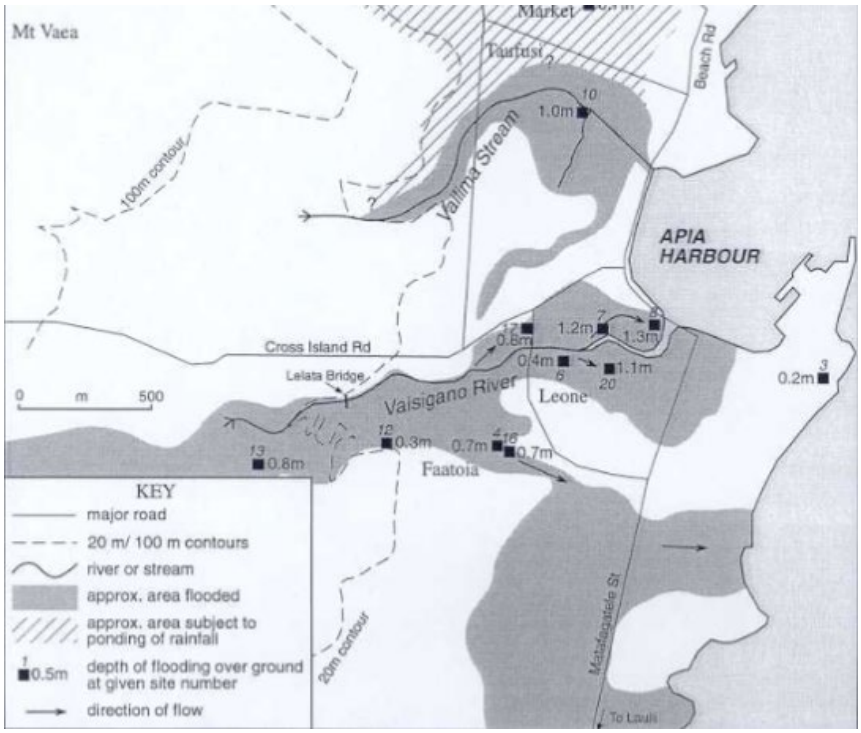

Figure 10. Flash flooding in Apia and Moata'a (Yeo, 2001).

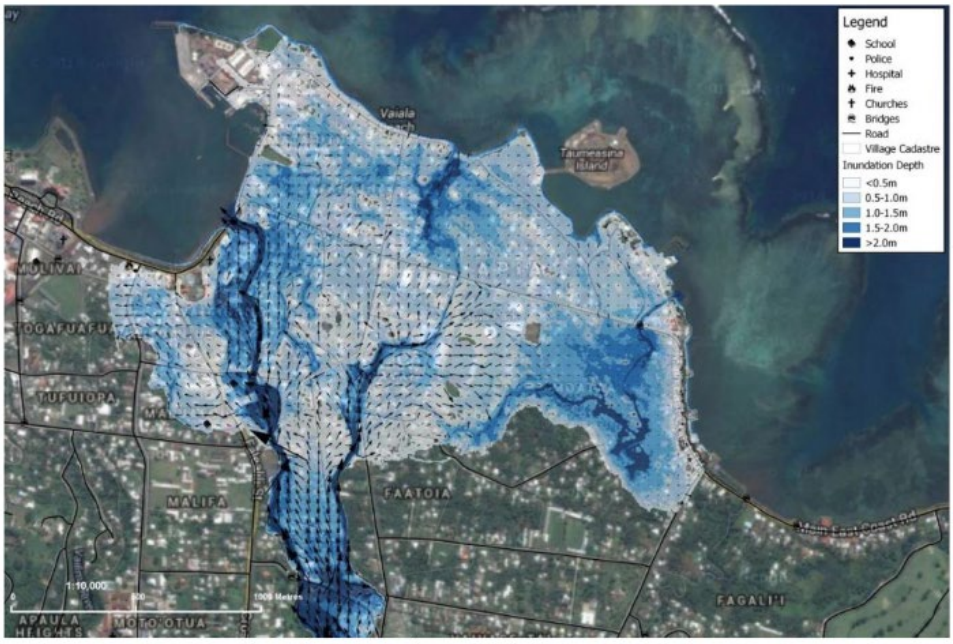

Figure 11. Flood map extent for extreme rainfall conditions obtained using a hydrodynamic model (Green Climate Fund, 2016).

COASTAL PROCESSES

Samoa is a group of volcanic islands formed in the late Quaternary period. Its soils are volcanic, derived from basalt and basic andesite and belong to the Inceptisol soil order (Schroth, 1970). The coral reef that surrounds the Samoan islands is a

highly biodiverse ecosystems that provides food, recreation and income, but at the same time, protection from waves and tropical storms.

Despite the coral reef protection, around 80% of the coastline is classified as "sensitive" or "highly sensitive" to coastal erosion (Green Climate Fund, citing GoS, 2015). Even though cyclones generate important coastal erosion, reefs reduce wave energy and the offshore currents.

Moata'a site remained relatively unchanged until 1970, when land reclamation, dredging, lagoon infilling and river diversion started to take place and considerably changed the coast by late 1980's (Solomon, 1994). There have been no systematic studies of the effects on these changes in the river/reef morphology and on the alluvial deposits. However, it is known that dredging in coastal areas reduces the material available to replenish the coasts and that modifications to the reef can increase the effect of currents. Figure 12 and Figure 13, shows how the coast in front of Moata'a village have been modified by land reclamation, occupation of coastal and mangrove areas and changes in the reef and sediments in the lagoons.

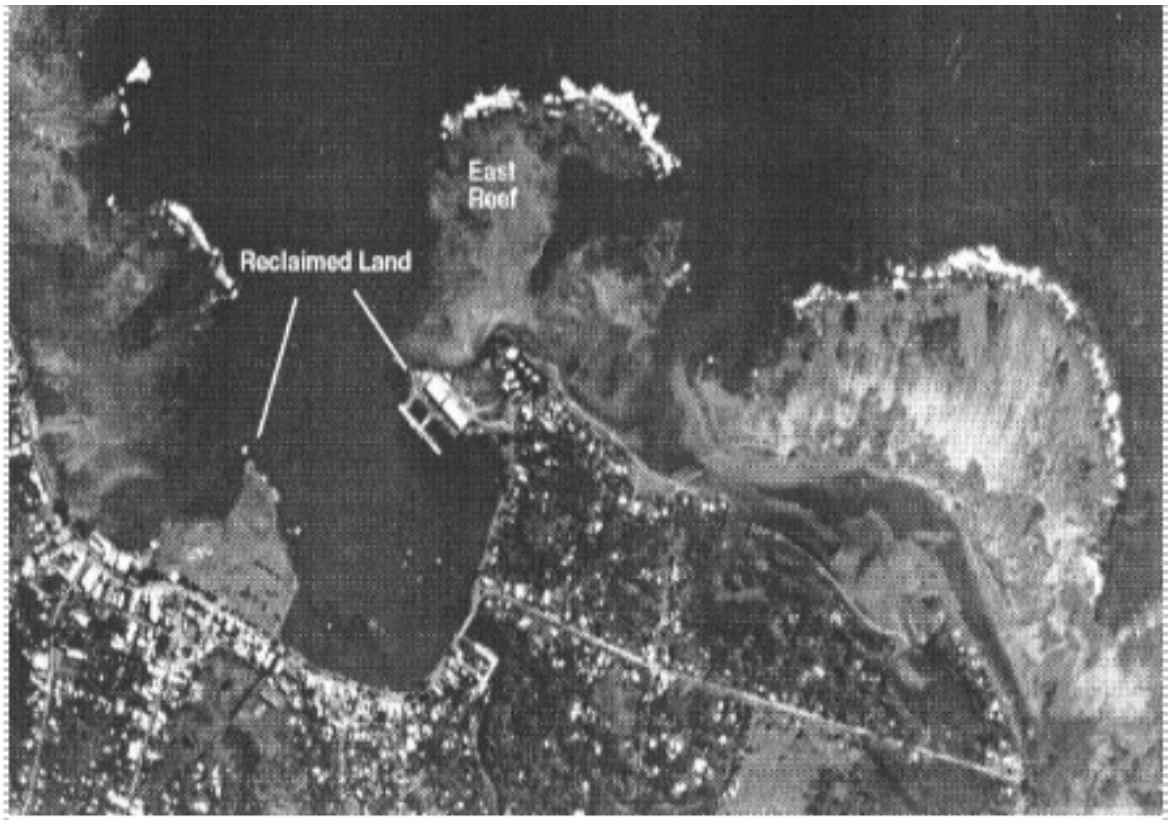

Figure 12. Apia and Moata'a aerial view 1970 (Solomon, 1994).

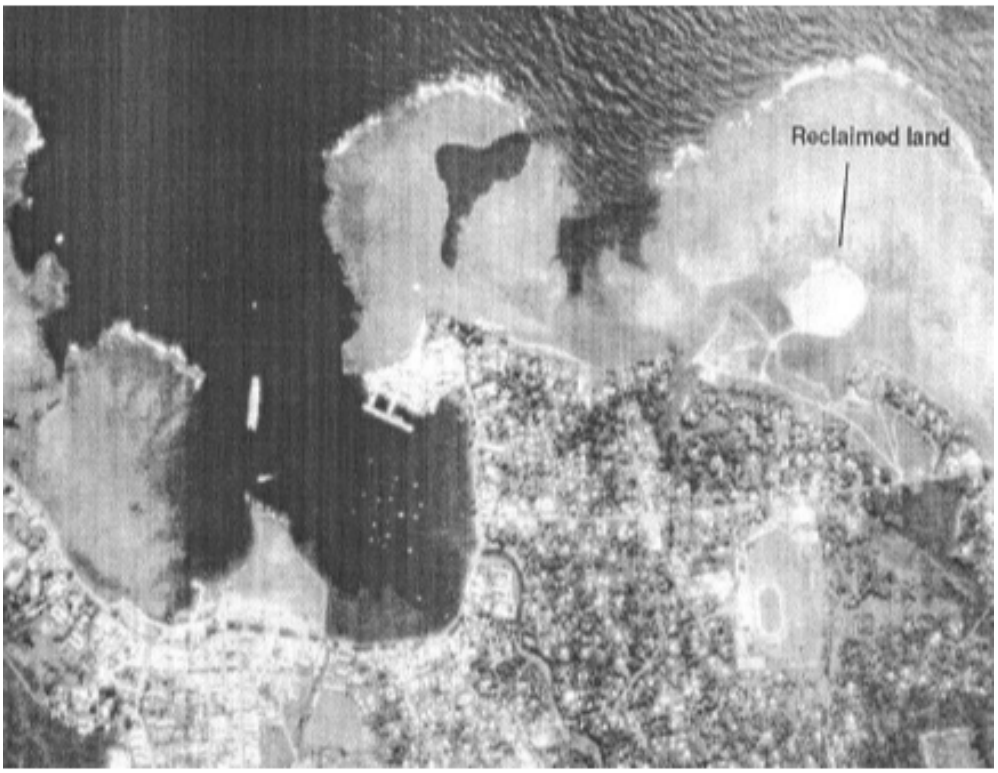

Figure 13. Apia and Moata'a aerial view 1987 (Solomon, 1994).

SEDIMENT EROSION AND DEPOSITION

Samoan soils are particularly susceptible to soil erosion because of the high slopes, replacement of native vegetation (tropical rainforest or shrub) for intensive agriculture and regular heavy rains, including those due to tropical storms/cyclones. As a result, significant soil erosion is expected, particularly in the upper catchment areas.

Floodplain sediments in Samoa are composed by fine sand and silt (Terry et al., 2006). It has been found that soils in Samoa have up to 70% porosity, hydraulic conductivity up to 1,000 cm/day, and bulk density of around 620 kg/m^3 (Van den Elsen et al., 2004). These characteristics can contribute to the generation of high runoff and sediment transport (including erosion and deposition), particularly under high intensity rainfall events. Terry et al. (2006) found that catchment sediment mobilised during cyclones produced sedimentation rates of up to 4+/-0.4 cm per year in the floodplains of the Vaisigano River, including Moata'a.

On the other hand, soil erosion in the Moata'a mangroves has been attributed mainly to land reclamation (Suluvale, 2001).

CLIMATE CHANGE

Samoa is already vulnerable to natural hazards and this vulnerability is expected to increase due to Climate Change. Globally, sea level has risen between 0.1 and 0.2 m during the 20th century (Ebi et al., 2006), with the Pacific Islands experiencing values at the upper end of the range, as shown by an average rise in relative sea level of 2.0 mm per year (Russell, 2011). This value could increase to up to 7 mm per year under climate change projections.

Projected reductions in coastal habitats (including mangrove wetlands) are mainly attributed to relative sea-level rise, resulting from climate change and global warming. The response of mangroves to sea-level rise depends on the mean sea level change rate relative to the mangrove surface elevation, tidal range, salinity regime, nutrient concentration, water quality (e.g., pH or pollutant inputs), inundation regime, slope of the terrain in the mangrove and adjacent areas, presence of obstacles to landward migration (e.g., urban development), sediment inputs, erosion and accretion of the mangrove (Krauss et al., 2014, Rodriguez et al., 2017). Reductions of mangrove habitat can be substantial in the Pacific Islands; for instance, (Gilman et al., 2007) found that by 2100 American Samoa could experience as much as 50% reduction of the Mangroves' areas due the sea level rise and the obstruction of landward migration by coastal developed areas.

Additional effects on mangrove areas due climate change and anthropogenic pressure include the introduction of invasive species, insect infestations, increases in infrequency and magnitude of extreme events (e.g., floods, cyclones), changes in precipitation, temperature, CO_2, unplanned developments, solid waste and destructive fishing techniques, to name a few.

CATCHMENT MANAGEMENT

Efforts have been made in the Moata'a village to better manage the catchment and protect the mangroves. For instance, the village matai council has approved a fine to avoid mangrove cutting or destruction (Saifaleupolu and Elisara, 2013). Some additional management activities planned or already implemented are listed below (Saifaleupolu and Elisara, 2017).

- Redesign and building of the causeway: a causeway originally built in the south part of Moata'a mangrove to connect the communities from the west to the east site (Figure 14) was redesigned to improve flow connectivity. The original causeway was constructed as an earth embankment which halted the connectivity of the flow, nutrients, fauna and sediments. As a result, the flora, fauna and water quality were significantly affected in the southern part of the mangroves. A better causeway was designed and built to restore the connectivity of the mangroves and recover their ecological services (Figure 15).

Figure 14. Causeway in 2013 (Saifaleupolu and Elisara, 2013)

Figure 15. Causeway in 2019

- Reforestation program: to counteract the anthropogenic pressure to the mangroves, a plan has been developed to create a nursery, determine replanting areas and remove invasive species. This plan follows the natural adaptation of the two mangrove species: Bruguiera spp at the landward locations, and Rhizophora spp at the seaward location
- Decontamination program: to improve water quality, investigations of the sources of heavy metals and microbiological contamination in the mangroves have been proposed to support a decontamination program
- Construction of structures: to counteract the effects of sea level rise and river flooding, construction of a retaining wall at a landward location and a sea wall in the coastal zone have been proposed.
- Development of affordable and economical fuel alternatives to the use of mangrove wood.

AVAILABLE INFORMATION

In this section, a summary of all the information gathered to date is presented. The information includes data from free and online sources and meteorological data provided by the MNRE.

DIGITAL ELEVATION MODEL (DEM)

A Digital Elevation Model (DEM) from the Shuttle Radar Topography Mission (SRTM DEM) (https://www2.jpl.nasa.gov/srtm/dataprod.htm) with a spatial resolution of one arc-second (30 x 30m) was retrieved from the United States Geological Service (USGS) Earth Resources Observation and Science (EROS) Center (https://earthexplorer.usgs.gov/). Figure 16 presents the DEM for the area, where the Vaisigano river catchment and the Moata'a wetlands catchment have been delineated using GIS software. Figure 17 shows a 3D representation of the topography, with an exaggeration in the vertical dimension.

The Moata'a wetland catchment is part of the floodplain of the Vaisigano river. The topography at the mouth of the river is gentler than in the headwaters where the slopes of the terrain are greater than 60% (30 degrees). Figure 18 shows the distribution of the slopes of both catchments, while Figure 19 present the hypsometric curve and the histogram of the slope for the Moata'a wetland catchment

and the Vaisigano river catchment, respectively. In the Moata'a catchment, more than 90% of the catchment is below 36 m and the slope is lower than 6% (Figure 19). On the other hand, the Vaisigano river catchment presents an average slope 24.55%. Approximately 20% of the area presents slopes that are greater than 60% (Figure 19).

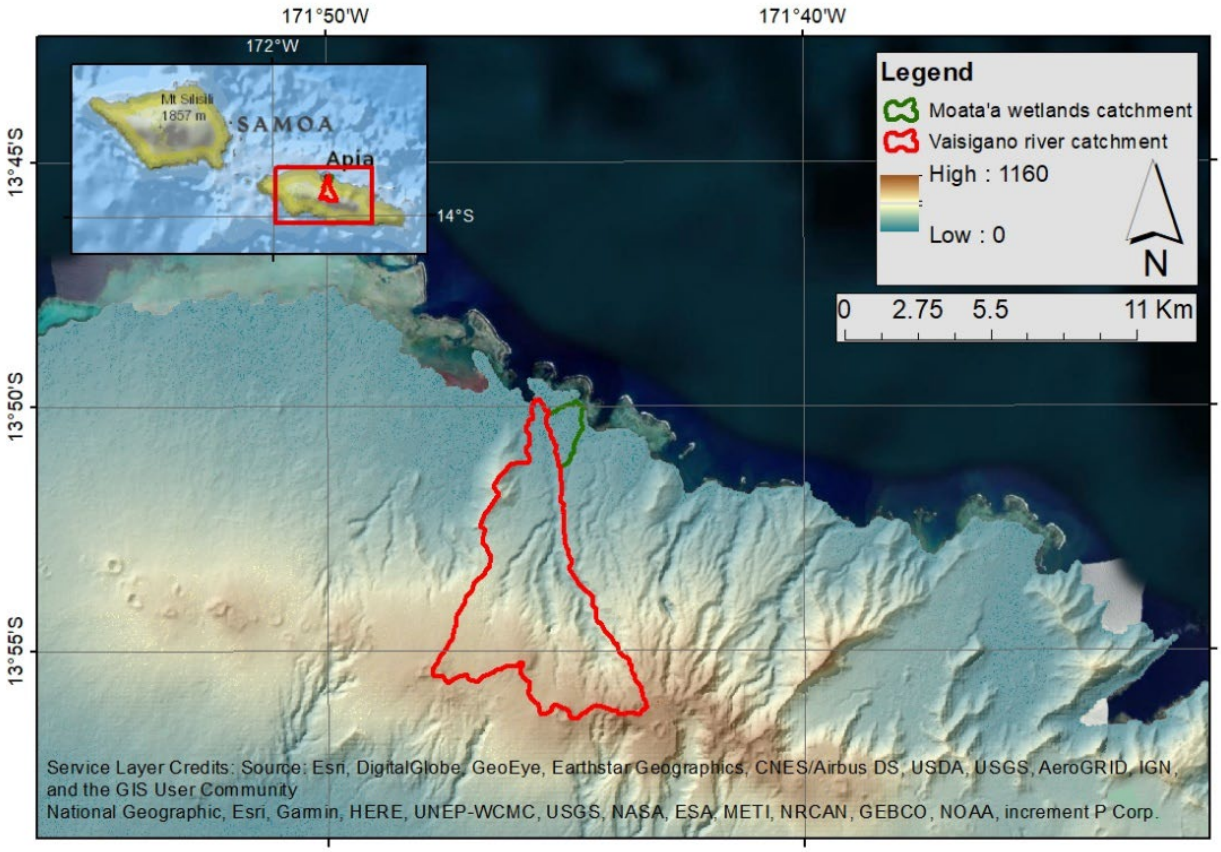

Figure 16. Topographical map.

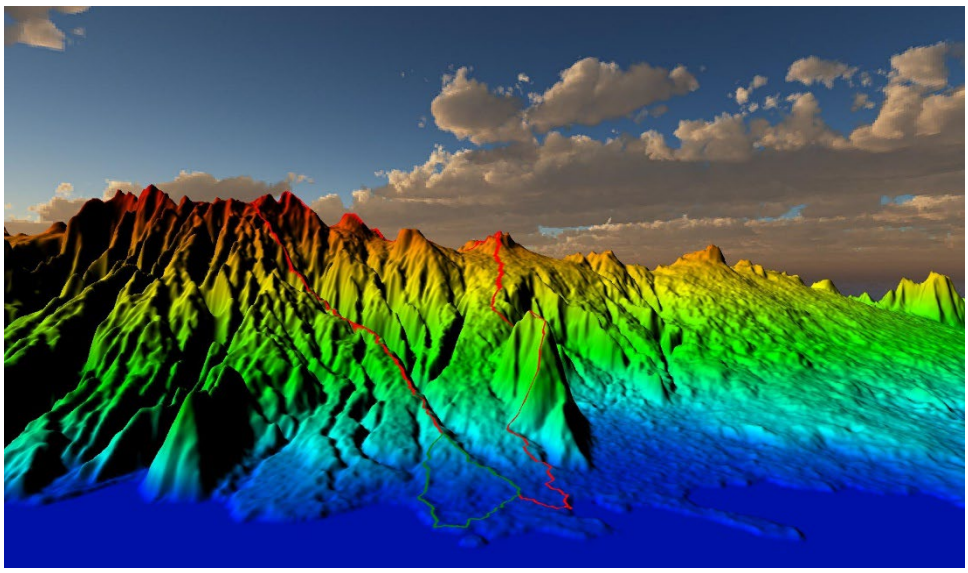

Figure 17. 3D representation of the catchments' topography.

The analysis of the topography allowed for a better understanding of the water dynamics of the system and highlighted the need for a higher resolution DEM, especially for the lower areas of the catchments.

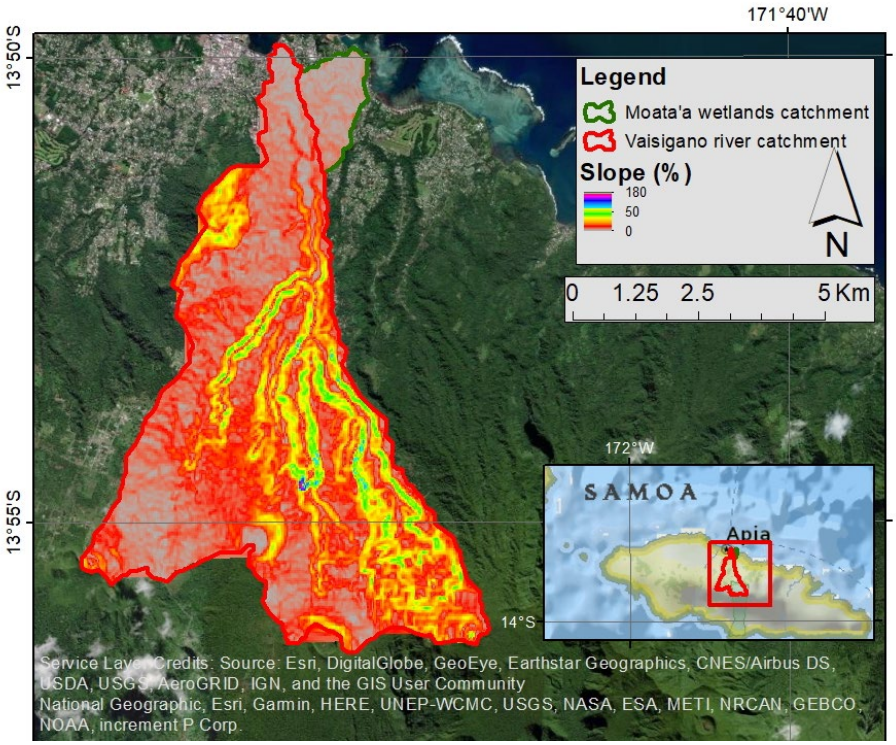

Figure 18. Slopes of the Vaisigano and Moata'a catchments.

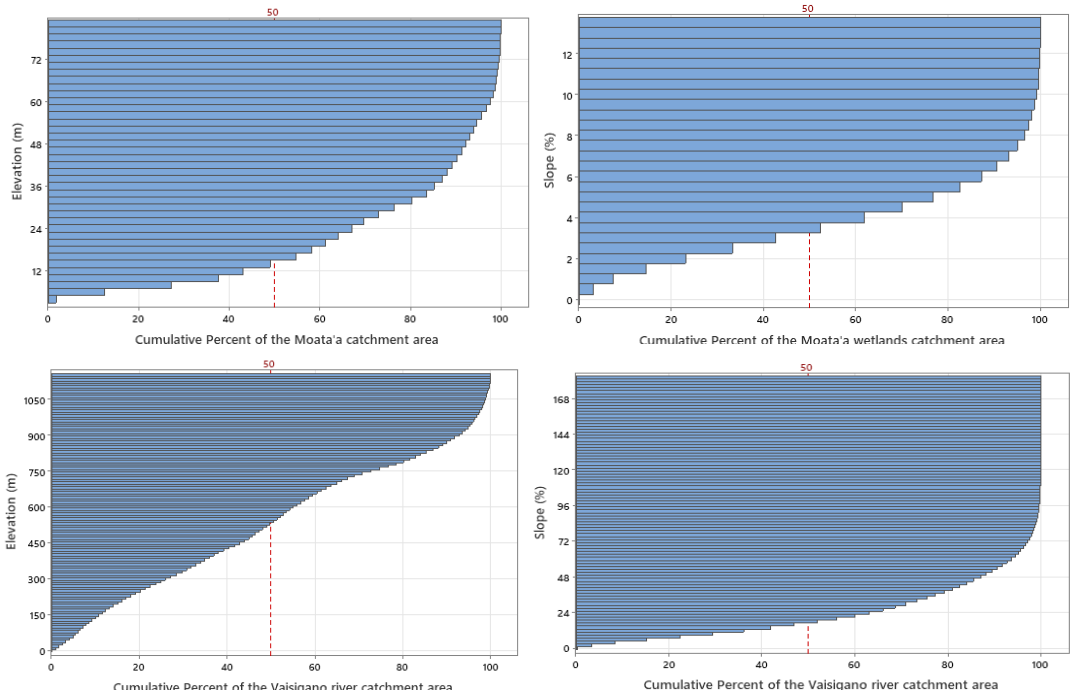

Figure 19. Hypsometric curve and histogram of the slope for Moata'a and Vaisigano catchments.

HYDRO-METEOROLOGICAL DATA

There are two hydrometeorological networks in Samoa, one operated by the Samoan MNRE and the other by the Samoa Meteorology Division (SAMET) (Figure 20). The MNRE network measures different variables such as rainfall, surface, and ground water levels. The SAMET network has climate, rainfall, and automatic weather stations (AWS) that measure precipitation, wind speed and direction, temperature, and atmospheric pressure (Figure 21).

The following sections present an analysis of precipitation, temperature, wind speed, relative humidity, solar radiation, surface water, and groundwater levels based on the information provided by SPREP.

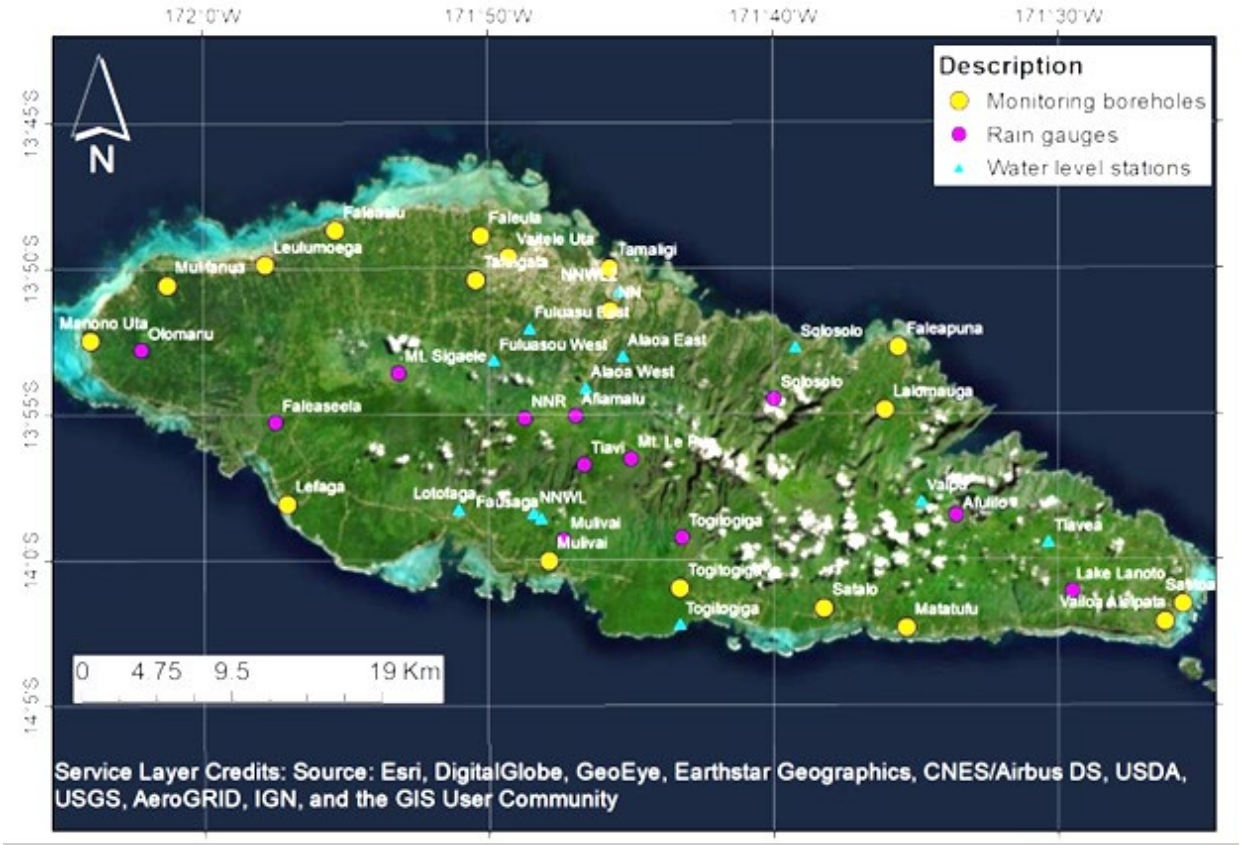

Figure 20. Ministry of Natural Resources and Environment (MNRE) hydrometeorological network.

PRECIPITATION

- *Subdaily data*

As stated by the Catalogue of rivers for pacific islands (WMO et al., 2012) the available rainfall data in Samoa is limited and part of the historical data is not easily

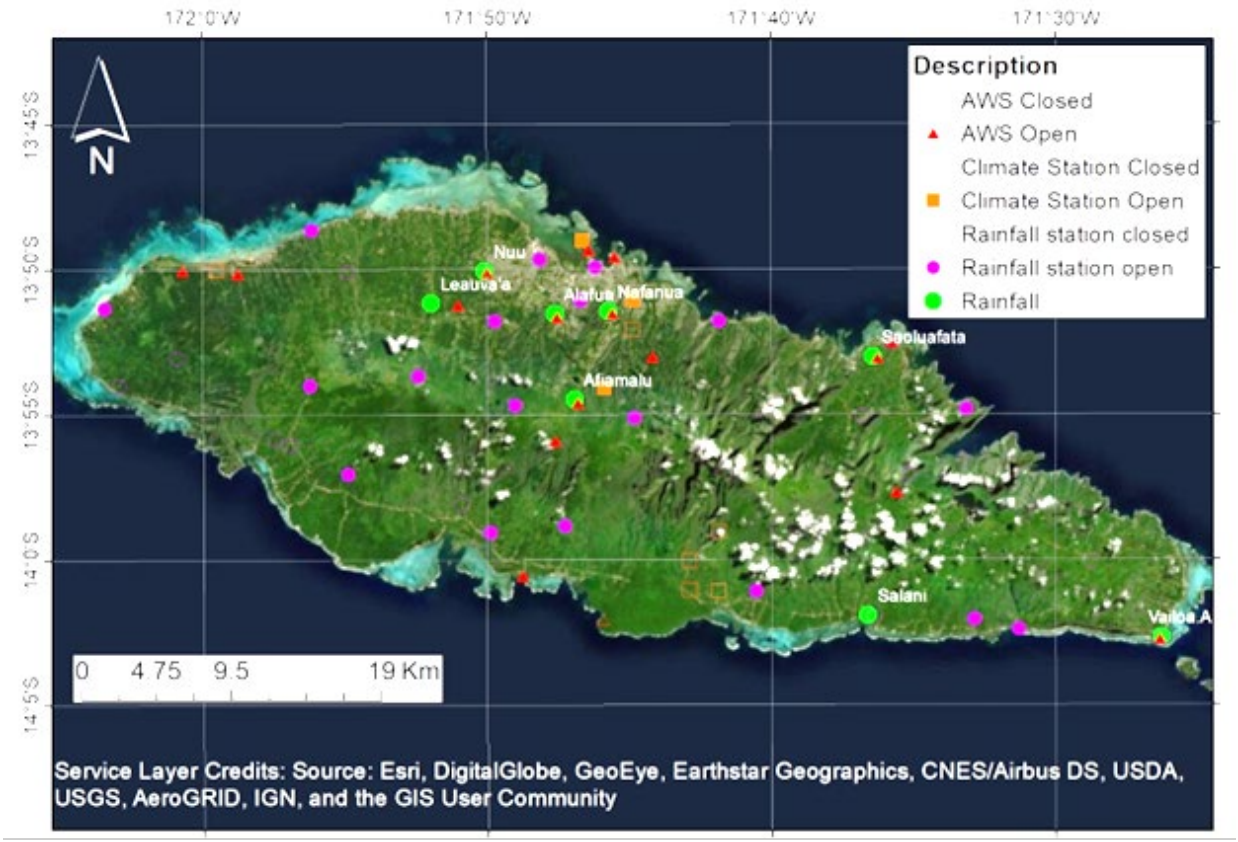

Figure 21. Samoa Meteorology Division (SAMET) meteorological network. AWS stands for Automatic Weather Station.

available or has not been archived. Information was gathered from eleven rainfall stations provided by MNRE, but the analysis was carried out only in the stations located within 15 km of the boundary of the catchments and on the same side of the divide (shaded in green and yellow in Table 3 – Figure 22).

A data quality analysis was performed, and data gaps were filled when possible. The procedure involved four steps: identifying the missing data, aggregating the data into a daily time step, assessing the correlation between stations, and completing the station with information from the other stations. The methodology applied to the SAMET stations was slightly different than the MNRE network due to the data type. In the first case, the stations had one data every 10 minutes, so a time step missing was identified as missing data. In contrast, the MNRE stations had one record for every 0.5 mm of rainfall, and the missing data were identified when successive values had a difference of more than 1.5 mm (three steps).

Table 3. Rainfall stations in the proximity of Moata'a.

Station name	Frequency	Period	Missing data or outliers (days)	Network
Afiamalu AWS	10 minutes	01/01/2015 - 31/12/2020	391	SAMET
Alafua AWS	10 minutes	01/01/2015 - 31/12/2020	1266	SAMET
Nuu AWS	10 minutes	01/01/2015 - 31/12/2020	734	SAMET
Salani Falealili AR	10 minutes	01/01/2015 - 31/12/2020	519	SAMET
Saoluafata Uta AWS	10 minutes	01/01/2015 - 31/12/2020	337	SAMET
Vailoa.A AR	10 minutes	01/01/2015 - 31/12/2020	43	SAMET
Nafanua AWS	10 minutes	01/01/2015 - 31/12/2020	775	SAMET
Leauva'a Uta AR	10 minutes	01/01/2015 - 31/12/2020	754	SAMET
Lake Lanoto'o	0.5 mm	11/09/2009 - 31/03/2019	82*	MNRE
Mt Sigaele	0.5 mm	11/09/2009 - 10/01/2018	7*	MNRE
Solosolo	0.5 mm	23/03/2009 - 28/01/2021	663*	MNRE

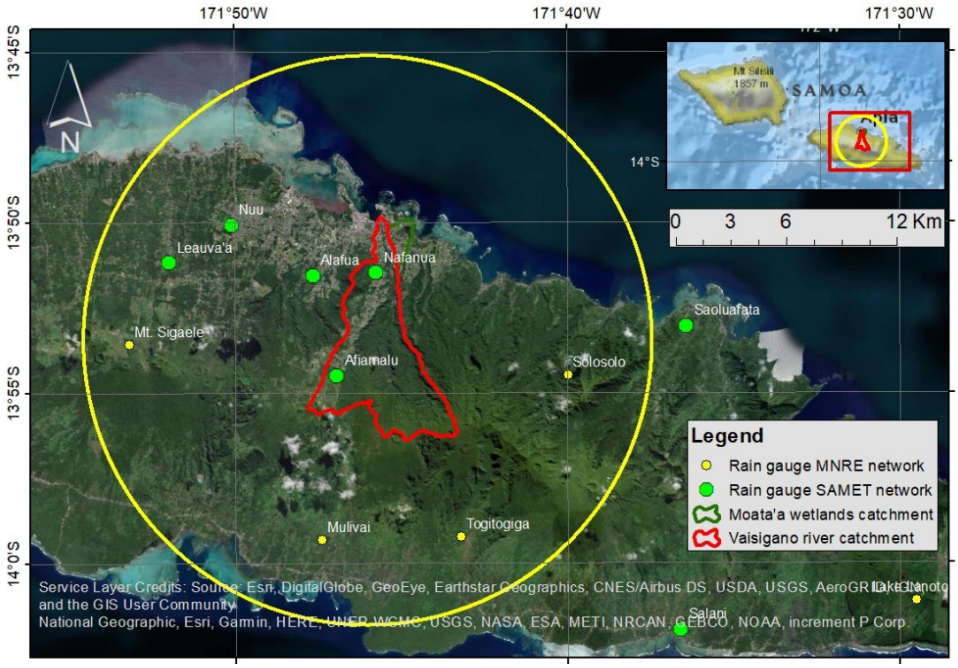

Figure 22. Location of the rainfall stations in the proximity of Moata'a.

The correlation among the stations was in general acceptable and completion of the series was carried out on in those stations who had a correlation coefficient R^2 higher than 0.5 (Table 4). After completion, the periods with missing data were reduced to 108 days in four stations (Afiamalu, Alafua, Nafanua and Leauvaa) and 245, 460 and 485 in the other three stations (Nuu, Mt. Sigaele and Solosolo, respectively).

Table 5 shows the amount of missing data per month for the four stations that have the most complete record (i.e., Afiamalu, Alafua, Nafanua and Leauvaa). Table 6 presents the monthly rainfall data for the seven stations analysed, highlighting the months during which completion of the series was not possible (pink cell with a -1).

Table 4. Correlation coefficient among the rainfall stations.

	Afiamalu	**Alafua**	**Nafanua**	**Nuu**	**Leauvaa**	**Mt. Sigaele**	**Solosolo**
Afiamalu	-	0.668	0.704	0.481	0.574	0.505	0.439
Alafua	0.668	-	0.928	0.822	0.787	0.207	0.584
Nafanua	0.704	0.892	-	0.727	0.657	0.455	0.508
Nuu	0.481	0.822	0.727	-	0.800	0.514	0.439
Leauvaa	0.574	0.787	0.657	0.800	-	0.403	0.416
Mt. Sigaele	0.505	0.207	0.455	0.514	0.40	-	0.112
Solosolo	0.439	0.584	0.508	0.439	0.42	0.1119	-

Table 5. Amount of missing data per month for Afiamalu, Alafua, Nafanua and Leauvaa stations.

Year	Jan	Feb	Mar	Apr	May	Jun	Jul	Aug	Sep	Oct	Nov	Dec
2015	0	0	0	1	0	0	0	0	0	0	0	0
2016	0	0	0	0	0	0	0	4	0	1	0	0
2017	0	0	0	0	0	0	0	0	1	1	0	0
2018	0	0	0	0	0	0	0	2	20	31	2	0
2019	2	0	0	22	13	3	0	2	1	0	0	1
2020	0	0	0	0	0	0	0	0	1	0	0	0

- *Daily data*

Daily precipitation data for the Afiamalu, Nafanua, Alafua and Apia stations was obtained from the Samoan MNRE and the SAMET (Figure 23). The records comprise the period from 01/01/1970 to 31/12/2020. A similar procedure to the one applied to sub-daily data was carried out, first analysing the correlation among stations and

then gap filling the missing data based on the correlation (Table 7). Figure 24 presents a synthesis of the total annual precipitation for each station.

Table 6. Monthly rainfall data for the seven stations analysed (incomplete data in pink).

Year		Jan	Feb	Mar	Apr	May	Jun	Jul	Aug	Sep	Oct	Nov	Dec
Afiamalu	2015	554	536	491	-1	331	200	141	165	18	302	873	588
	2016	369	261	412	695	372	124	47	-1	137	-1	378	735
	2017	410	1014	169	438	1046	203	183	316	-1	-1	542	713
	2018	994	885	443	499	216	110	95	-1	-1	-1	-1	723
	2019	-1	769	184	-1	-1	-1	535	-1	-1	206	358	-1
	2020	939	1264	282	232	318	336	295	93	-1	512	412	1225
Alafua	2015	419	418	254	-1	282	92	11	85	7	195	660	336
	2016	125	362	367	480	414	112	59	-1	72	-1	163	625
	2017	324	554	144	318	847	126	174	287	-1	-1	413	607
	2018	587	777	219	484	201	96	80	-1	-1	-1	-1	418
	2019	-1	639	113	-1	-1	-1	363	-1	-1	166	131	-1
	2020	482	824	91	232	144	270	223	36	-1	326	219	658
Nafanua	2015	361	405	307	-1	275	101	8	97	7	184	750	336
	2016	141	383	305	542	419	142	62	-1	121	-1	185	667
	2017	349	681	108	354	918	127	195	228	-1	-1	383	648
	2018	632	837	236	521	217	96	76	-1	-1	-1	-1	508
	2019	-1	541	130	-1	-1	-1	376	-1	-1	186	144	-1
	2020	539	902	98	229	143	327	241	47	-1	329	211	735
Nuu	2015	317	366	327	120	212	73	11	71	10	214	677	349
	2016	96	201	229	485	349	82	43	97	49	72	142	508
	2017	327	515	123	307	883	156	118	268	56	159	408	706
	2018	344	693	281	385	143	85	65	-1	-1	-1	-1	336
	2019	-1	514	-1	-1	-1	-1	-1	-1	-1	179	114	-1
	2020	520	860	120	165	213	252	172	30	-1	306	201	709
Leauvaa	2015	374	425	278	-1	217	75	46	57	12	266	702	346
	2016	127	206	317	511	314	87	54	-1	53	-1	267	490
	2017	303	616	164	334	809	153	111	252	-1	-1	384	665
	2018	313	785	219	537	156	84	76	-1	-1	-1	-1	395
	2019	-1	605	100	-1	-1	-1	306	-1	-1	172	98	-1
	2020	676	994	87	116	166	145	114	30	-1	288	189	668
Mt. Sigaele	2015	365	520	342	213	301	122	55	31	9	-1	239	175
	2016	71	4	0	0	0	0	11	197	267	345	502	667
	2017	390	609	229	359	909	252	173	312	62	333	458	545
	2018	336	420	-1	234	-1	-1	-1	-1	-1	-1	-1	-1
	2019	-1	-1	-1	-1	-1	-1	-1	-1	-1	109	69	-1
	2020	315	-1	73	-1	129	153	104	-1	-1	-1	-1	430
Solosolo	2015	454	506	576	301	434	183	117	163	10	289	951	615
	2016	195	343	424	683	534	172	51	20	31	65	156	436
	2017	235	64	45	-1	-1	-1	70	269	-1	-1	-1	-1
	2018	-1	-1	-1	-1	-1	-1	-1	-1	-1	-1	-1	-1
	2019	-1	-1	-1	-1	-1	-1	-1	-1	-1	-1	2	-1
	2020	-1	-1	-1	-1	-1	255	208	41	-1	298	196	-1

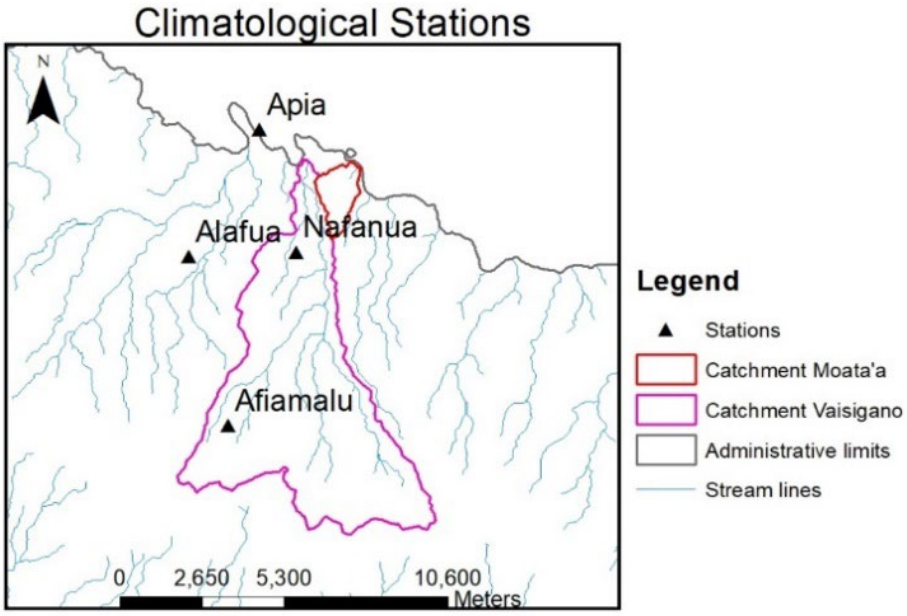

Figure 23. Location of the climatological stations.

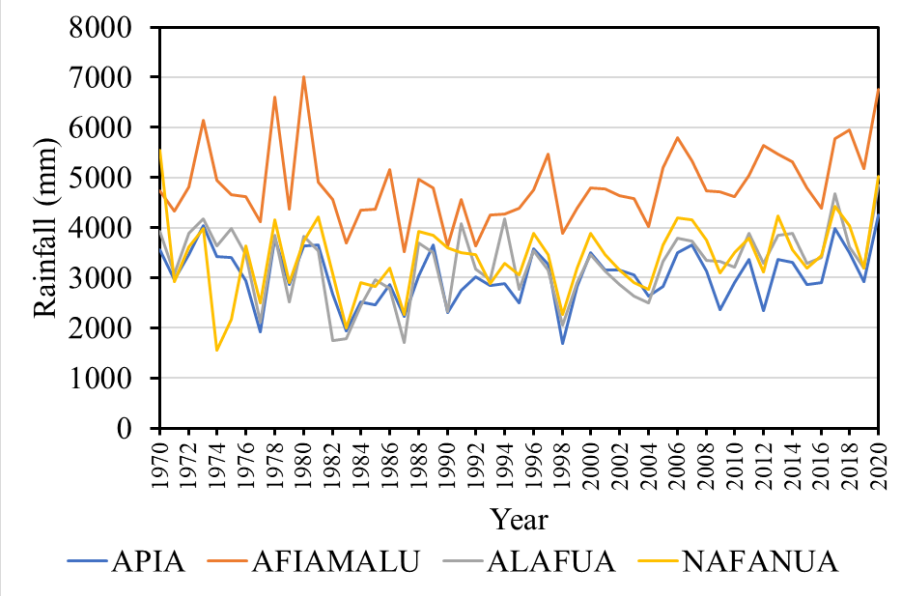

Figure 24. Annual rainfall from the selected climatological stations.

Table 7. Precipitation missing daily data.

Station	Apia	Afiamalu	Nafanua	Alafua
Missing data	1%	2%	35%	13%

TEMPERATURE

The Samoan MNRE and the SAMET provided the daily minimum and maximum temperature in four stations: Apia, Afiamalu, Nafanua y Alafua from 1970 to 2020. Table 8 summarises the available information for each station. Figure 25 presents the monthly average minimum and maximum temperature.

Table 8. Minimum and maximum temperature missing data.

Station	Apia	Afiamalu	Nafanua	Alafua
Minimum Temperature	1%	13%	>50%	45%
Maximum Temperature	5%	23%	>50%	47%

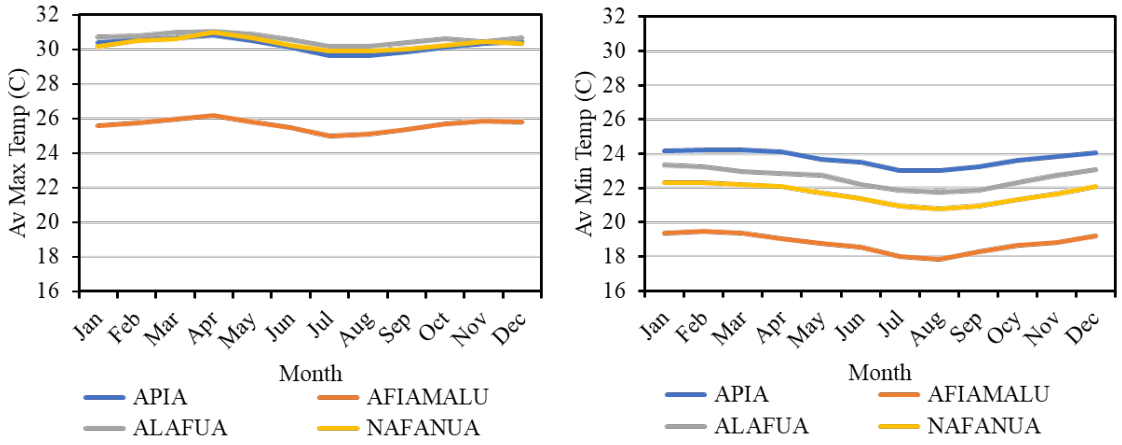

Figure 25. Monthly average temperature. Left: maximum temperatures. Right: minimum temperatures.

WIND SPEED

The daily data of wind speed was provided for Apia, Afiamalu, Nafanua and Alafua stations by the MNRE and SAMET for the period from 1970 to 2020. Table 9 shows the quality of the data and Figure 26 presents the annual average wind speed at Apia.

Table 9. Wind speed missing data.

Station	Apia	Afiamalu	Nafanua	Alafua
Missing data	1%	8%	40%	33%

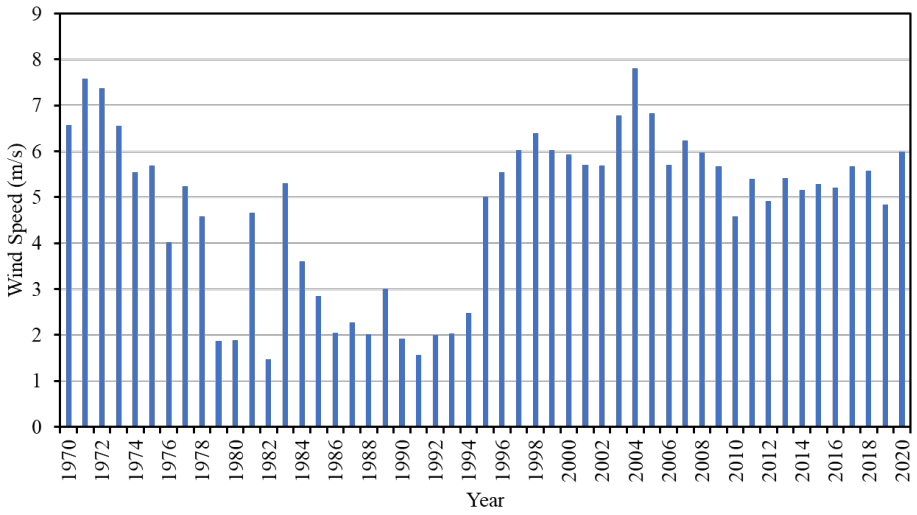

Figure 26. Annual average wind speed at Apia.

RELATIVE HUMIDITY

The relative humidity data from the mentioned meteorological network corresponds to Apia, Afiamalu, Nafanua and Alafua stations. The missing data at each station is summarised in Table 10, while Figure 27 depicts the average relative humidity at Afiamalu station.

Table 10. Relative humidity missing data.

Station	Apia	Afiamalu	Nafanua	Alafua
Missing data	1%	8%	40%	33%

SOLAR RADIATION

The MNRE and SAMET provided the daily net solar radiation at Afimalu Station, from July 2010 to December 2020. There was a 15% of missing data in the series. Figure 27 presents the monthly average net solar radiation and relative humidity at Afiamalu station.

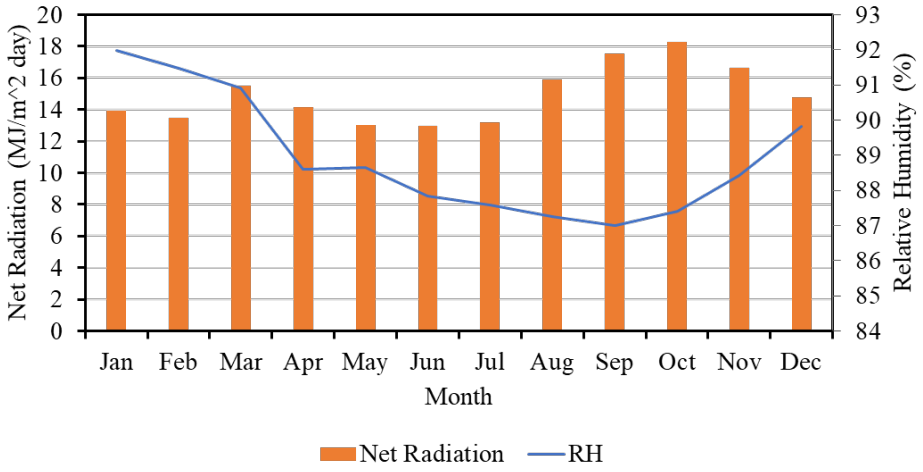

Figure 27. Average net radiation and Relative Humidity at Afiamalu.

WATER LEVELS

The MNRE data provided included three water level stations (Table 11 and Figure 28). The first two are located on the Fuluasou river catchment, while the third one is in the headwaters of the Vaisigano river (Alaoa East). The following analysis corresponds to the Alaoa East, as it is located in the area of interest.

Although intervals with an absence of data were not identified, there is an unusually high value in December 2012 coinciding with historic flooding (Cyclone Evan), and a noticeable difference in the patterns of water level variations after that point (Figure 29 and Figure 28). Filer et al. (2019) mentioned the water level sensor failed during cyclone Evan once the water level reached 5.5 m, and in 2018 during cyclone Gita. For modelling calibration purposes, the period from January 2012 to December 2017 was adopted, dismissing the week after cyclone Evan (December 2012).

Table 11. Available water level stations.

Station name	Type	Frequency	Period
Fuluasou West	Water level	15 minutes	21/09/2017- 10/02/2018
Fuluasou East		15 minutes	20/10/2017- 03/08/2021
Alaoa East		15 minutes	21/01/2009- 03/08/2021

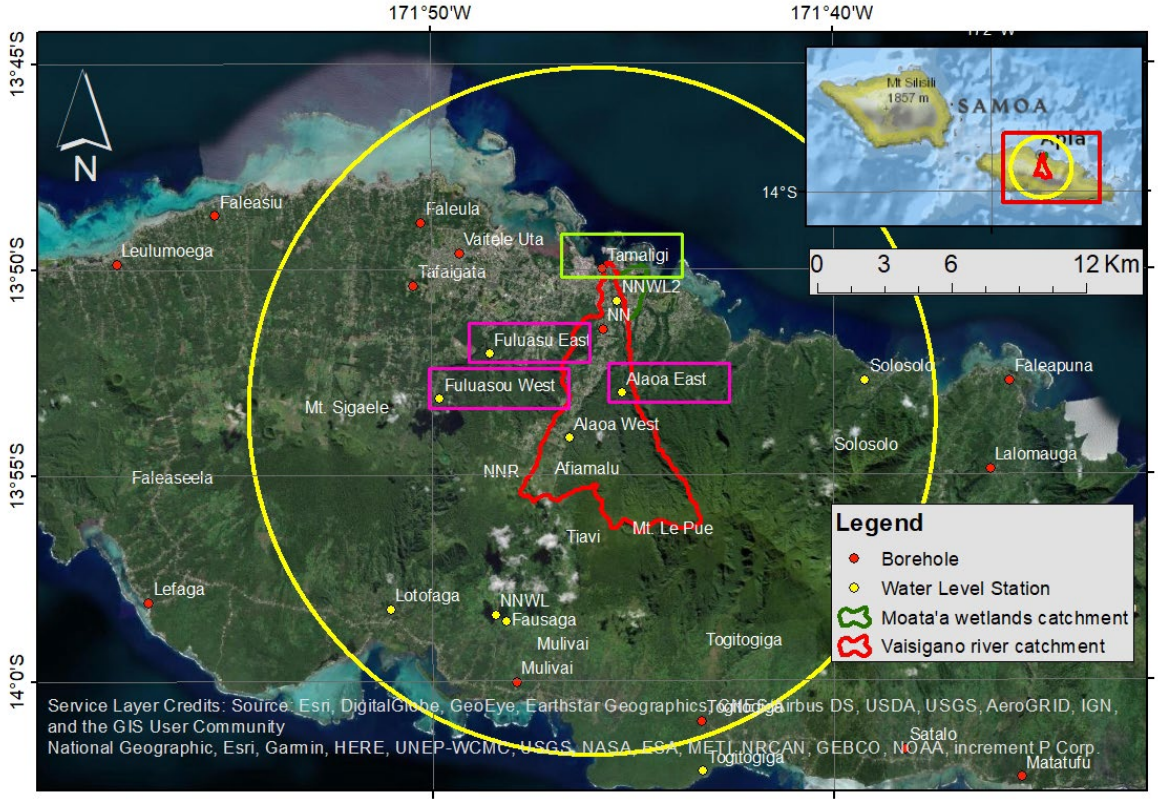

Figure 28. Water level and borehole stations. Pink box: Water level station, Green box: borehole monitoring point.

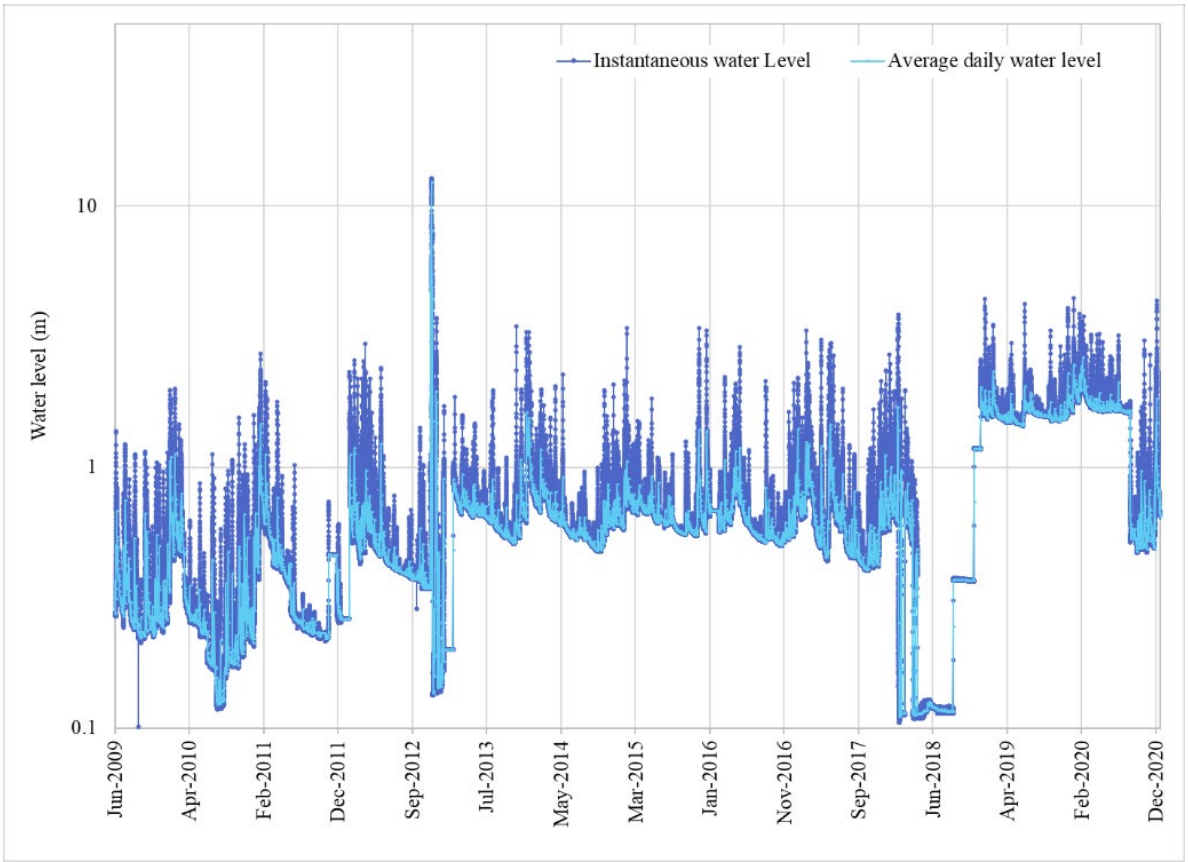

Figure 29. Instantaneous and average daily water levels at Aleoa East station.

GROUNDWATER LEVEL (BOREHOLES)

The Tamaligi station is near the mouth of the Vaisigano River, and has a 30-min. groundwater level record of 15 months with eight days missing (Table 12). A comparison was performed between the record from the borehole with the Alaoa East water levels and with the precipitation from the Afiamalu station (Figure 30). It can be seen that there is a strong correlation between the precipitation, surface water in the catchment and groundwater.

Table 12. Available groundwater level data.

Station name	Type	Frequency	Period	Missing data (days)	Network
Tamaligi	Monitoring boreholes	30 minutes	16/06/2017 - 03/10/2018	8	MNRE

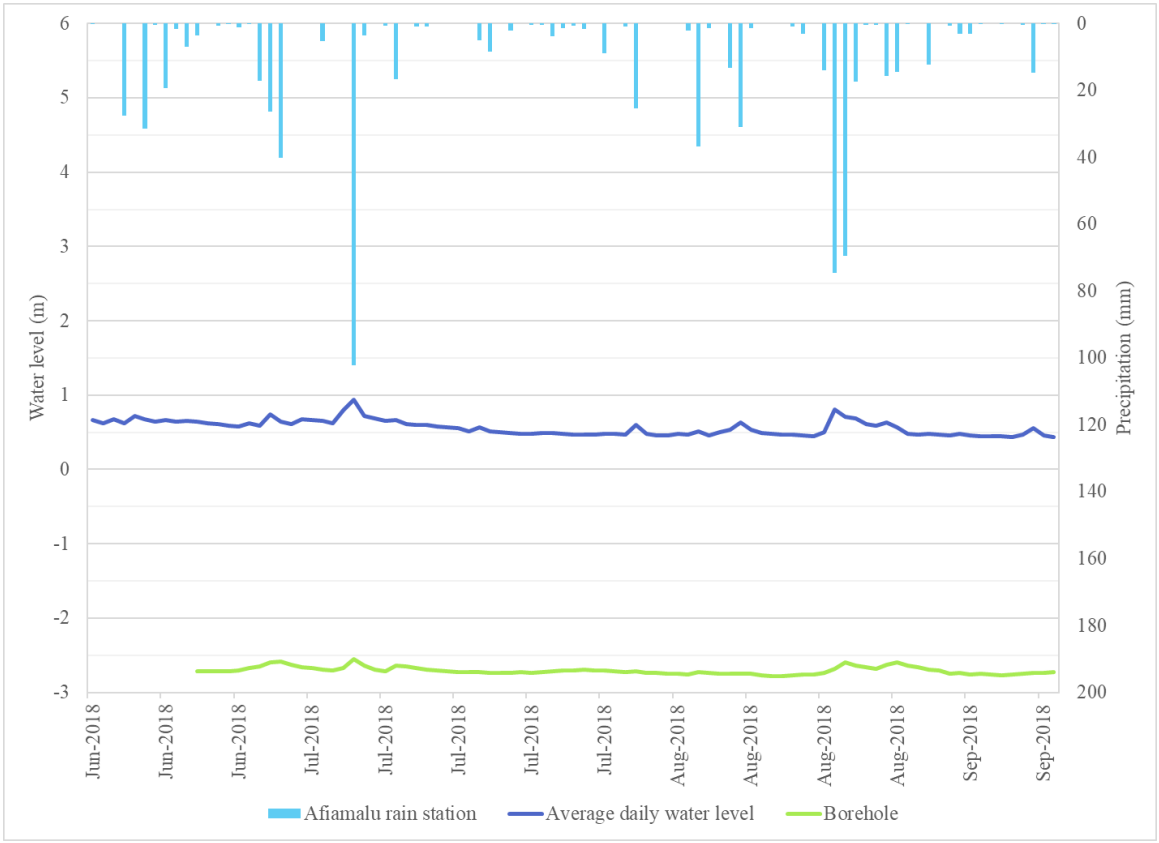

Figure 30. Water levels, precipitation and groundwater level (borehole).

SEDIMENT DATA

In the absence of ground information on sediment concentrations, satellite data available for the area from Landsat and Sentinel-2 was retrieved from the data portal of the USGS EROS Center (https://earthexplorer.usgs.gov/). The Case-2 Regional CoastColour (C2RCC) processor (Brockmann et al., 2016) was applied to the satellite images. The C2RCC is based on the Case 2 Regional processor, originally developed by Doerffer and Schiller (2007). It estimates the inherent optical properties (IOPs), such as absorption and scattering coefficients from the water leaving radiance reflectance measured at the top of the atmosphere. With those values, it calculates the concentrations of optically active substances such as total suspended matter and chlorophyll a, among others. C2RCC has been validated in numerous studies for the different sensors with reliable results for Case-2 water (Brockmann et al., 2016, Nazirova et al., 2021). It is available through ESA's Sentinel toolbox SNAP (https://step.esa.int/). Only images with less than 20% cloud cover were selected for the analysis, which resulted in 168 images (Table 13).

Table 13. Information available in the area with a cloud cover under 20%.

Mission	From	To	Quantity
Sentinel-2 A and B	02/12/2015	18/06/2022	154 images
Landsat 8	13/07/2013	19/05/2022	14 images

TIDAL REGIME RECORDS

The hourly sea level and meteorological data from 1993 to 2021 (http://www.bom.gov.au/pacific/samoa/index.shtml) was retrieved from the Australian Bureau of Meteorology. The daily averaged sea level data is shown in Figure 31, where it can be seen that the sea level has risen 200 mm in the last 30 years, with a rate of 6.7 mm/year. This value is about three times the previous estimates of 2 mm/year by Russell (2011).

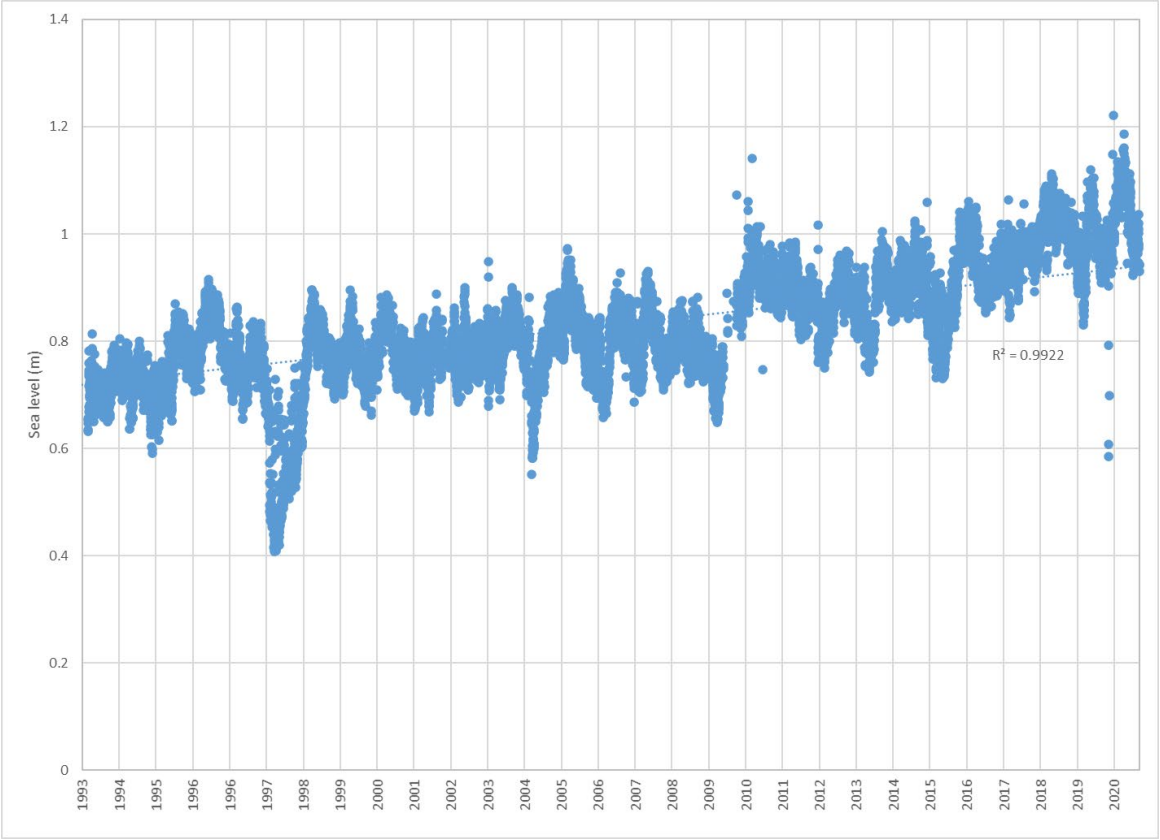

Figure 31. Daily average see level in Samoa (Apia).

TROPICAL CYCLONES

As mentioned before, Samoa is an area frequently affected by tropical cyclones and tropical depressions (TCs). Since 1970 there have been more than 23 Cyclones

passing directly though Samoa. Table 14 shows the dates and the names of the strongest cyclones on record.

Table 14. Cyclones Affecting Samoa (Extended from Terry et al., 2006).

Date	Name
11-25 Feb 1970	Dolly
31 Jan - 7 Feb 1973	Elenore
29 Jan 5 Feb 1975	Val
11-12 Dec 1976	Laurie
9-13 Dec 1976	Kim
17-24 Mar 1981	Fran
4-8 Feb 1987	Uma
22-26 Apr 1987	Zuman
2-9 Jan 1989	Fili
6-9 Jan 1989	Gina
30 Jan 10 Feb 1990	Ofa
4-16 Dec 1991	Val
29 Dec 1992 – 5 Jan 1993	Nina
31 Jan - 4 Feb 1993	Lin
13-19 Jan 1997	Evan
2-6 Jan 1998	Ron
26-28 Jan 1998	Tui
25 Dec 2003 – 8 Jan 2004	Heta
10-25 Feb 2004	Olaf
19-30 Jan 2011	Wilma
9-27 Dec 2012	Evan
13-25 Apr 2016	Amos
3-22 Feb 2018	Gita

Nevertheless, there are other multiple TC not passing directly over Samoa, but that affect the precipitation and sediment export in the island. To quantify the impact of TC data from the Southwest Pacific Enhanced Archive of Tropical Cyclones, SPEArTC (Diamond et al., 2012) was used. SPEArTC has been acknowledged as the most complete repository for this area (Magee et al., 2016, Sharma et al., 2020). The database records at 6-hourly intervals the coordinates and central pressures of each cyclone and tropical depression throughout its life since 1840 (noting that TC data post-mid-1940s is more reliable/complete and the earlier data must be used with caution).

It was considered that cyclones' tracks that were within 5º of the centre of the catchment (13.9ºS, 171.75ºW – Figure 32), could potentially affect the catchment. Several authors have used this approach to relate the impact of TCs on extreme precipitation events (Dare et al., 2012, Deo et al., 2021, Khouakhi et al., 2017, Villarini and Denniston, 2016). The analysis period was from 1970 to 2017.

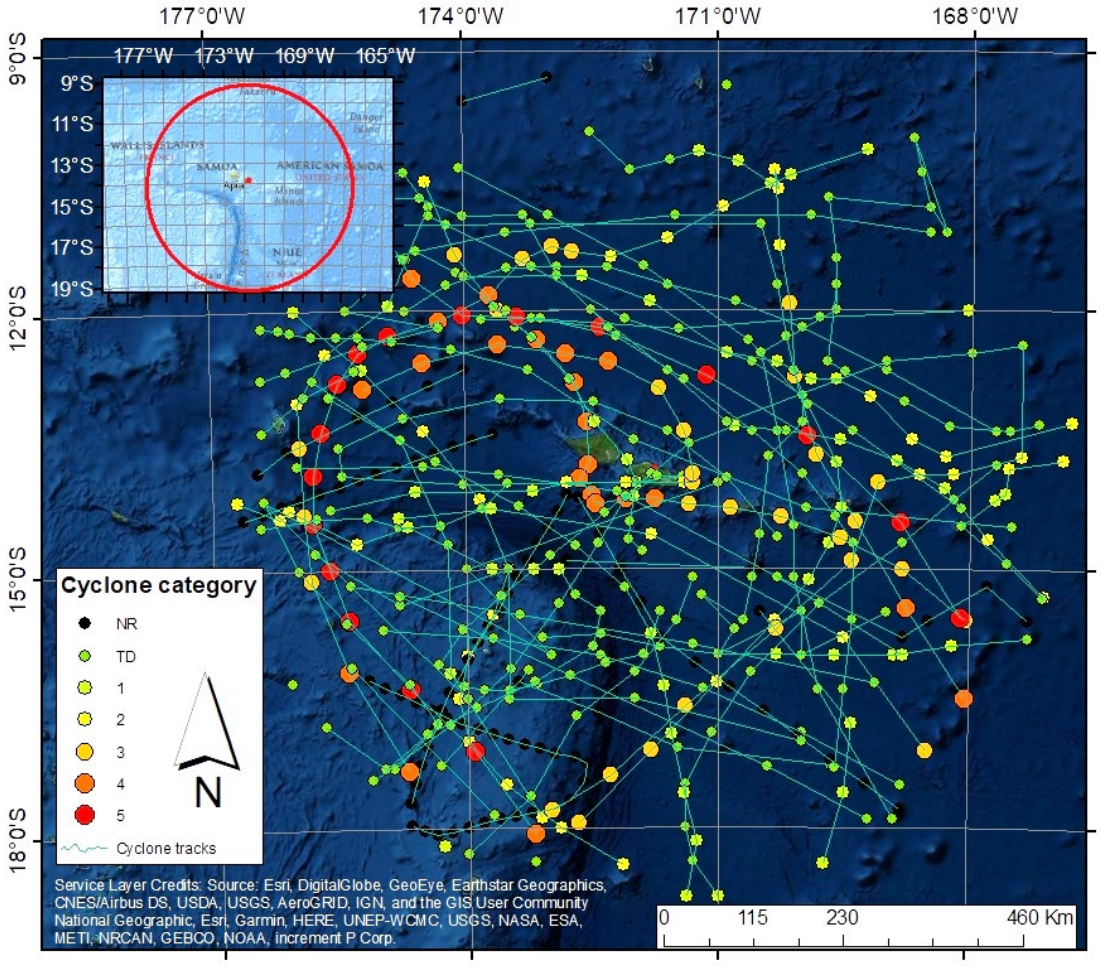

Figure 32. Trajectories of cyclones within 5º of the centre of Moata'a catchment from 1970 to 2017.

It was found that, on average, 1.125 tropical cyclones and depressions affect the area per season. Figure 33 shows the number of cyclones per season and category of the cyclone. The category classification was done following the Australian Bureau of Meteorology definition (Table 15). The duration of the cyclone varies from 1 to 8 days, lasting on average 3.14 days.

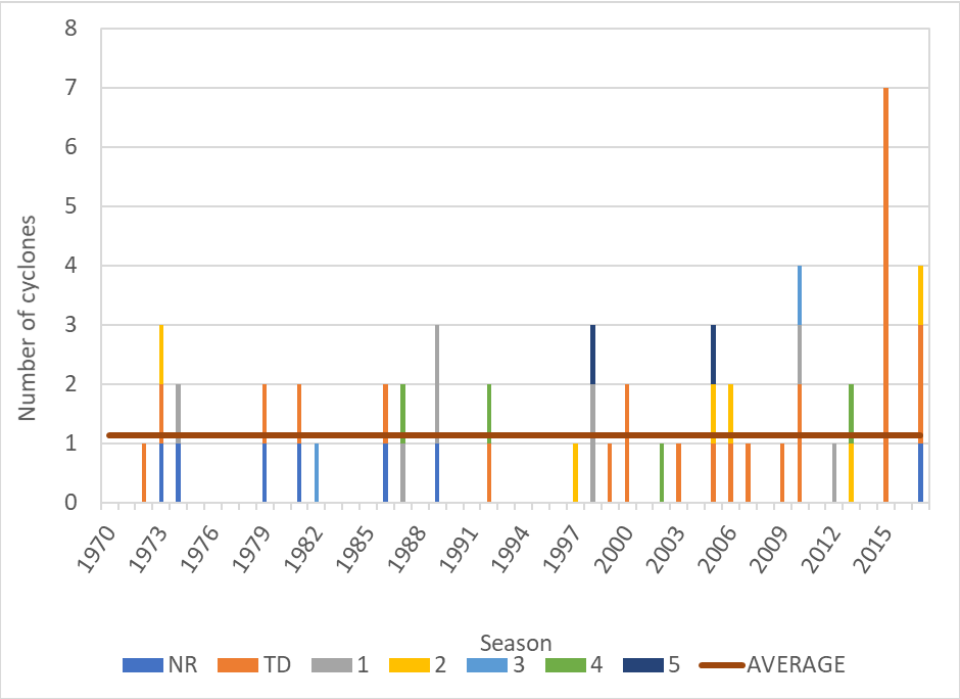

Figure 33. Distribution of the number of cyclones per year and separated by cyclone category (1-5) including non-rated (NR) and Tropical Depressions (TD)

Table 15. Tropical Cyclone category explanation (http://www.bom.gov.au/cyclone/tropical-cyclone-knowledge-centre/understanding/tc-info/.)

Category	Maximum Mean Wind (km/h)	Typical Strongest Gust (km/h)	Typical Effects
1	63 - 88	< 125	Damaging winds. Negligible house damage. Damage to some crops, trees and caravans. Craft may drag moorings.
2	89 - 117	125 - 164	Destructive winds. Minor house damage. Significant damage to signs, trees and caravans. Heavy damage to some crops. Risk of power failure.
3	118 - 159	165 - 224	Very destructive winds. Some roof and structural damage. Some caravans were destroyed. Power failures likely. (e.g., Clare, Olwyn)
4	160 - 199	225 - 279	Significant roofing loss and structural damage. Many caravans were destroyed and blown away. Dangerous airborne debris. Widespread power failures. (e.g., Tracy, Debbie, Lam)
5	> 200	> 279	Extremely dangerous with widespread destruction. (e.g., Vance, Marcia, Yasi)

METHODOLOGY

The methodology is divided into three components (Figure 34). The first component includes modelling the Vaisigano and Moata'a catchments to determine the amount of water and sediments that enter the mangrove area. The second component consists of the eco-geomorphological modelling of the mangrove wetland to evaluate the mangrove response under different conditions. Finally, the resilience assessment is conducted by analysing the response of the Moata'a mangrove under different future scenarios.

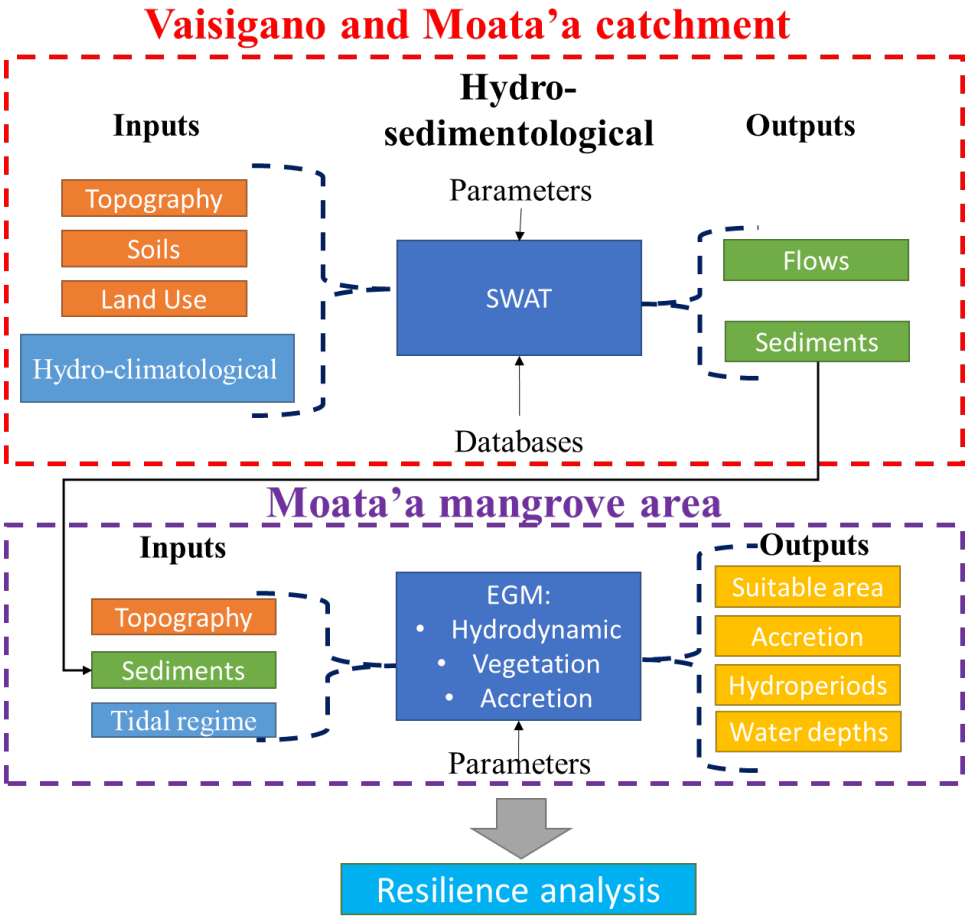

Figure 34. Moata'a mangrove resilience analysis methodology.

HYDRO-SEDIMENTOLOGICAL MODEL (HSM)

In this section, we describe the Soil and Water Assessment Tool (SWAT) model used for the hydro-sedimentological assessment of the Moata'a mangroves catchment. SWAT was selected as it has been widely tested for estimating the

impacts of land use changes, climate change and/or land management practices on soil erosion (Hajigholizadeh et al., 2018). The model is freely available (https://swat.tamu.edu/) and allows the estimation of water and sediments exports in a catchment (Briak et al., 2016) on a continuous basis.

The sediment erosion, transport and deposition processes modelled are complex and depend on the climatologic, topographic, soils and land use conditions present in the catchment. SWAT is a physically based model that simulates flow, sediment/soil erosion and water quality (optional) outputs at a range of temporal scales (daily, monthly or annual). The user of the model must determine the parameters that best suit the conditions of the study site and can base the decision on values found in other studies, measurements or databases available within the SWAT software package. Figure 35 shows the SWAT model conceptualization.

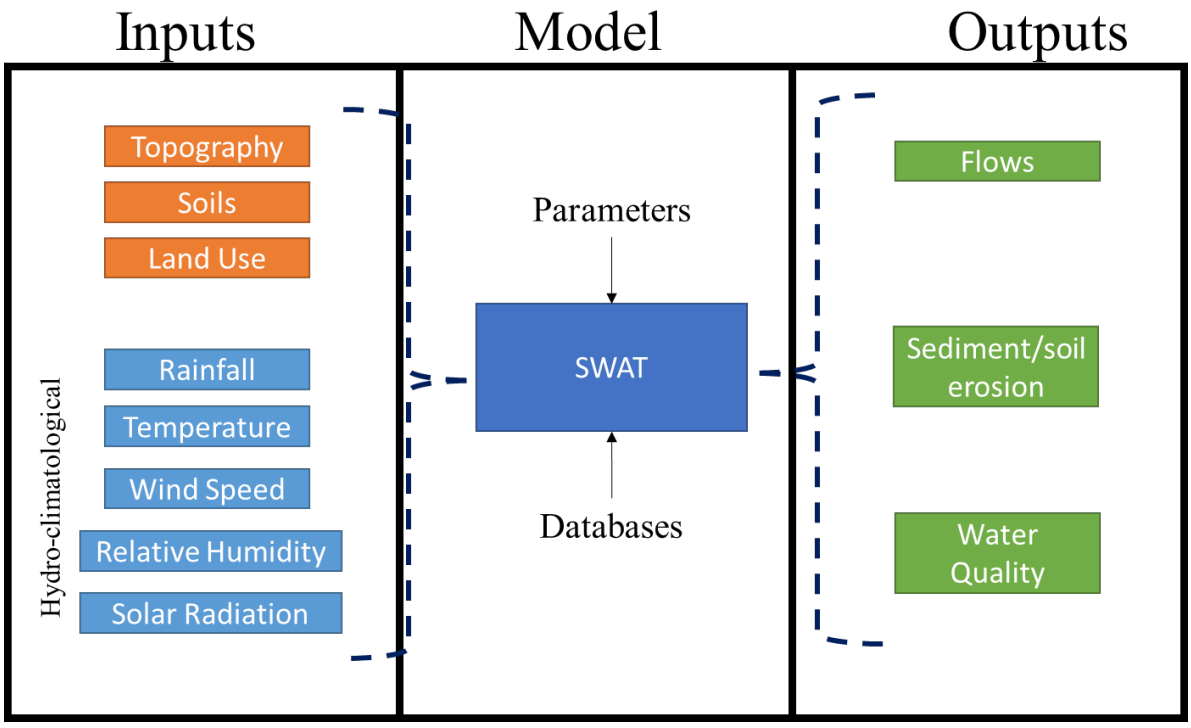

Figure 35. SWAT model conceptualization.

The SWAT model includes a climate-hydrology module to determine the fraction of the rainwater contributing to runoff, infiltration, evaporation, soil moisture and groundwater. The hydrological balance equation is solved in each Hydrological Response Unit (HRU) to estimate the runoff that will reach the channel network

(Arnold et al., 1998). The hydrological balance equation is expressed in mm as (Arnold et al., 1998):

$$SW_t = SW_o + R_i - R_{off,i} - ET_{a,i} - W_s - Q_{gw} \qquad 1$$

where, SW_t and SW_o are the soil water content at day t and at the initial time, respectively, R_i is the precipitation, R_{off} is the surface runoff, ET is the actual evapotranspiration, W_s is the flow entering the vadose zone and Q_{gw} is the groundwater flow.

The amount of surface runoff is then routed through the channel network. The model uses the Muskingum routing or a variable storage coefficient method to route the flow. This water routing module determines the amount of transported of sediments, nutrients, and pollutants.

The quantity of sediments generated per unit of time are obtained using the MUSLE equation (Williams and Berndt, 1977) applied to each HRU:

$$y = 11.8(Qq_p)^{0.56} KCSLP \qquad 2$$

where, y is the sediment yield, Q is the runoff volume, q_p is the peak runoff rate, K is the soil erodibility factor, C is the crop management factor, S and L are the slope length-gradient factors and P is the erosion control practice (Williams and Berndt, 1977).

SWAT requires inputs of meteorologic, topography, soil type and land use data. Climatic inputs include rainfall, temperature, wind speed, relative humidity and solar radiation, and are used to drive the hydrological process. The topography, soil type and land use data are input as maps covering the extension of the catchment. The topography is entered as a raster file (Digital Elevation Model - DEM), while soil type and land use can be entered as shape or raster files. The spatial data is used to divide the area into sub-catchments and HRUs (Neitsch et al., 2011). HRU are areas of similar land uses, soils, and slopes which are defined based on user-defined thresholds.

Additionally, the user needs to define the parameters that best suit the conditions of the study case. SWAT has on-board pre-defined databases of land cover,

plant growth, tillage, pesticides, fertilizers, and urban land types that can be used to set the parameters of the model. However, the user is free to set values outside the ones found in the databases, based on experience or other studies.

ECO-GEOMORPHOLOGICAL MODELLING (EGM)

The eco-geomorphological modelling framework adopted in this work to study the response of the Moata'a mangrove to sea-level rise was developed and implemented by Rodriguez et al. (2017), Sandi et al. (2018), and Breda et al. (2021). The framework combines hydrodynamic, vegetation and sedimentation/accretion models which are explained in the next subsections.

HYDRODYNAMIC MODULE

The hydrodynamic model calculates the distribution of water levels and velocities over the simulation domain using a scheme of cells originally proposed by Cunge and developed by Riccardi (2000) (Cunge 1975; cited by Riccardi, 2000). The model solves the simplified Saint-Venant equations of mass and momentum for shallow water on a rectangular cell-grid.

The conservation of mass for each cell is expressed in the model as (Riccardi, 2000):

$$S_i \frac{dz_i}{dt} = \sum_{k=1}^{j} Q_{k,i} \qquad 3$$

where, S_i is the cell area i, z_i is the water depth and $Q_{k,i}$ is the flow between neighboring cells. The discharge flow between cells is based on the conservations of momentum equation and depends on the water surface gradient, gravity, hydrostatic pressure, and friction forces. The system of equations is numerically solved using a Gauss-Seidel iteration method (Riccardi, 2000) and the parameters of the model are the roughness coefficients. The hydrodynamic model allows the calculation of the mean water depth below high tide and the percentage of days per year that the cell is inundated (denominated as hydroperiod), which are used for the calculation of the vegetation (mangrove) growth.

VEGETATION MODULE

The mangrove biomass on the simulation domain grows depending on the mean depth below high tide (D) and is calculated in each cell as:

$$B = aD + bD^2 + c \qquad 4$$

where, a, b, and c, are empirical coefficients. The establishment of mangrove in a cell is based on the hydroperiod (H) and mean depth below high tide (D). The thresholds of H and D to determine the mangrove survival vary according to the mangrove species (D'Alpaos et al., 2007, Lovelock et al., 2015, Saco and Rodríguez, 2013). This study adopted a minimum D of 20 cm and a H equal or lower than 0.5, which are recommended for the *Rhizophora samoensis* and *Bruguiera gymnorrhiza* species. These two threshold values are compared with the tidal values estimated from the water levels calculated by the hydrodynamic model and used to determine if the hydrodynamic conditions are suitable for mangrove establishment.

The mangroves generated in the vegetation model affects the surface roughness of the hydrodynamic module. When the mangrove establishes in the cell, the roughness coefficient increases to 0.4, compared to 0.035 for channels and 0.12 for other vegetation and grass land.

SEDIMENTATION/ACCRETION MODULE

The mangroves trap sediments and transfer biomass to the soil increasing the soil surface elevation. This process is denominated bio-geomorphic accretion and is calculated following Rodriguez et al. (2017). The equation used to calculate the change in surface elevation in the marshes depends on the concentration of sediments in the water, the biomass of mangroves and the mean depth below high tide:

$$\frac{dE}{dt} = C(q + kB)D \qquad 5$$

where, E is the surface elevation, C is the suspended sediment concentration, B is the aboveground biomass, D is the mean depth below high tide, k is the trapping efficiency coefficient and q is a depositional parameter. The values of the parameters q and k are a function of the vegetation and sediment characteristics,

while the suspended sediment concentration C is spatially variable depending on the input maximum concentration and D (Rodriguez et al., 2017).

EGM INPUT DATA AND OUTPUT DATA

The eco-geomorphological model requires three main inputs: temporal series of tide elevations, a digital elevation model (DEM) of the study area and a series of sediment concentration that enter to the domain. With the three inputs, the model executes the hydrodynamics, vegetation and sedimentation/accretion model and provides outputs of area that is suitable for mangrove establishment and values of accretion, hydroperiods and water depths.

HYDRO-SEDIMENTOLOGICAL ASSESSMENT OF THE CATCHMENT

VAISIGANO RIVER CATCHMENT

This section describes the application of the SWAT model to the Vaisigano river catchment. The objective of the modelling was to calculate the amount of water and sediments transferred to Moata'a mangroves during extreme events. First, the input data used to drive the processes in the model are described. Second, the calibration of the model using data from the Alaoa East gauging station is presented. Finally, the procedure to generate the flows and sediments to be used in the Moata'a catchment is explained.

INPUT DATA AND MODEL SETUP

- *Climatological data*

Climatological data was obtained from the Samoan MNRE and the SAMET. For the Vaisigano river catchment four nearby stations are available, with a record period from 01/01/1970 to 31/12/2020: Afiamalu, Nafanua, Alafua and Apia (Figure 23). The four stations have precipitation, maximum and minimum air temperature, and relative humidity daily data. The solar radiation daily data corresponds to Afiamalu station, from 02/07/2010 - 31/12/2020. Table 16 summarises the available data for the catchment.

The data required for the hydrological modelling included daily precipitation, temperature, relative humidity, wind speed and solar radiation. SWAT runs using daily meteorological data but accepts lower temporal resolution data that is disaggregated using an onboard weather generator. The criterion for data selection was to use daily data when the amount of missing data was small enough so that a gap filling procedure based on the correlation between stations could be used. When the data gaps were too important, the monthly data was used jointly with the weather generator. Based on these analyses and the quality of our data (Table 16), the modelling was conducted using daily data of precipitation from the four stations, daily temperature, wind speed and relative humidity only from Afiamalu and Apia stations, and monthly solar radiation from Afiamalu station.

Table 16. Available information for hydro-sedimentological modelling.

Station	Available periods and missing data				
	Rainfall	Maximum & minimum T°	Solar radiation	Wind Speed	Relative Humidity
Afiamalu	1970 - 2020	1970 - 2020	2010 – 2020	1970 – 2020	1970 – 2020
	2%	23% Tmax - 13% Tmin	15%	8%	8%
Alafua	1970 - 2020	1970 - 2020	-	1970 - 2020	1970 - 2020
	13%	45% Tmax - 47% Tmin	-	37%	40%
Nafanua	1970 – 2020	1970 - 2020	-	1970 - 2020	1970 - 2020
	35%	>50% Tmax- >50% Tmin	-	33%	33%
Apia	1970 - 2020	1970 - 2020	-	1970 - 2020	1970 - 2020
	1%	5% Tmax -1% Tmin	-	1%	1%

- *Topography*

A 30 x 30m Digital Elevation Model (DEM) from the Shuttle Radar Topography Mission (SRTM DEM) (https://www2.jpl.nasa.gov/srtm/dataprod.htm) was used (Figure 36). It was retrieved from USGS EROS Center (https://earthexplorer.usgs.gov/).

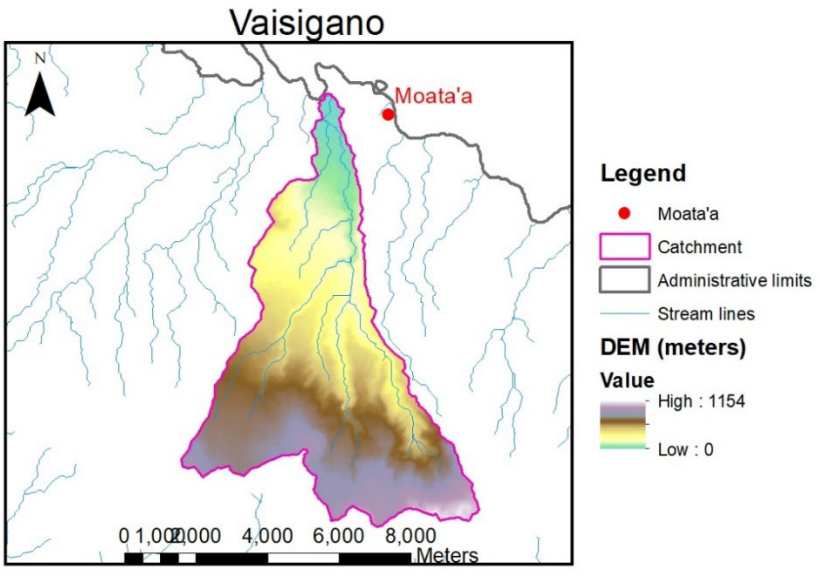

Figure 36. Vaisigano river catchment topography.

- *Soil type*

The soil type layer was retrieved from the Harmonized World Soil Database (HWSD) developed by the Food and Agriculture Organization (FAO) of the United Nations (UN) and the UN Educational, Scientific and Cultural Organization (UNESCO) published and updated since 1981 (Sanchez et al., 2009). This digital layer is low resolution (1:5000000), but the information related to each soil Mapping Unit was useful to determine soil properties like texture, slope classes, depth of profile and composition, among other characteristics. Furthermore, the classification was compatible with SWAT database for soil properties, which is based on the FAO/UNESCO soil types. There are two dominant soils in the catchment: Eutric Cambisols and Ferralic Cambisols. These types of soils have uniform medium-textured profiles, with organic surface horizons overlying reddish or brownish subsoils. It is a moderate well drained soil with high content of clay (FAO, 1978).

- *Land use data*

The different land uses in the catchment were identified and digitised from the land use map presented by the Samoa – City Development Strategy (UN-Habitat, 2015). Afterwards, they were classified according to the land use type set for model purposes into agriculture, forest, urban high density, and urban low density (Figure 37).

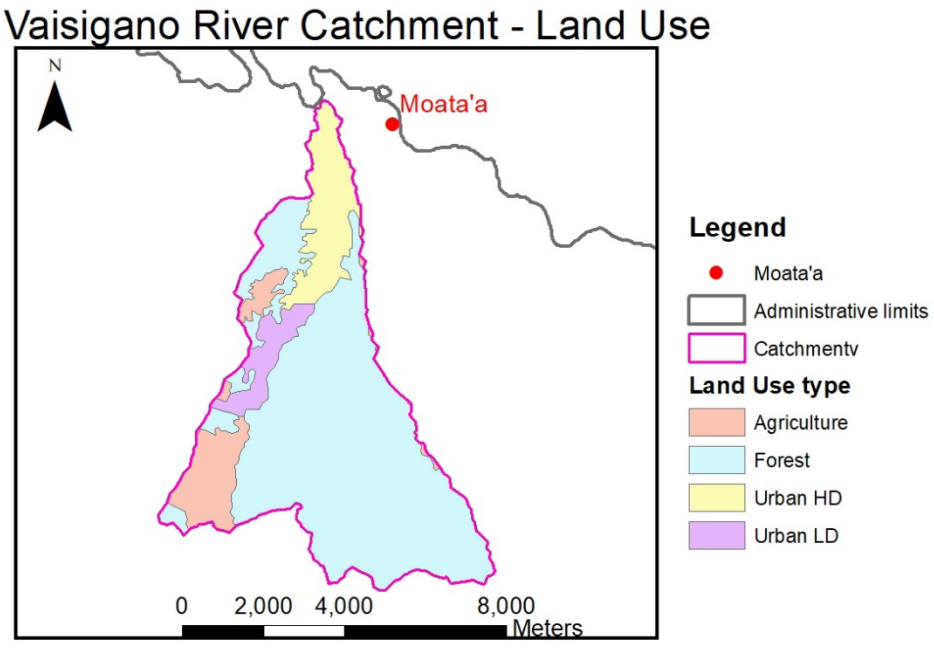

Figure 37. Vaisigano river catchment land use.

The catchment was delineated based on the topography with a flow accumulation threshold of 50 ha. Eleven subcatchments were obtained, representing the drainage network reported in previous works (Filer et al., 2019, Williams et al., 2021). The outlet of the catchment was set 300 m upstream of the Lelata bridge in order to ensure that tidal effect were not affecting the outlet and that all the flow was contained within the river cross section and not in the floodplain. After the catchment delineation, the subcatchments were split into 94 HRUs based on the overlaying of land use, soil type and slope classes (Figure 38). The model was setup to run daily from 1970 to 2020s.

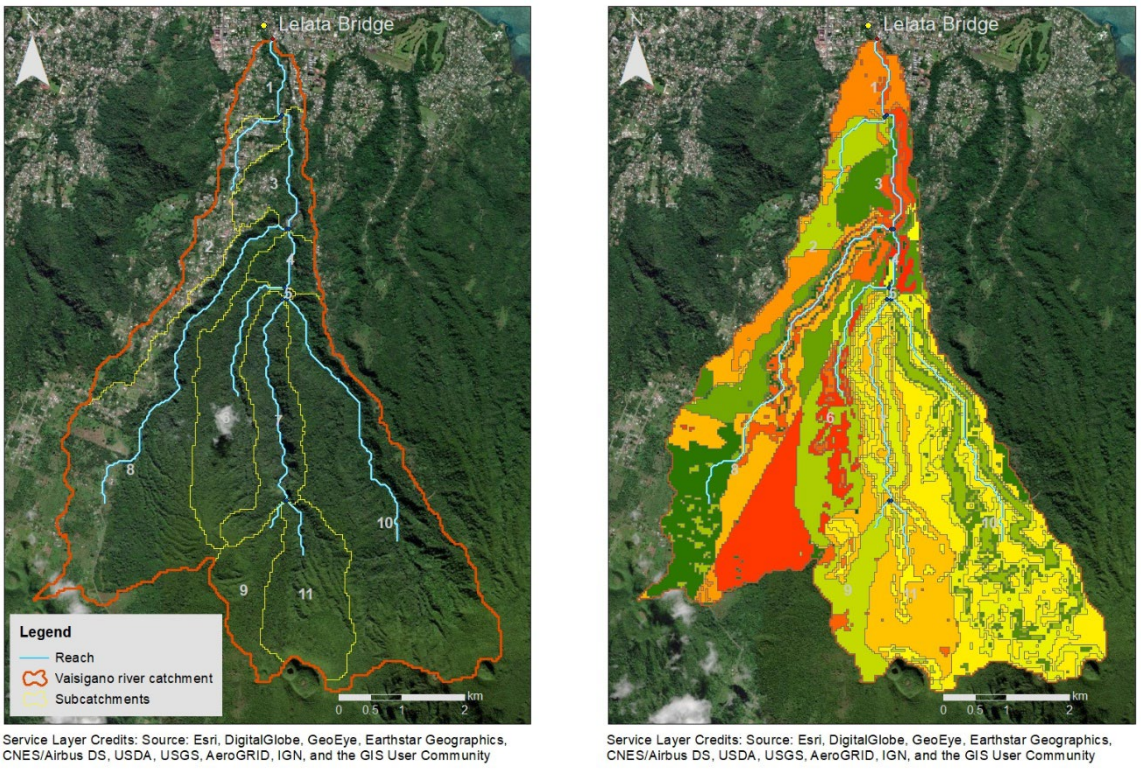

Figure 38. Spatial discretisation of the catchment for the hydrological model. Left: Subcatchments. Right: HRUs

The calibration was performed using data from water level of the Vaisigano river (Alaoa East) gauging station (Table 11) provided by the MNRE and the rating curved presented in Williams et al. (2021) to transform the water levels into discharges. Following Filer et al. (2019), the data from 2012 to 2018 was used to calibrate the model.

Most of the parameters in SWAT have a physical meaning (Arnold et al., 1998), so a manual calibration was performed by modifying the parameters related to surface flow and base flow. Regarding the sediment process, only the support practice factor for natural areas were changed (eg. Forest, (Benavidez et al., 2018, Li et al., 2014)). Table 17 summarises the adopted values and the range of parameters suggested by the bibliography. It can be seen in the table that the calibrated parameters are well within the suggested range of values.

Table 17. SWAT calibrated parameters

	Parameter	Description	Range	Influencing factor	References	Adopted value
Surface Runoff	CN2	Curve number at moisture condition II	30 - 98	(calibrated) land use, soil and slope	(Neitsch et al., 2011)	Average catchment 52.4
	CH_N2	Channel Manning's roughness coefficient	0 - 0.67	(calibrated) channel bed and banks characteristics	(Briak et al., 2016, Filer et al., 2019, Vilaysane et al., 2015)	Channel: 0.04
	OV_N	Manning's roughness coefficient for overland flow	0.1 - 12	(calibrated) land use and vegetative cover	(Ricci et al., 2018, Filer et al., 2019)	Agriculture: 0.14; Urban: 0.1, Forest: 0.8
Base flow	ALPHA_BF	Baseflow recession constant	0 - 1	(calibrated) Soil type	(Neitsch et al., 2011)	0.000005
	GWQMN	Threshold water level in the shallow aquifer	0 - 5000 mm	(calibrated) Soil type	(Neitsch et al., 2011)	0
Sediment	USLE_P	Support practice factor	0 - 1	management practice	(Benavidez et al., 2018, Li et al., 2014)	Natural areas: 0.5; Agriculture: 1

Figure 39 shows the comparison of the monthly average simulated and observed flow at Alaoa East River gauge. There is a good correlation between the flows, and the relation between the observed and simulated accumulated water volume for the entire period is equal to 1.03, which is considered a good fit (Filer et al., 2019).

The metrics used to evaluate the performance of the model were the Nash-Sutcliffe efficiency (NSE), percent bias (PBIAS), the root mean square error to the standard deviation of measured data (RSR), and the correlation coefficient R^2. Following Moriasi et al. (2007), our model performed very good according to the PBIAS indicator and good for all the other metrics (Table 18).

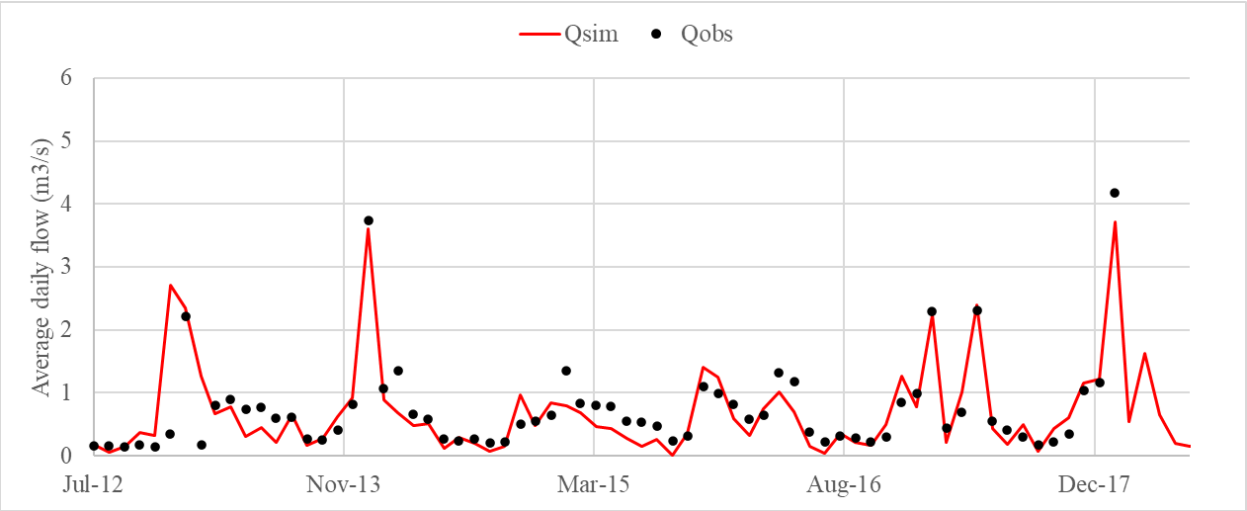

Figure 39. Simulated and observed flows at Alaoa East River gauge.

Table 18. Performance indicators at Alaoa East River gauge.

Metric	Value	Rating
R^2	0.741	Good
NSE	0.710	Good
PBIAS	-2.6%	Very good
RSR	0.538	Good

VAISIGANO RIVER CATCHMENT HSM RESULTS

Once the model was calibrated, simulations were conducted for the period 1970-2020 and the model results at the outlet of the catchment (Lelata bridge) were used to estimate the flow and sediment inputs from the Vaisigano into the Moata'a catchment due to the flow transfer during floods. According to Filer et al. (2019) the lower-lying areas around the lower floodplain get flooded at least once per year during the wet season. Statistical analysis of the flows at the outlet (see for example ARR (2016)) showed that the daily average discharge of 19.8 m^3/s has an average recurrence interval of one year. It was assumed that all the discharges equal or greater than this threshold would overflow, and that a 10% of the Vaisigano discharge would transfer to the Moata'a catchment. The concentration of sediments of the transferred discharge was assumed to be equal to the concentration at the outlet of the catchment (Figure 40). A total of 88 events over 51 years resulted in overflows to the Moata'a catchment.

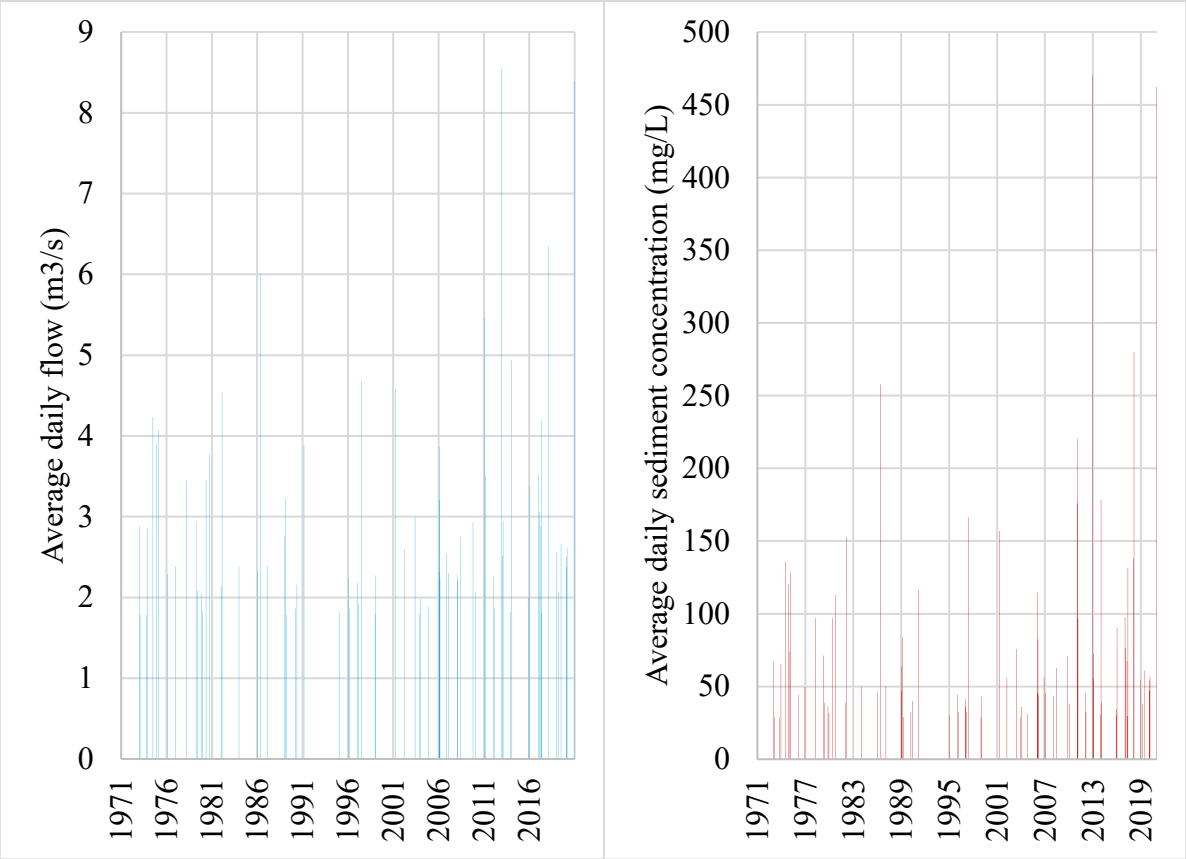

Figure 40. Flow and sediment transfer from the Vaisigano river catchment to the Moata'a catchment

HSM MOATA'A CATCHMENT

This section presents the SWAT model for Moata'a catchment. The objective of the modelling was to calculate the amount of water and sediments being delivered to the Moata'a mangrove area. These values are the inputs for the modelling of the ecological response of the Moata'a mangroves to be presented later in the report. The first subsection of this section describes input data used in the model. The second subsection presents the flows and sediments delivered to the Moata'a mangrove area.

INPUT DATA AND MODEL SETUP

Because the Moata'a catchment is part of the lower floodplain of the Vaisigano river catchment, similar type of information used for the Vaisigano catchment was used but limited to the area of influence of the Moata'a catchment. Figure 41 presents topographic data, while Figure 42 shows the land use of the catchment. In the case of the meteorological data, only Nafanua and Apia stations were considered,

because of the location of the catchment and the proximity of the stations (Figure 23).

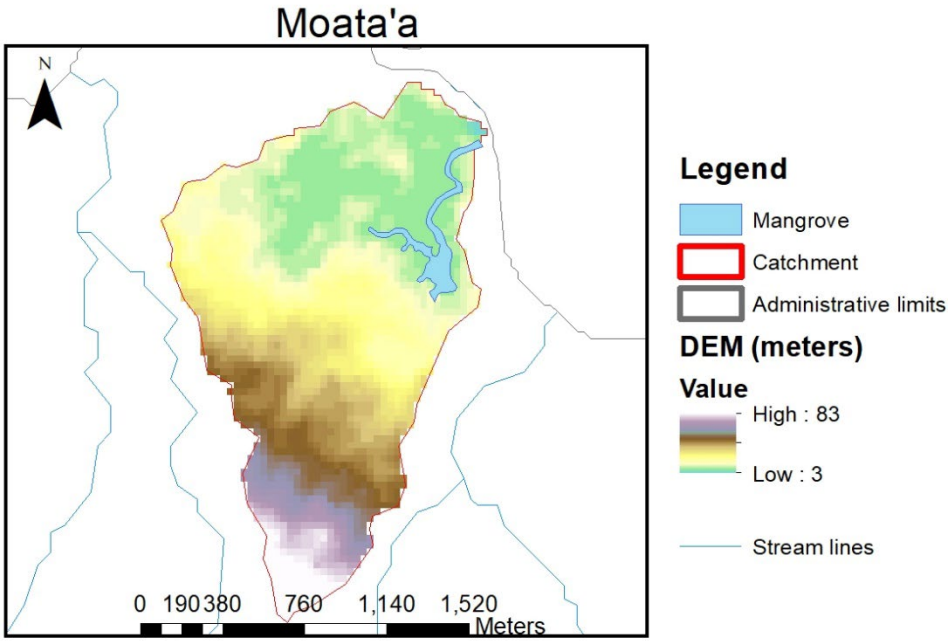

Figure 41. Moata’a catchment topography.

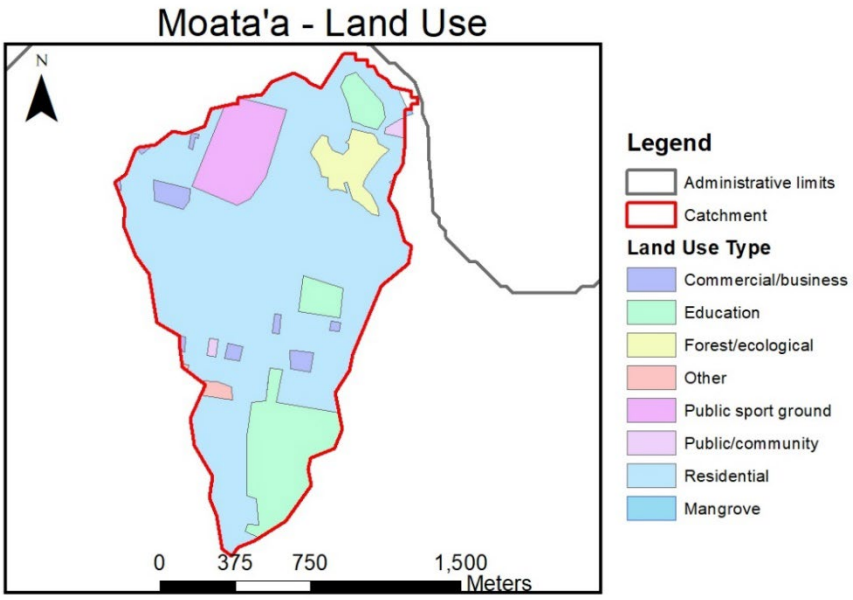

Figure 42. Moata’a catchment land use.

The setup of the model based on topography, soil type and land use, consisted of two subcatchments and sixteen HRUs. For modelling purposes, the land use was re-classified into five categories: residential, commercial, institutional, urban low density and wetlands (Figure 43). The overflow outputs from the Vaisigano river

catchment were added as an input into the northern subcatchment (subcatchment 1 - Figure 43). The calibrated parameters of the Vaisigano river were used to run the model.

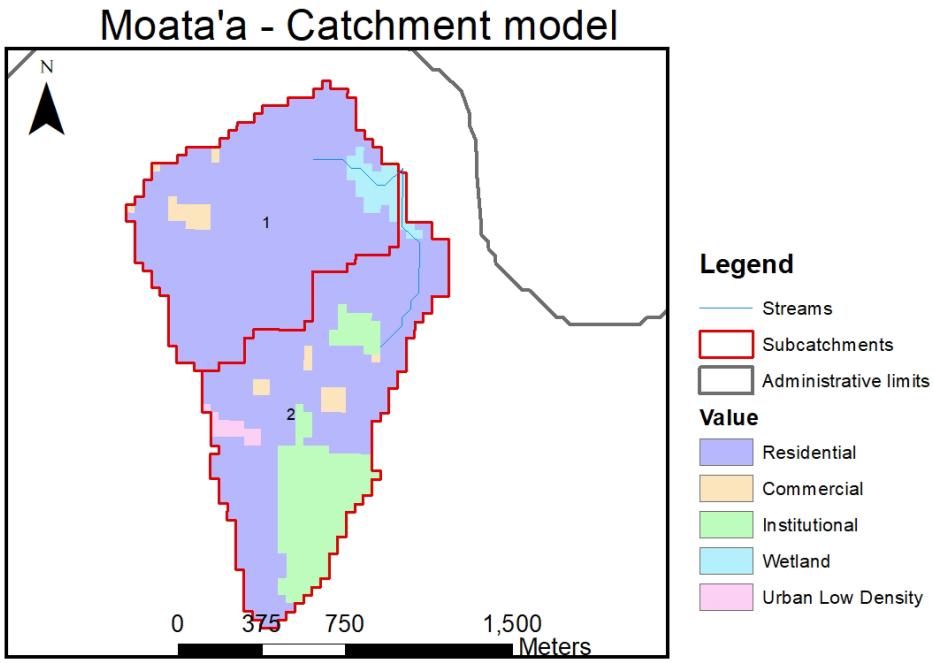

Figure 43. Moata'a catchment and land uses for modelling purposes.

MOATA'A CATCHMENT HSM RESULTS

To determine the input of sediments and water to the Moata'a mangrove, the SWAT model was run on a daily time scale from 1970 to 2020 and included the transfer flows from the Vaisigano catchment. The outputs from the two subcatchments draining into the wetland were aggregated into a single value for analysis purposes. Flows and total sediment from subcatchment 1 and 2 were added and then an overall sediment concentration was calculated. Figure 44 shows 30 years of average daily sediment concentration, where a pulsed behaviour with peaks up to 200 mg/L can be observed. However, those peaks are short-lived and are heavily reduced when the data is presented in terms of average monthly data, as shown in Figure 45. Figure 45 also shows that January-April is the period with higher sediment concentrations.

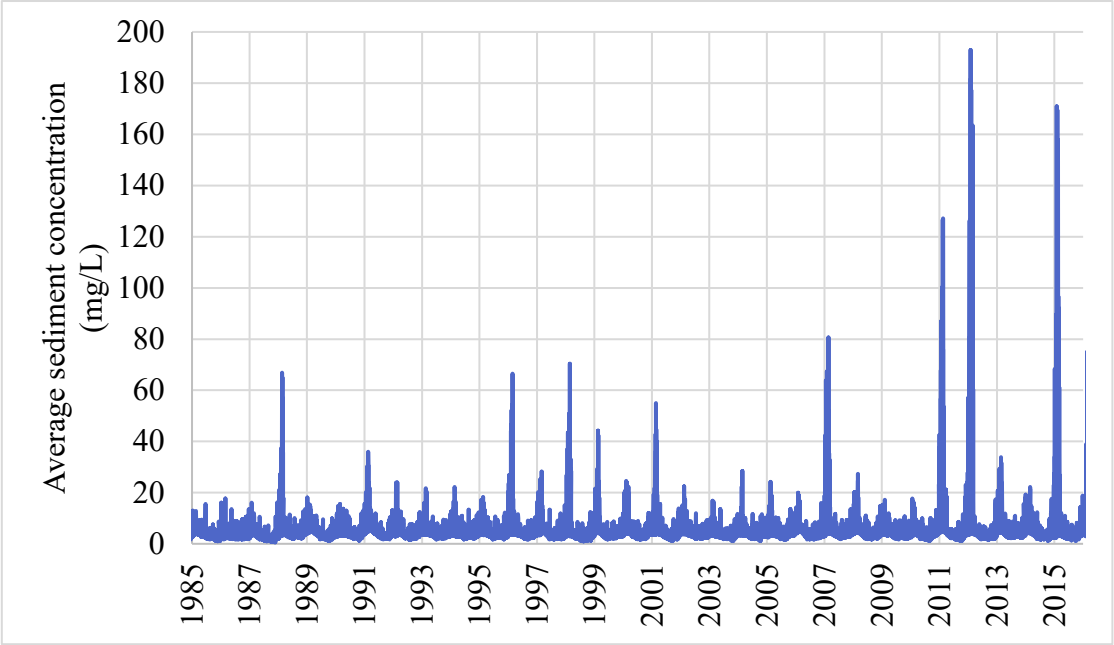

Figure 44. Simulated daily sediment concentration from the tributaries to the Moata'a wetland.

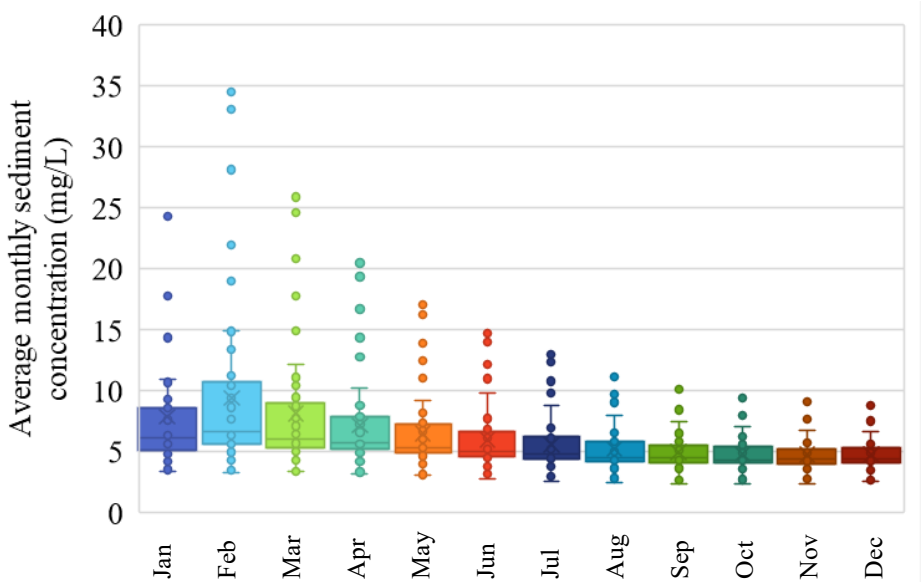

Figure 45. Simulated average monthly sediment concentration

A verification of our results for the sediment concentration in the Moata'a mangrove area was carried out using satellite data. The Case-2 Regional CoastColour (C2RCC) processor (Brockmann et al., 2016) was applied to the satellite images. The C2RCC was described in section 0.

Figure 46 shows the substantial sediment concentration in the area from a Sentinel-2 image on the 16th of March 2018, a month after cyclone Gita struck the area. This cyclone was the first significant storm of the season 2017 – 2018 and was

classified as category one when it passed near Samoa. Figure 46 indicates that, even though the concentrations were very high (up to 50 mg/L) in the marine areas between the coast and the reef, concentrations within the Moata'a mangroves were only around 0.2-4 mg/L. The hydro-sedimentological model results for the Moata'a mangroves area presented in Figure 47 capture the high peaks in concentration due to the cyclone, and for the particular day of the satellite image of Figure 46 (16th of March) it provides a value of 3.4 mg/L, well within the range of sediment concentration retrieved from satellite data. It can be also noticed that sediment concentrations in the coast close to the wetland entrance are much higher.

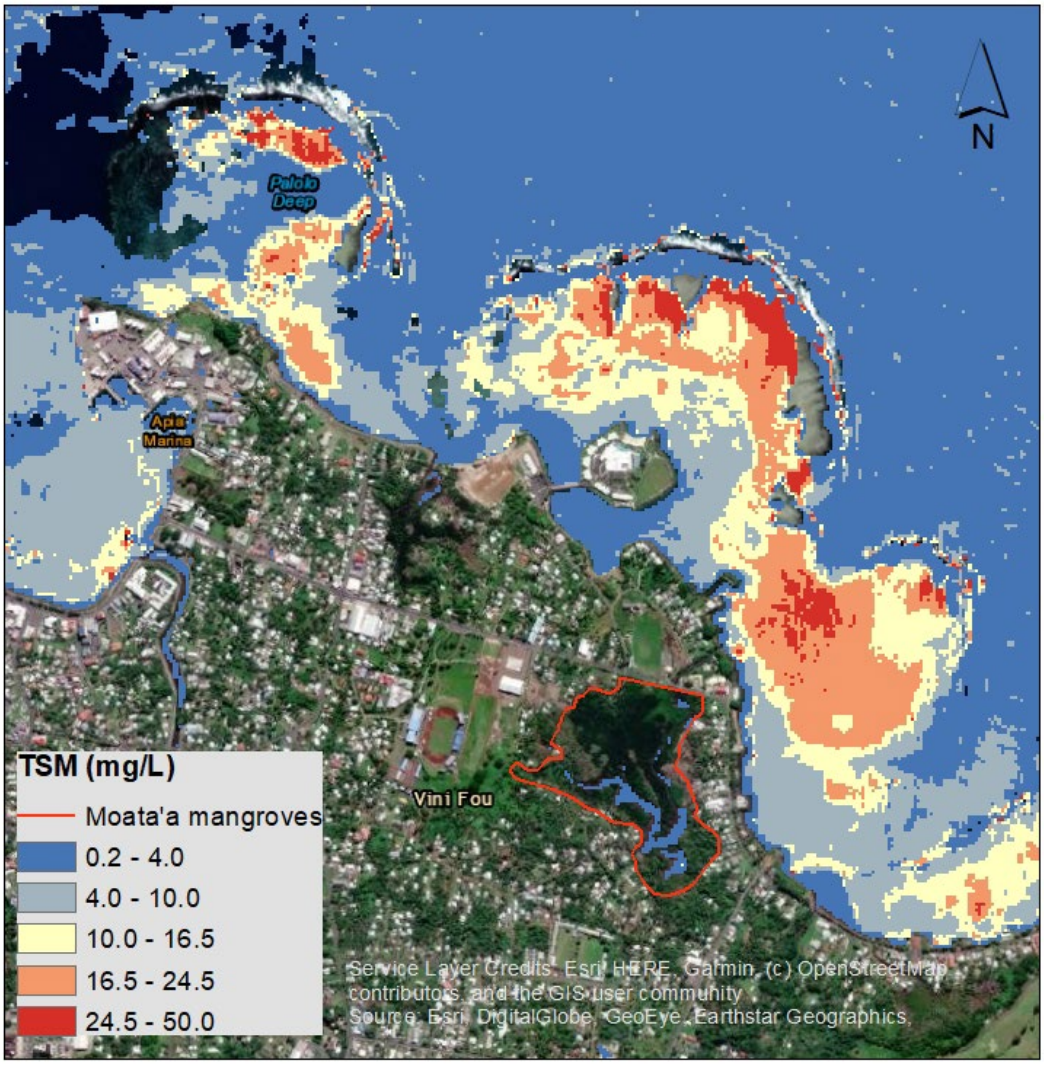

Figure 46. Total Suspended Mater retrieved from Sentinel-2 for 16 March 2018.

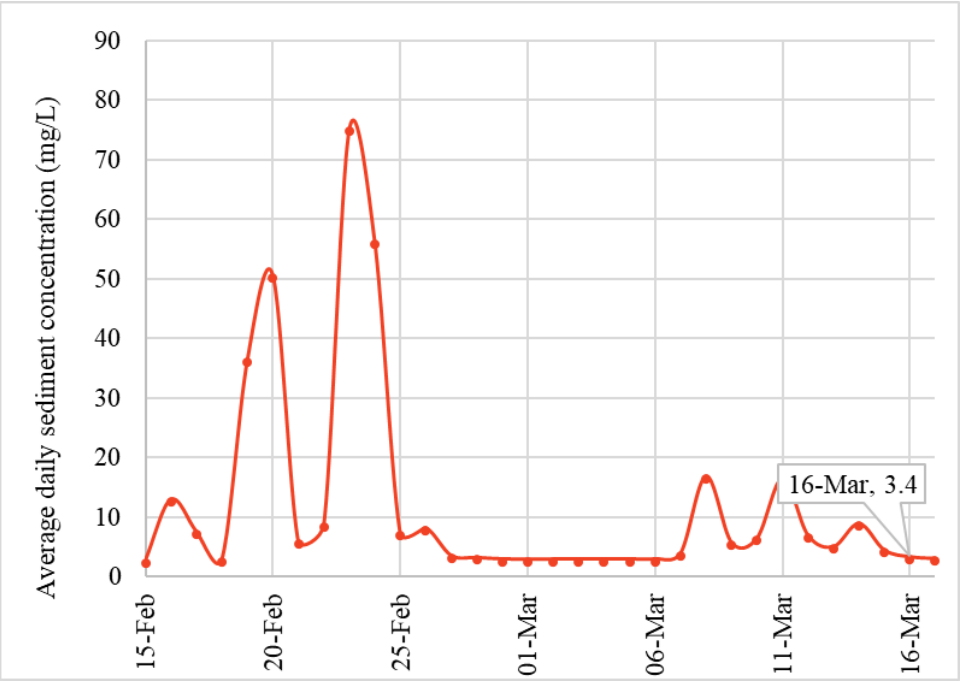

Figure 47. Simulated average daily sediment concentration at the Moata'a inlet. From mid-February to mid-March 2018.

EGM OF THE MOATA'A WETLAND: INPUTS AND MODEL SET UP.

The main input of the model is the topography of the wetland and the surrounding area. The digital elevation model was retrieved from USGS EROS Center (https://earthexplorer.usgs.gov/) with data gathered as part of the Radar Topography Mission (SRTM DEM) (https://www2.jpl.nasa.gov/srtm/dataprod.htm). Using this DEM, a 10 by 10 meter resolution representation of the Moata'a mangrove area was generated and presented in Figure 48. In the figure, the low laying areas represented in the dark blue colours are more exposed to inundation by tides.

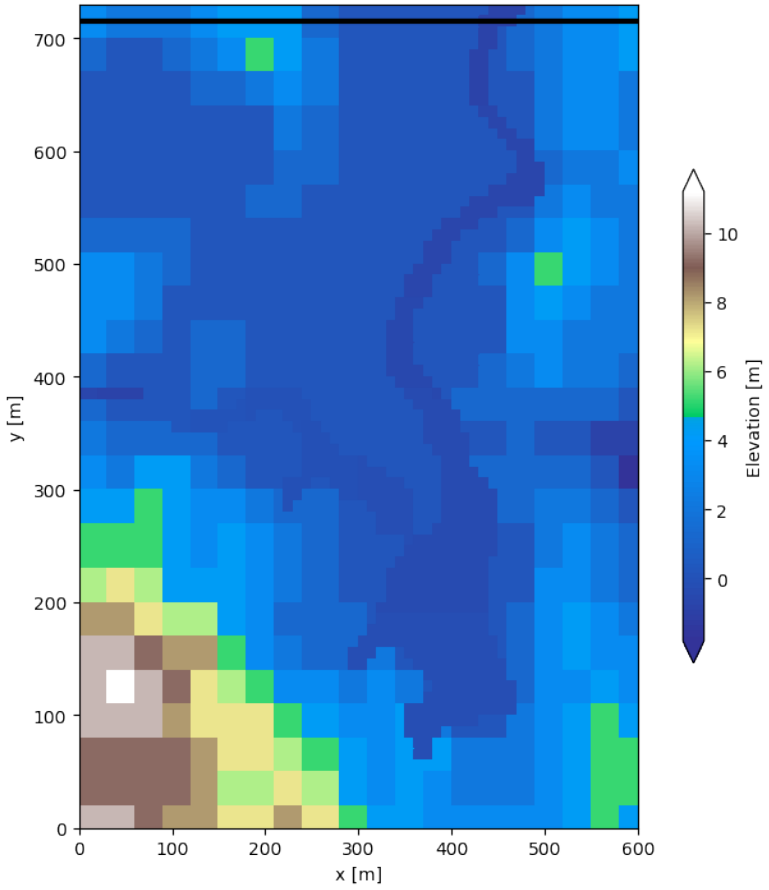

Figure 48. Digital elevation model of the Moata'a mangrove wetland.

The tidal regime drives the hydrodynamic process through the wetland. The hourly sea level data (1993 – 2021) from the Australian Bureau of Meteorology at Apia was used to derive the main characteristics of the tidal regime (http://www.bom.gov.au/pacific/samoa/index.shtml). For simulation purposes, the

average amplitude was set at 1.5 m with a period of 12 hours. Figure 49 shows the tidal time series at the entrance of the wetland.

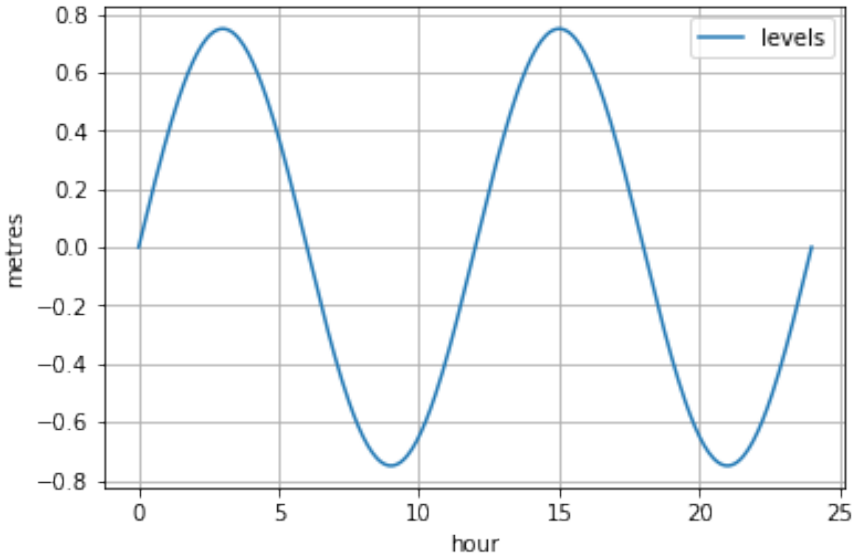

Figure 49. Tide levels

The sediment input is the product of the analysis in the Vaisigano and Moata'a catchment using the Soil & Water Assessment Tool (SWAT), described in section 0 added to the existing sediment levels in the coastal area close to the wetland entrance. A 40 mg/L sediment concentration was determined based on SWAT results and analysis of satellite images for the coastal areas close to the wetland entrance that show concentration levels that can be recirculated by the tides into the wetland.

The wetland domain consists of an area of 600 m wide by 730 m long, divided into a grid of 10m-by-10m cells (4380 in total) (Figure 50). There are two types of cells, channel and overland. The upper two rows simulate the road in the northern part of the wetland, and it is represented by an embankment. The cells are connected in two dimensions by links through which flow and sediment are conveyed. Figure 50 shows the modelling domain where it can be seen the difference between channel (lighter coloured area) and overland cells (the rest of the domain).

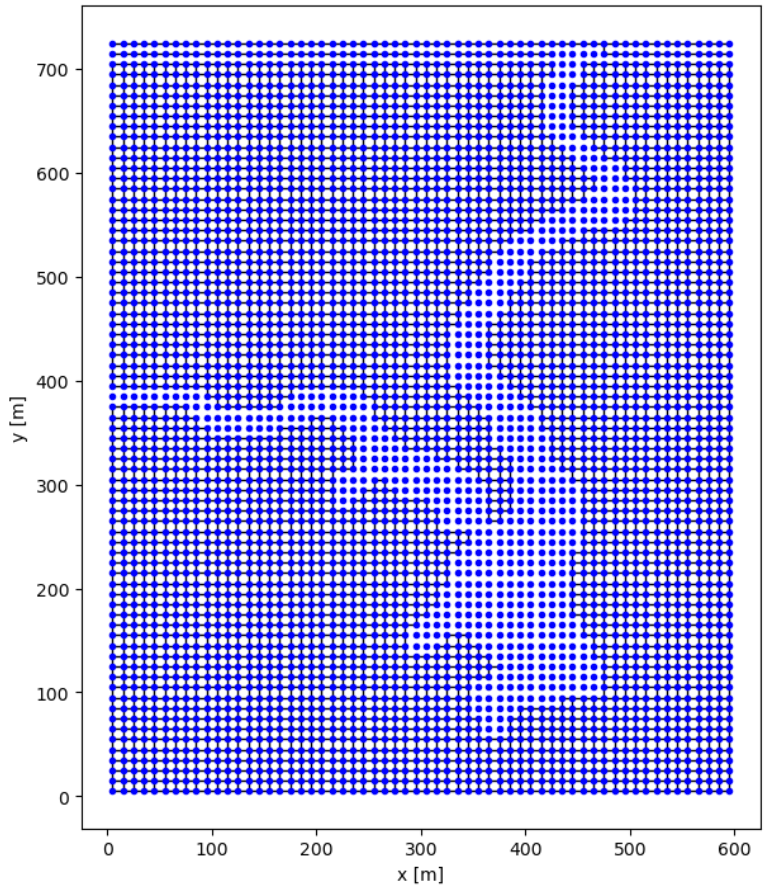

Figure 50. Simulation domain.

EGM MODEL RESULTS

Two scenarios were analysed in this section. The first one represented current condition of the Moata'a mangroves (with no sea-level rise) and a sediment concentration input of 40 mg/L. The second scenario represented climate change conditions with a sea-level rise of 0.7 meters in 100 years (corresponding to RCP8.5) (IPCC, 2021) and a sediment concentration input of 40 mg/L. Additionally, a sensitivity analysis was performed for the climate change scenario to determine the effect of DEM uncertainty on the predictions.

For the current scenario, the model was able to predict the spatial distribution of areas that are suitable for the mangrove habitat in the Moata'a area. Figure 51 shows that the mangroves establish in areas around the channel and mainly in the left side margin. In that area, the mangroves have more area to expand, and the low terrain conditions allow frequent inundation. The values of hydroperiod (H) and mean depth below high tide (D) produce conditions with enough oxygen for respiration of the mangroves through their lenticels (pores in the bark and roots).

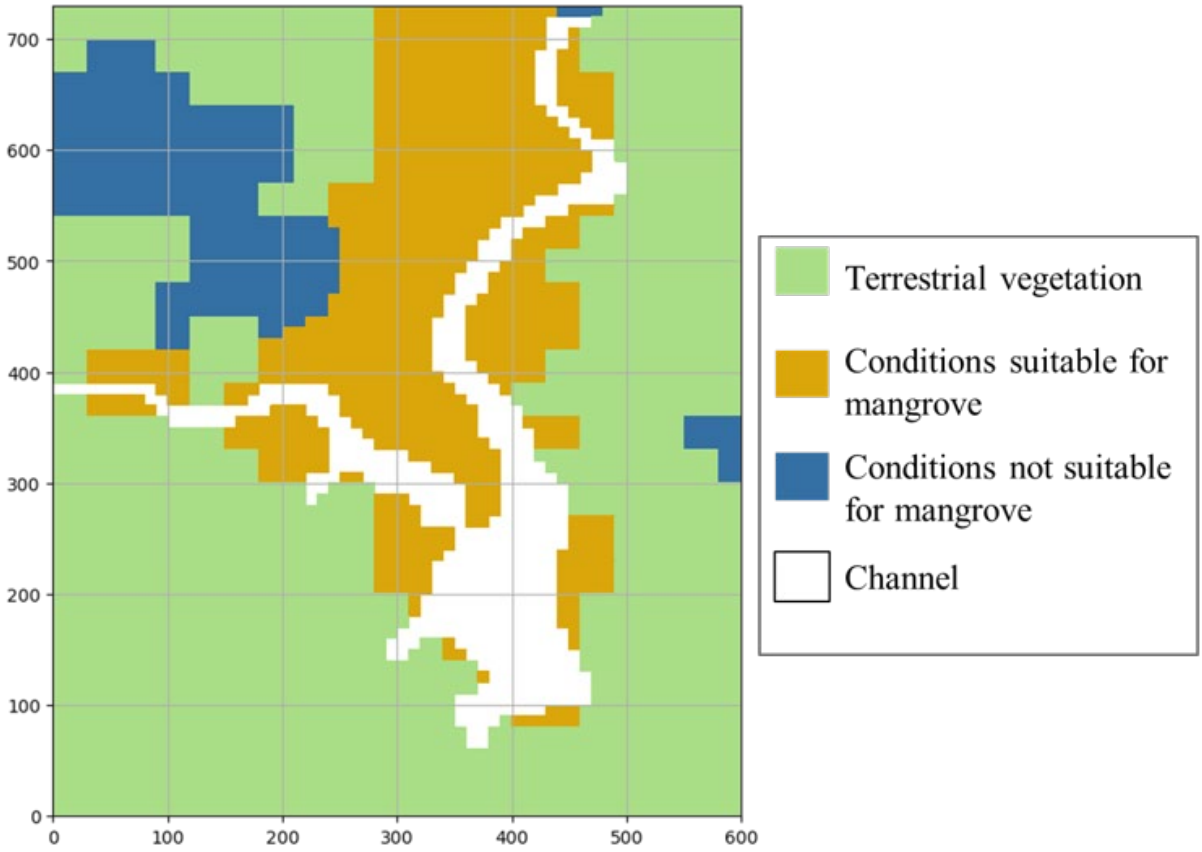

Figure 51. Initial mangrove distribution.

Mangrove retreat is expected due to SLR, and the model results are very sensitive to the magnitude of SLR (see Figure 52). The starting sea level of our simulations have an uncertainty due to limitations on the accuracy of the SRTM data. A sensitivity analysis was carried out by increasing and decreasing the starting sea level by 10 cm, accounting for potential uncertainties in the DEM data. Figure 52 shows that there is significant uncertainty in the amount of area that could be unsuitable in the future for mangroves due sea level rise. After 20 years of sea level rise (7 mm per year) the area suitable for mangrove establishment reduces by 5%, but uncertainty on initial sea levels could vary this reduction from 1% to 50%. After 40 years, the drop in area is 25% with error limits between 4% and 52%, while after 60 years the rate of reduction starts to decline. After 100 years, the reduction in suitable area is expected to be 37% with error margins between 32% and 57%.

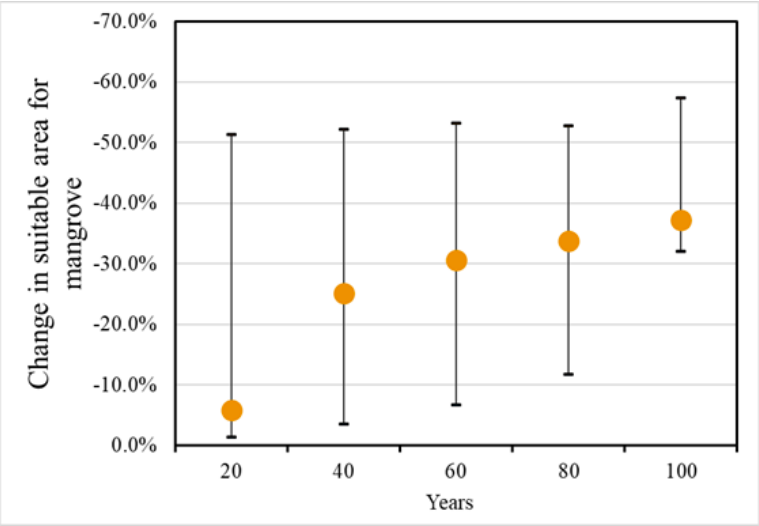

Figure 52. Change in mangrove area with sea level rise (SLR).

Figure 53 presents the accretion in the mangrove area in terms of average elevation in the entire area occupied by mangroves. The figure shows initial increases in elevation because of the accretion promoted by the root systems that are trapping sediments. Even though the elevation is increasing, it is not enough to offset the sea level rise. It can also be notice that the rate of accretion is slowing down from 9 mm in the first 20 years to 3 mm in the next 20 and to 2 mm from 60 to 80 years. This is partly due to a reduction in mangrove area that produces accretion (Figure 52). After this point, accretion stalls because of further reduction of mangrove areas. Combined with the sea level rise, this situation produces widespread drowning of the mangroves.

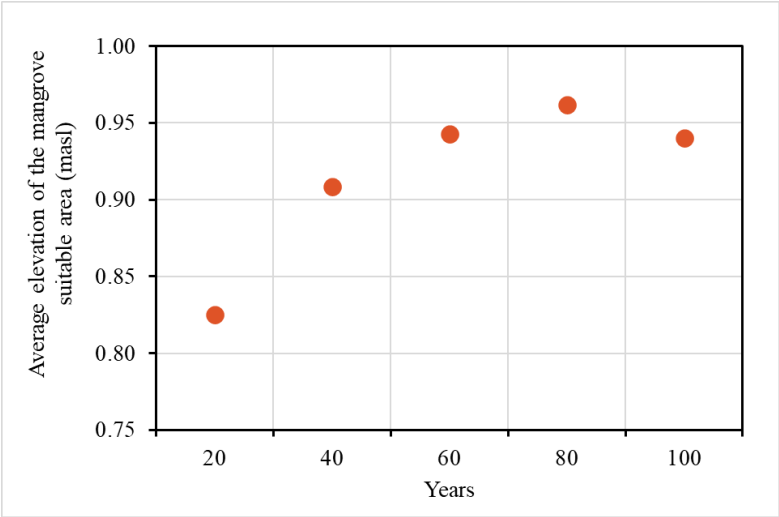

Figure 53. Average elevation of the mangrove area

Figure 54 shows the changes in the average above-ground biomass for the last years of simulation. The reduction in biomass shown in the figure is not only due to the reduction of the area covered by the mangroves, but also because the surviving mangroves have a lower biomass (smaller trees).

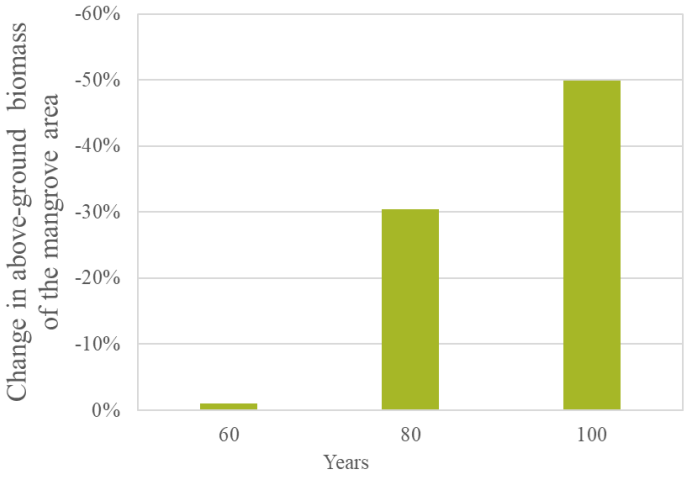

Figure 54. Change in above-ground biomass of the mangrove area.

Because mangrove establishment and survival depend on the hydroperiod, it is of interest to visualise how hydroperiod changes over time (Figure 55). The increase of the hydroperiod in the first years corresponds with the reduction of the mangrove area (Figure 52). Larger hydroperiods mean that the mangrove is inundated more time during the year, affecting the sustainability and increasing the mortality. Even though the mangroves close the lenticels during high tide to avoid drowning, if this condition persists (as in sea level rise), it could lead to mangrove mortality.

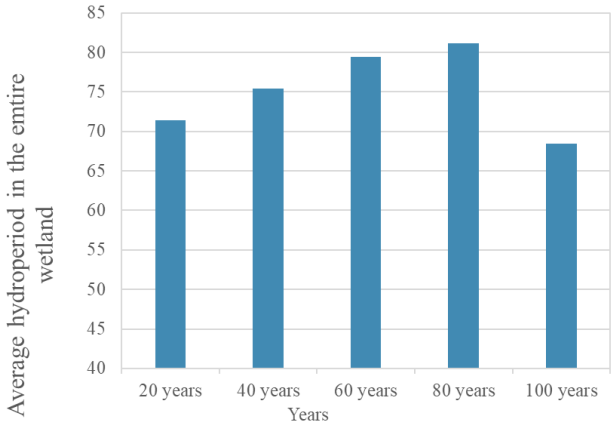

Figure 55. Average hydroperiod in the wetland.

RESILIENCE ANALYSIS

Three scenarios are analysed in this report to assess the effect of the sediments production in the catchment and how it affects the accretion rates in the Moata'a mangrove to deal with sea level rise. The first scenario studies the effect of the construction of a dam and flood protection levees in the Vaisigano river, the second scenario examines the influence of land use change from forested to agricultural areas in the Vaisigano catchment, and the third scenario investigates the change in sediment loads with increased rainfall intensity due to climate change.

SIMULATION SCENARIOS

- *Flood protection levees and dam project in the Vaisigano river*

As a result of historical flooding events, levees on the banks of the Vaisigano river have already been constructed. A 700m segment was finished in late 2018, extending from the Vaisigano Bridge at the river mouth to the Faatoia Bridge (Figure 56). The objective of the levee is to prevent water to exceed the riverbanks and reduce the risk of flooding in the surrounding urban areas.

Figure 56. Levees in the Vaisigano river at the Faatoia Bridge. Figure taken from Google Maps.

A second levee segment has been proposed (Filer et al., 2019), which extends from the Faatoia Bridge to the Lelata bridge (Figure 57). Even though the levees reduce the risk of flooding and minimise the economic impacts of flooding events, they also prevent the passage of fauna and sediments from the river to the floodplain.

Figure 57. Levees in the Vaisigano river. Segment 1 (already constructed) and segment 2 (proposed by Filer et al. (2019)).Figure taken from Google Maps.

The proposed levee in the Vaisigano river (Figure 58) could cut the main supply of sediments that enter to the Moata'a mangroves during high flows, which can affect the accretion rates and the future resilience against sea level rise. Additionally, there is a proposed project by the Asian Development Bank to build the Alaoa multipurpose dam in the upper reaches of the Vaisigano River (Figure 59). This dam will provide further protection against flooding, increase the resilience of the water supply and increment the energy production capacity of the island. Like the levee project, the dam can significantly reduce the amount of sediments entering the Moata'a mangroves, affecting its resilience. In this report, the Moata'a mangrove resilience is analysed under reduced sediment supply of 25% and 50% (product of the proposed levee construction and/or dam construction) in conjunction with sea level rise.

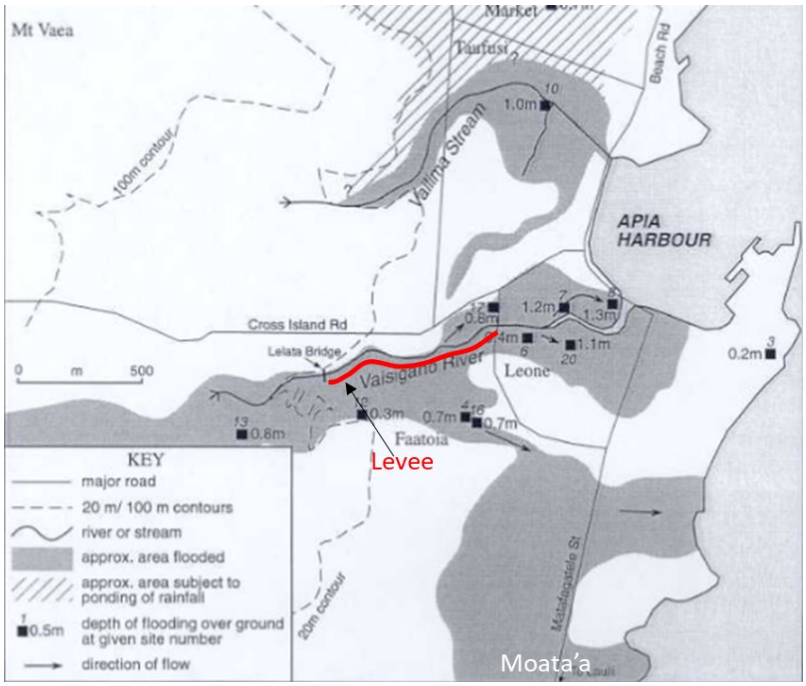

Figure 58. Levee (traced in red) in the Vaisigano river. Figure modified from (Yeo, 2001).

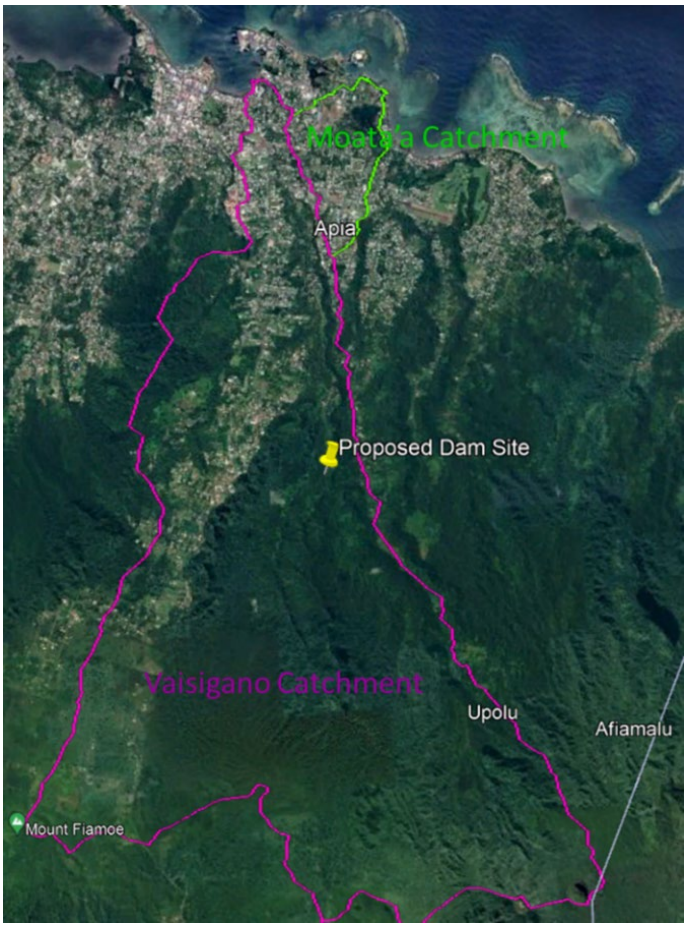

Figure 59. Proposed location for the multipurpose dam in the Vaisigano river.

- *Land use change in the Vaisigano catchment area*

Anthropogenic pressures can modify the natural landscape by expanding urban, agricultural, or livestock areas. Global demands of goods and commodities produced in the island, industrialization of agricultural processes and increase of local demand (due to the price increment of imported goods) could lead to the expansion of agricultural areas in the Vaisigano catchment.

The current land use of the area includes 73% of forest, 10% of agriculture and 17% of high- and low-density urban use. Based on the Land and Survey Department of Samoa, there are soils that are physically and chemically suitable for agricultural purposes (even though in practice they cannot be converted because they lay on forest-protected areas). The land use was modified to analyse the effect in the sediment production in the catchment that would alter the sediment input to Moata'a mangrove. The agricultural areas were increased by 17% according to the soils that are suitable for that purpose, resulting in a distribution of land use of 57% forest, 27% agricultural land and 17% high- and low-density urban areas. In Figure 60, the comparison of the current and changed land uses is presented. The hydro-sedimentological model was run first to obtain alterations in sediment production and then the EGM was used to simulate the response of the Moata'a mangroves to the land use change (alteration in sediment input) and sea level rise. Land use changes in the Moata'a catchment were not investigated as the catchment contributes very little sediment and flows to the wetlands.

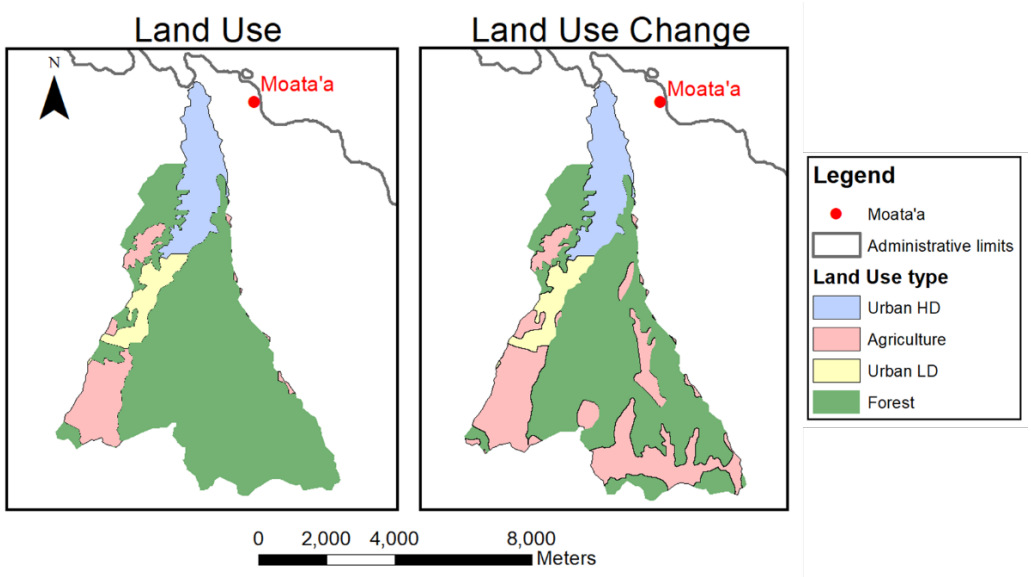

Figure 60. Land use change in the Vaisigano catchment.

- *Increase on rainfall intensity due to climate change*

Climate change is already altering the frequency and intensity of rainfall events and droughts, rising sea levels, melting glaciers and warming oceans. Moata'a mangroves will be affected not only by sea level rise but also by more frequent and intense tropical storms, cyclones and extreme rainfall events. More rainfall could bring additional soil erosion and increase the sediment input into the mangroves.

Based on the Intergovernmental Panel on Climate Change's (IPCC) Sixth Assessment Report (AR6), the western equatorial pacific is likely to expect more rainfall under all emission scenarios. Warmer conditions will increase the atmospheric moisture in this region, bringing more frequent and intense extreme rainfall. The increase in intensity is expected to be between 7% and 30% due to an increment in temperature between 1°C and 4°C (IPCC, 2021). To evaluate the sediment production in the worst-case scenario, this report analyses the production of sediments in the catchment using the hydro-sedimentological model under a 30% increase in rainfall. Subsequently, the EGM is used to analyse the resilience of the Moata'a mangrove to sea level rise with the increased input of sediments.

MANGROVE RESILIENCE RESULTS

As presented in the previous section, the effects of three different sediment inputs on the Moata'a mangrove are analysed in conjunction with sea level rise. The scenarios consider the change of sediments due to: 1) flood protection levees and dam project in the Vaisigano river, 2) land use change in the Vaisigano catchment area, and 3) increase on rainfall intensity due to climate change. The results are used to assess the resilience of Moata'a wetland under different scenarios and considering 2020 as baseline year.

FLOOD PROTECTION LEVEES AND DAM PROJECT (SEDIMENT SUPPLY REDUCTION)

Under this condition, two possible scenarios of sediment supply reduction were analysed. In the first scenario, the reduction was 50% of the current conditions, while the second scenario reduced the sediment supply by 25%. The model results highlighted that under a shortage of sediment supply, the accretion rate cannot keep up with the sea level rise rate leading to a substantial decrease in the area suitable

for mangrove growth (Figure 61). The results indicate that mangroves are not able to thrive because they are inundated more than 50% of the time, which may generate drowning conditions (as shown in Figure 62).

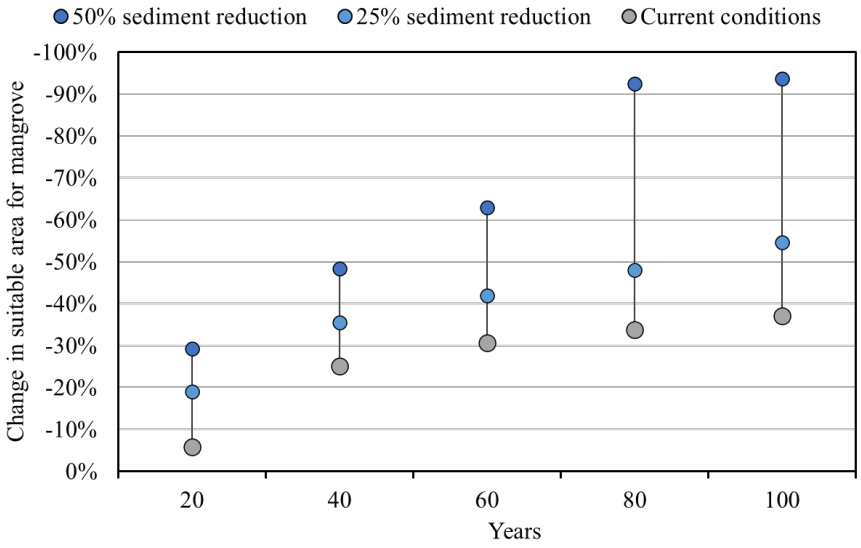

Figure 61. Change in suitable area for mangroves under two scenarios of sediment supply reduction.

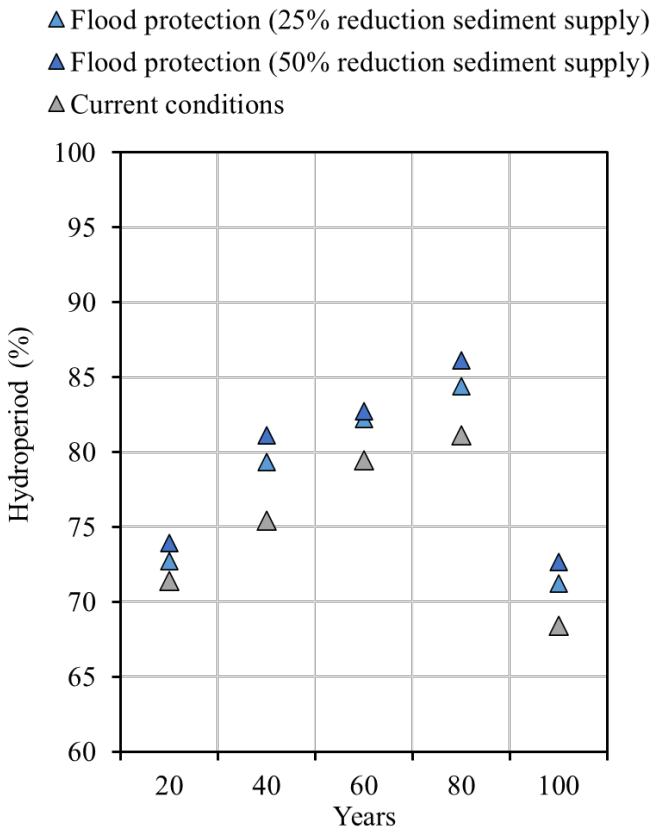

Figure 62. Average hydroperiod in the wetlands.

LAND USE CHANGE (SEDIMENT SUPPLY INCREASE)

The expansion of the agriculture area on the Vaisigano catchment may generate an increase in sediment inputs in the Moata'a mangrove but this may be associated with an increase in pollutants and reduction of water quality. Figure 63 shows that when new agricultural areas were added to the Vaisigano catchment, it resulted in a 10% increase in sediment production compared to the current scenario condition. The results from the ecogeomorphological model showed this increase of 10% has in the sediment concentration has little effect in the Moata'a mangrove, with reductions in the mangrove suitable area of 27% in 100 years (Figure 64), which not that different (considering uncertainty) from the 37% expected reduction under the current land use conditions. Notice that according to the land classification, the soils of the potential new agricultural areas have low nutrient content, so they will require intense use of fertilisers. This study did not consider the quality of the runoff water, so although the effects of more sediment are not negative for the wetland, the concentration of fertilizers in the runoff may increase and produce other adverse effects on the mangroves.

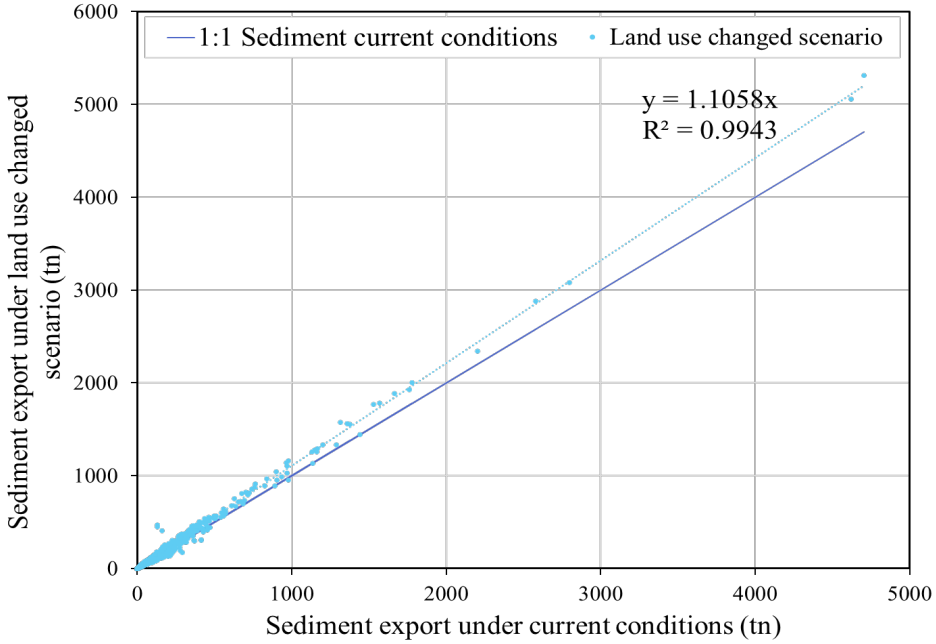

Figure 63. Increase in sediment export under land use changed scenario.

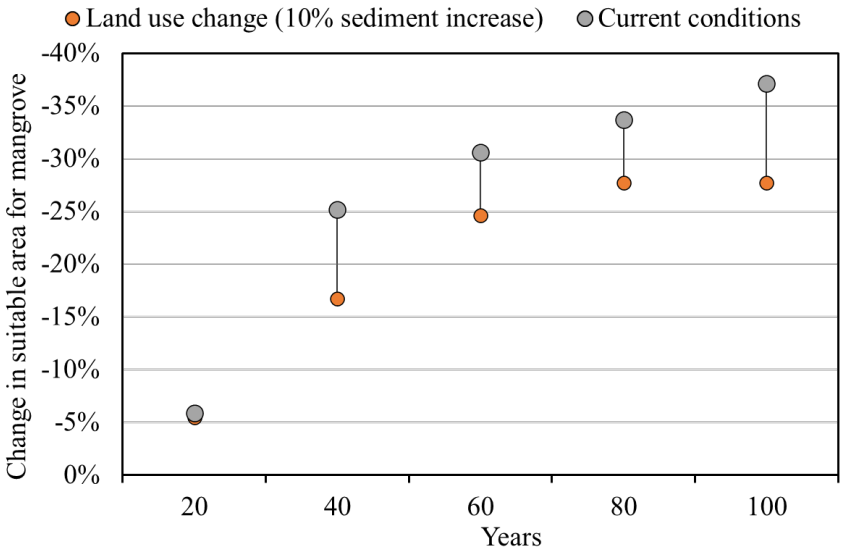

Figure 64. Change in suitable area for mangroves over time.

INCREASE ON RAINFALL INTENSITY (SEDIMENT SUPPLY INCREASE)

The results from the hydro-sedimentological model (SWAT) showed an increment in the sediment export from the Vaisigano catchment area by a factor of around 2 when a 30% increase in rainfall intensity was considered (Figure 65). The same increase in intensity was considered for all rainfall events, including those associated with cyclones. The ecogeomorphological simulations were performed doubling the sediment concentration (100% increase). Under this scenario, the accretion rate was equal to or larger than the sea level rise rate, allowing the mangroves to maintain suitable conditions for their development. As a result, the reduction in the suitable area for mangroves was almost inexistent (lower than 5%) for the entire period of simulation (Figure 66). This means that under these conditions, the Moata'a mangrove may be more resilient to sea level rise. However, the increase in 100% sediment concentration for the entire period of simulation can be considered an upper limit, and it is more likely that the increase in sediment will be gradual. In Figure 66 the results of the simulations considering a gradual increase in sediment concentration over time, starting at zero and reaching a 100% increase at the end of the 100 years simulation period. It can be seen in the figure that under these conditions the area suitable for mangroves will be reduced by about 23% after the first 60 years of simulation. It should be also noticed that the effects of storm surges, wind damages or other possible effects of extreme events were not considered in this study and should be incorporated in future work.

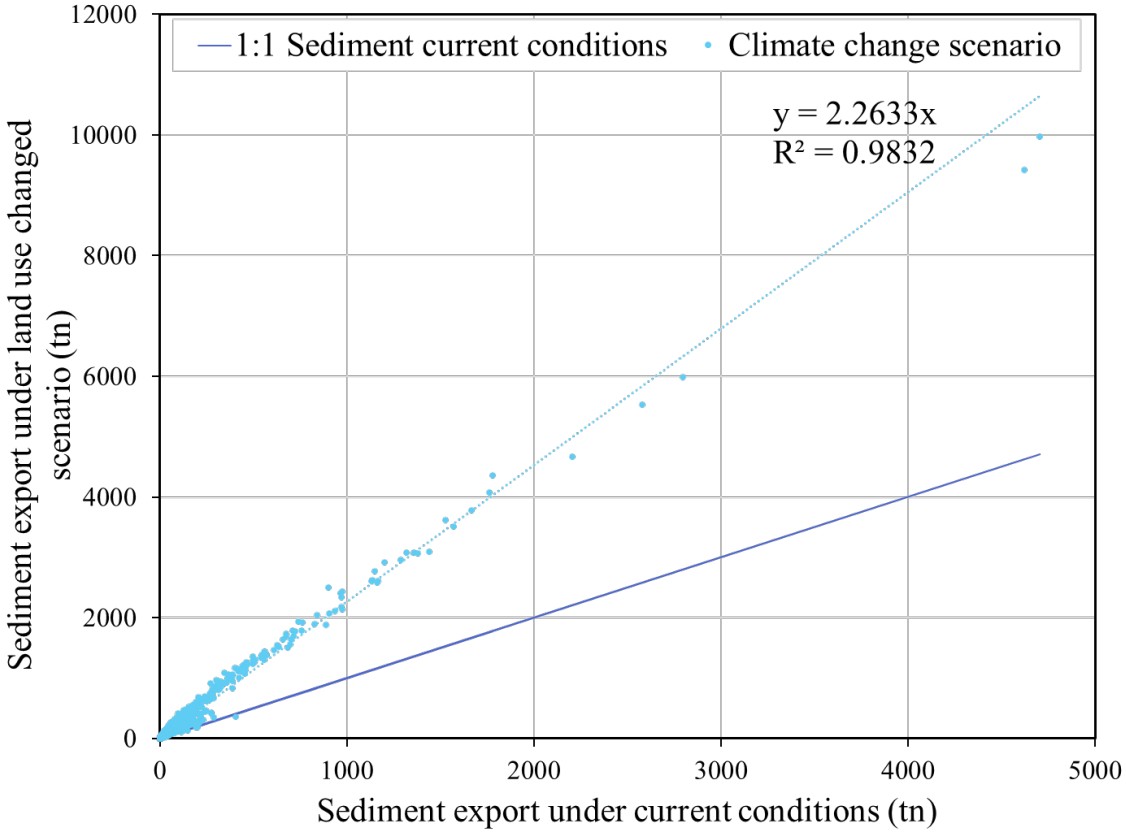

Figure 65. Increase of sediment supply under climate change scenario of increased rainfall.

Figure 66. Change in suitable area for mangroves under climate change scenario of increased rainfall.

SCENARIOS COMPARISON

The comparison between current conditions (considering 2020 as baseline year) and possible future scenarios highlighted the strong relationship between mangrove resilience and sediment inputs to the mangrove. Figure 67 shows that a substantial reduction in the sediment supply could lead to the loss of half of the mangrove suitable area in approximately 50 years (dark and light blue lines). On the other hand, a significant increase in sediment supply could lead to less than a 5% change in the mangrove suitable area. This can be explained by looking at the changes in the accretion capacity of the mangroves. It can be seen in Figure 68 that the accretion changes (and associated area suitable for mangroves) are more sensitive to sediment reduction than sediment increments. For instance, the accretion ability of the mangroves is reduced up to 60% in the case of a 50% reduction in the sediment supply. In comparison, accretion can increase to 40% for an increase in sediments of 100%. It should be noticed that all the simulated scenarios showed some degree of decrease in the area suitable for mangroves, highlighting the threat of sea level rise for mangrove resilience. The scenario with a gradual increase of sediment supply from 0 to 100% over the 100 years of simulation has not been included in Figure 67 as the results are similar to the scenario of 10% increase due to land use changes.

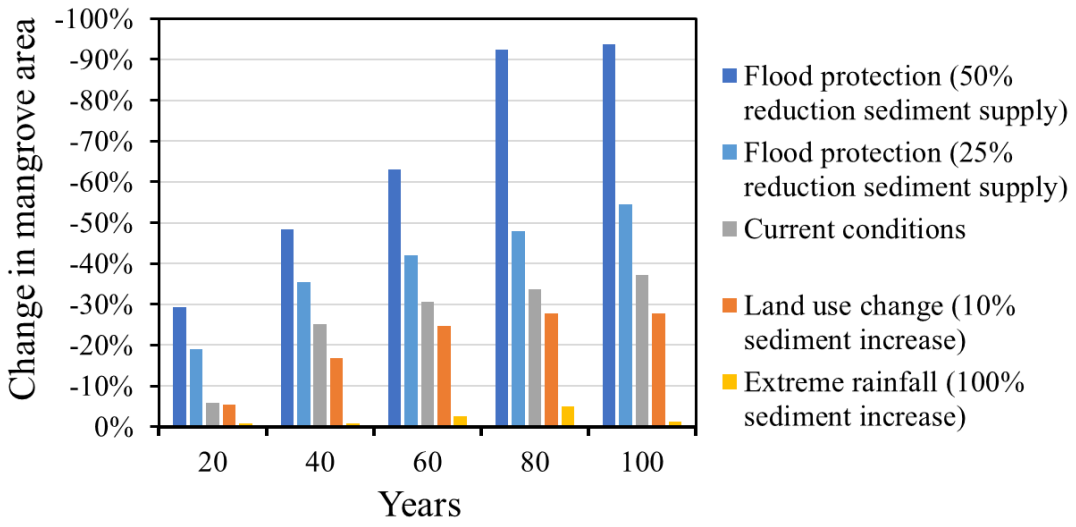

Figure 67. Change in mangrove suitable area under different scenarios.

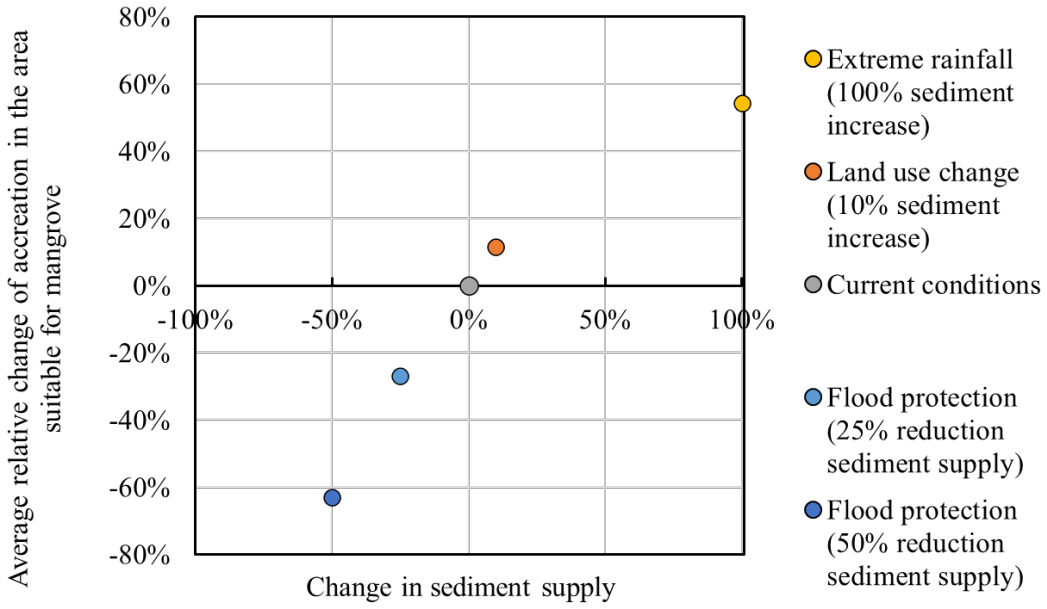

Figure 68. Average relative change in accretion respect the current condition under different sediments supply.

FINAL REMARKS

The Moata'a mangroves are under pressure due to human impacts and climate effects. The resilience of the mangrove will depend on the rate of accretion versus the rate of sea-level rise and the measures to protect the existing mangroves against anthropogenic stressors. In this study, hydro-sedimentological and eco-geomorphological models were implemented in Moata'a area to analyse the resilience of the mangroves to sea-level rise and changes in sediment inputs from the catchments.

Mangroves may collapse if the anthropogenic pressures and sea-level rise exceed the system thresholds. The resilience of the Moata'a mangroves was analysed using modelling tools to improve the understanding of how ecological and physical processes react under different input conditions and predict the mangrove functionality and persistence. These models are subject to significant uncertainties (both due to data limitations and process simplification) but can guide an adaptive management approach, which could enhance the mangrove resilience in conjunction with appropriate engineering interventions.

Understanding the mangrove functionality is vital for determining adequate design alternatives to enhance mangrove resilience. Mangroves have innate adaptability to conditions that make them more flexible in responding to extreme events compared with hard engineering solutions. Mangroves can increase the soil elevation, migrate to different areas, and recover from the impacts of extreme events. Hard engineering solutions that do not consider the mangrove functionality may threaten the mangrove's survival by limiting the sediment supply or restricting the mangrove migration areas.

HSM CONSIDERATIONS

The amount of water and sediments generated in the catchment were determined using a physically based, watershed scale model (SWAT). Climatic (rainfall, temperature, wind speed, relative humidity and solar radiation), topography, soil type and land use data were used to generate daily series of flow and sediment delivered to the Moata'a mangroves area for the period 1970-2020.

The hydro-sedimentological model proved to be suitable to represent the flows in the Vaisigano river catchment with a good performance against measured data during calibration. Under extreme events, the contribution of flows and sediments of the Vaisigano river catchment to the Moata'a catchment during important floods were determined based on historical information. These inputs from the Vaisigano catchment were incorporated into the hydro-sedimentogical model of the Moata'a catchment. The resulting sediment concentrations reaching the mangroves areas provided by the model compared favourably with sediment concentrations obtained using remote sensing products. The results of the calibrated and validated hydro-sedimentological models presented in this report played a vital rol for the mangrove ecosystem analysis and assessment of the resilience under climate change.

EGM CONSIDERATIONS

The distribution of the mangroves, accretion and hydroperiods were determined using the model. The model was able to represent the spatial distribution of suitable area for mangrove habitat given the current conditions. Under sea-level rise scenarios, it was observed that despite the uncertainties a significant amount of the suitable area for mangrove establishment can potentially disappear after 100 years.

This is a result of a decrease in accretion rates and an increase in hydroperiod, which can lead to the drowning of mangroves and the reduction of the suitable area.

ECOSYSTEM RESILIENCE

The resilience of the Moata'a mangrove was studied by analysing the response of the ecosystem under different sediment inputs in conjunction with sea level rise. As in many other mangrove wetlands, it was identified that there is a noticeable relationship between the sediment concentrations entering the wetland and the mangrove accretion capacity. The flood protection levees and dam project scenario that resulted in substantial decreases of sediment to the wetland considerably reduced the resilience of the system, while the scenarios of increased rainfall intensity that resulted in large increases of sediment greatly improved the resilience.

The scenario of land use changes had a more moderate positive effect on the mangroves resilience as the sediment inputs increased by a smaller amount. This last scenario did not consider the potential effects of water quality (increased pollution) that could also affect resilience. Even though the land use change scenario could increase the sediment inputs, it could also increment the pollutants and affect the sustainability of the mangrove. It is not recommended to change land uses to increase sediment input to the mangrove and it is important to promote the conservation of forest areas to maintain water quality levels.

Based on the results presented in this report, measures that can increase mangrove resilience include:

- *Maintain connectivity between mangroves, the catchment and the coast*

The interactions between hydrodynamic, sedimentological and ecological processes in the mangroves are highly dependent on each other, and the connectivity allows the persistence of the functionality of the mangroves. The main connectivity includes the link with the Vaisigano river catchment, which provides essential water and sediments to the wetland. Maintaining access to this source of sediment and freshwater is vital to enhance the wetland survival over time.

The connectivity could also be preserved by avoiding changing the hydroperiod/water regime. Dredging/filling and construction of dams, roads, and

dikes affect and disrupt the hydrological regime in the wetland. Moreover, it is necessary to avoid altering natural features such as barrier islands, sandbars or reefs that protect from wave erosion and storm surge and at the same time maintain sediment reach tides that promote mangrove accretion.

Another practice to maintain the connectivity in the mangroves is to reduce the water/sediment stagnation. Creeks and drainages in the mangroves allow sediment/water distribution and seed dispersal (Figure 69). Stagnated areas could drown mangroves and decrease the water quality conditions. One major recommendation is to maintain the drainage/creeks unobstructed by residues or barriers. Channel banks that are consolidated and have dense mangroves would maintain these channels open and free of barriers.

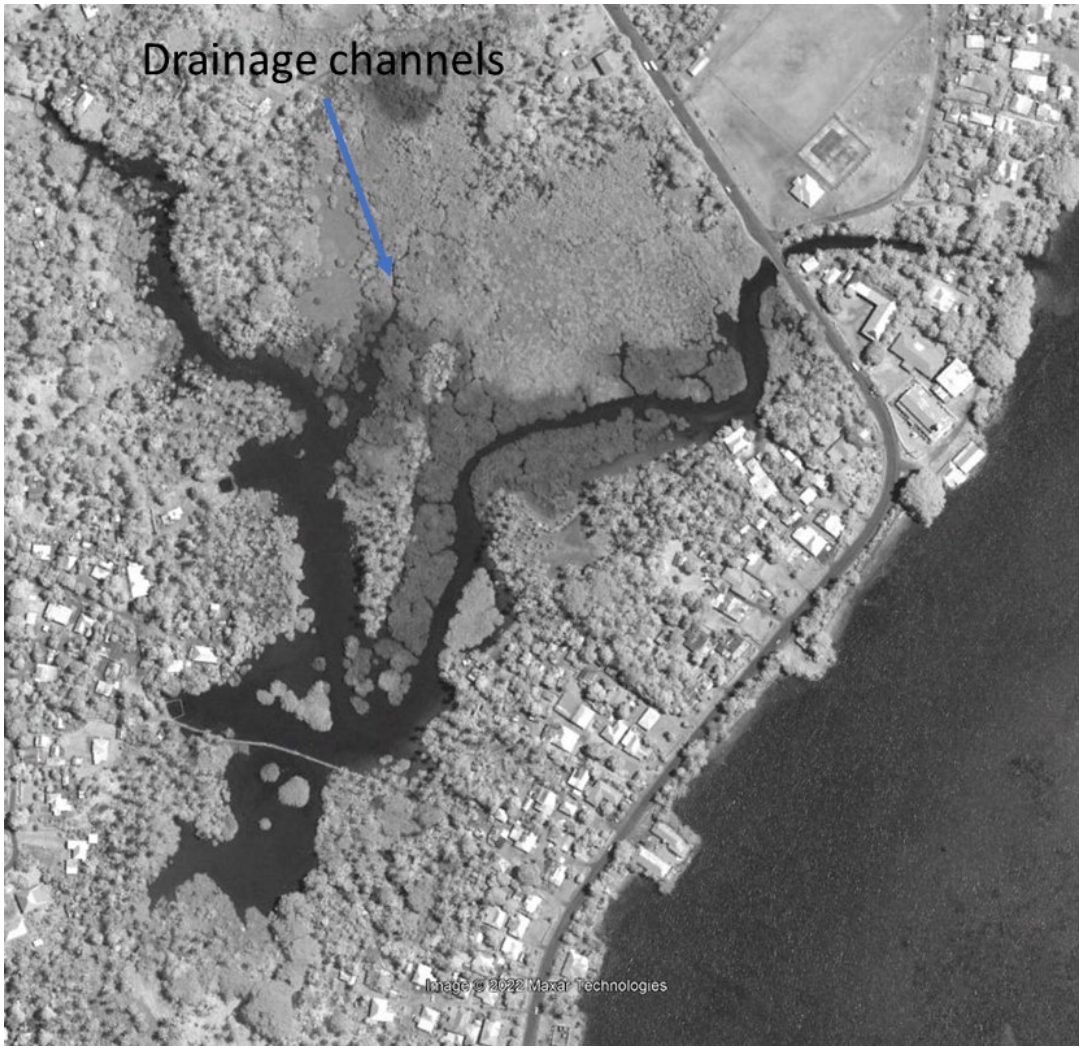

Figure 69. Drainage channel connectivity in the Moata'a mangrove area (Google earth. Imagery date: 17/04/2009).

- *Establish buffer zones*

Buffer zones are low-laying areas that are suitable for the colonization of mangroves and are clear from human settlements. These areas act as coastal protection against storm surges and erosion, provide a transition between the mangroves and human settlements and allow for the expansion of mangroves due to sea-level rise.

These zones should be between 10-100 meters along riverbanks, and biodiversity-friendly practices should be developed around them (McLeod and Salm, 2006). For example, a potential 100-m buffer zone around the Moata'a current mangrove area is presented in Figure 70. However, the buffer zones must have the correct elevation for the mangroves to be able to colonise them during sea level rise, so a detailed ground survey and further modelling must be conducted before the establishment of the buffer zones. These potential mangrove colonisation areas should not be disrupted by the presence of dikes or seawalls and can be supported by replanting of mangroves and restoration of degraded areas.

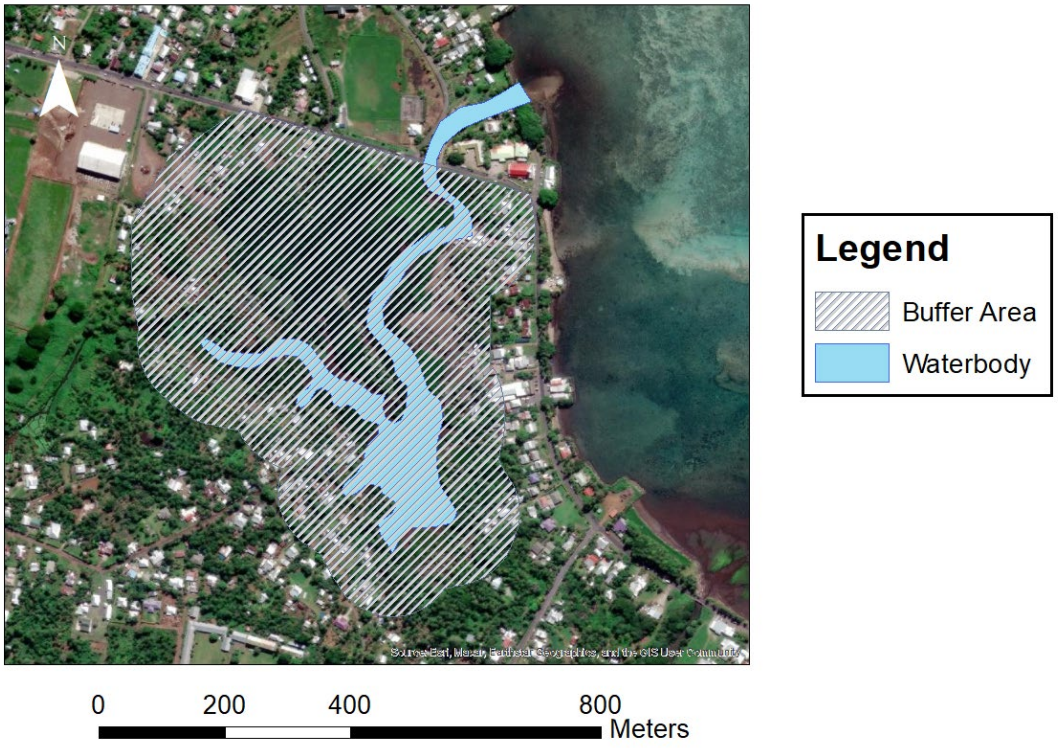

Figure 70. Example of a 100-m buffer zone around the Moata'a mangroves (Imagery source: Esri, DigitalGlobe, GeoEye, Earthstar Geographics, CNES/Airbus D S, USDA, USGS, Aero GRID, IGN, and the GIS User Community).

- *Monitoring of Moata'a mangrove area using field and remote sensing techniques*

Regular monitoring is required to assess the effectiveness of the implemented measures. Reduction in the uncertainty of the model and assessment of the effectiveness of implemented measures could be addressed by field campaigns and remote sensing studies. Some of the data that can be collected are: a detailed topography and bathymetry in the mangrove areas combining drone-based LIDAR with in-situ RTK GPS measurements, vegetation extension using high resolution remote sensing imagery, biomass measurements (e.g. tree density, stem diameter, height and roots), ecological processes (e.g., tree growth, size of new recruits), sediment concentration measurements (e.g., optical backscatter sensors, turbidity measurements, grab samples) and deposition/accretion measurements using Surface Elevation Tables (SET). These data may reduce the uncertainty of the results and would allow a better understanding of the ecosystem and the effectiveness of the implementation of measures that enhance mangrove resilience. Additionally, the monitoring may give early warning signals to take preventive and remedial actions.

- *Further study*

It is important to notice that the effects of other variables were not considered in this report and are recommended to be included in future studies. Some of the variables that could be considered are the effect of the increase in water/air temperature (affecting tree growth), changes in salinity, tree mortality/damage due extreme weather events, water quality (e.g., fertilizers, pesticides and fungicides product of agricultural runoff), groundwater levels, tectonic movements, excess of leaf litter and sediment accumulation (which can lead to mortality of some mangrove species), inter-species competition, and mangrove health condition (deteriorated mangroves are less resilient).

REFERENCES

Arnold, J. G., Srinivasan, R., Muttiah, R. S. & Williams, J. R. 1998. Large area hydrologic modeling and assessment part I: Model Development. *JAWRA Journal of the American Water Resources Association,* 34**,** 73-89.

Benavidez, R., Jackson, B., Maxwell, D. & Norton, K. 2018. A review of the (Revised) Universal Soil Loss Equation (R/USLE): with a view to increasing its global applicability and improving soil loss estimates. *Hydrology and Earth System Sciences Discussions***,** 1-34.

Breda, A., Saco, P. M., Sandi, S. G., Saintilan, N., Riccardi, G. & Rodríguez, J. F. 2021. Accretion, retreat and transgression of coastal wetlands experiencing sea-level rise. *Hydrol. Earth Syst. Sci.,* 25**,** 769-786.

Briak, H., Moussadek, R., Aboumaria, K. & Mrabet, R. 2016. Assessing sediment yield in Kalaya gauged watershed (Northern Morocco) using GIS and SWAT model. *International Soil and Water Conservation Research,* 4**,** 177-185.

Brockmann, C., Doerffer, R., Peters, M., Kerstin, S., Embacher, S. & Ruescas, A. Evolution of the C2RCC neural network for Sentinel 2 and 3 for the retrieval of ocean colour products in normal and extreme optically complex waters. Living Planet Symposium, 2016. 54.

D'alpaos, A., Lanzoni, S., Marani, M. & Rinaldo, A. 2007. Landscape evolution in tidal embayments: Modeling the interplay of erosion, sedimentation, and vegetation dynamics. *Journal of Geophysical Research: Earth Surface,* 112.

Dare, R. A., Davidson, N. E. & Mcbride, J. L. 2012. Tropical Cyclone Contribution to Rainfall over Australia. *Monthly Weather Review,* 140**,** 3606-3619.

Deo, A., Chand, S. S., Ramsay, H., Holbrook, N. J., Mcgree, S., Magee, A., Bell, S., Titimaea, M., Haruhiru, A., Malsale, P., Mulitalo, S., Daphne, A., Prakash, B., Vainikolo, V. & Koshiba, S. 2021. Tropical cyclone contribution to extreme rainfall over southwest Pacific Island nations. *Climate Dynamics*.

Diamond, H. J., Lorrey, A. M., Knapp, K. R. & Levinson, D. H. 2012. Development of an enhanced tropical cyclone tracks database for the southwest Pacific from 1840 to 2010. *International Journal of Climatology,* 32**,** 2240-2250.

Doerffer, R. & Schiller, H. 2007. The MERIS Case 2 water algorithm. *International Journal of Remote Sensing,* 28**,** 517-535.

Ebi, K. L., Lewis, N. D. & Corvalan, C. 2006. Climate variability and change and their potential health effects in small island states: information for adaptation planning in the health sector. *Environmental health perspectives,* 114**,** 1957-1963.

Filer, B., Dearnley, C., Buchanan, M. & Caddis, B. 2019. Review of the Interdependence of Flood Mitigation Options for the Vaisigano River Catchment. Brisbane, Australia.: BMT Eastern Australia Pty Ltd.

Gilman, E., Ellison, J. & Coleman, R. 2007. Assessment of Mangrove Response to Projected Relative Sea-Level Rise And Recent Historical Reconstruction of Shoreline Position. *Environmental Monitoring and Assessment,* 124**,** 105-130.

Green Climate Fund 2016. FP037: Integrated Flood Management to Enhance Climate Resilience of the Vaisigano River Catchment in Samoa - Annex II: Feasibility Study. *In:* (UNDP), U. N. D. P. (ed.). Samoa.

Hajigholizadeh, M., Melesse, A. M. & Fuentes, H. R. 2018. Erosion and Sediment Transport Modelling in Shallow Waters: A Review on Approaches, Models and Applications. *International Journal of Environmental Research and Public Health,* 15**,** 518.

Ipcc 2021. *Climate Change 2021: The Physical Science Basis. Contribution of Working Group I to the Sixth Assessment Report of the Intergovernmental Panel on Climate Change,* Cambridge, United Kingdom and New York, NY, USA, Cambridge University Press.

Jaffe, B., Buckley, M., Richmond, B., Strotz, L., Etienne, S., Clark, K., Watt, S., Gelfenbaum, G. & Goff, J. 2011. Flow speed estimated by inverse modeling of sandy sediment deposited by the 29 September 2009 tsunami near Satitoa, east Upolu, Samoa. *Earth-Science Reviews,* 107**,** 23-37.

Khouakhi, A., Villarini, G. & Vecchi, G. A. 2017. Contribution of Tropical Cyclones to Rainfall at the Global Scale. *Journal of Climate,* 30**,** 359-372.

Krauss, K. W., Mckee, K. L., Lovelock, C. E., Cahoon, D. R., Saintilan, N., Reef, R. & Chen, L. 2014. How mangrove forests adjust to rising sea level. *New Phytologist,* 202**,** 19-34.

Li, L., Wang, Y. & Liu, C. 2014. Effects of land use changes on soil erosion in a fast developing area. *International Journal of Environmental Science and Technology,* 11**,** 1549-1562.

Lovelock, C. E., Cahoon, D. R., Friess, D. A., Guntenspergen, G. R., Krauss, K. W., Reef, R., Rogers, K., Saunders, M. L., Sidik, F. & Swales, A. 2015. The vulnerability of Indo-Pacific mangrove forests to sea-level rise. *Nature,* 526**,** 559.

Magee, A. D., Verdon-Kidd, D. C. & Kiem, A. S. 2016. An intercomparison of tropical cyclone best-track products for the southwest Pacific. *Natural Hazards and Earth System Sciences,* 16**,** 1431-1447.

Mcleod, E. & Salm, R. V. 2006. *Managing mangroves for resilience to climate change*, World Conservation Union (IUCN) Gland, Switzerland.

Moriasi, D. N., Arnold, J. G., Van Liew, M. W., Bingner, R. L., Harmel, R. D. & Veith, T. L. 2007. Model evaluation guidelines for systematic quantification of accuracy in watershed simulations. *Transactions of the ASABE,* 2007 v.50 no.3**,** pp. 885-0.

Nazirova, K., Alferyeva, Y., Lavrova, O., Shur, Y., Soloviev, D., Bocharova, T. & Strochkov, A. 2021. Comparison of In Situ and Remote-Sensing Methods to Determine Turbidity and Concentration of Suspended Matter in the Estuary Zone of the Mzymta River, Black Sea. *Remote Sensing,* 13**,** 143.

Neitsch, S. L., Arnold, J. G., Kiniry, J. R. & Williams, J. R. 2011. Soil and Water Assessment Tool Theoretical Documentation Version 2009. *Texas Water Resources Institute Technical Report No 406*. College Station, Texas.: Texas A&M University System.

Planning and Urban Management Agency & Ministry of Natural Resources and Environment 2015. Samoa – City Development Strategy. *In:* PROGRAMME, U. N. H. S. (ed.) *UN-Habitat*. Fukuoka, Japan: UN-Habitat.

Riccardi, G. 2000. A cell model for hydrological-hydraulic modeling. *Journal of Environmental Hydrology,* 8.

Ricci, G. F., De Girolamo, A. M., Abdelwahab, O. M. M. & Gentile, F. 2018. Identifying sediment source areas in a Mediterranean watershed using the SWAT model. *Land Degradation & Development,* 29**,** 1233-1248.

Rodriguez, J. F., Saco, P. M., Sandi, S., Saintilan, N. & Riccardi, G. 2017. Potential increase in coastal wetland vulnerability to sea-level rise suggested by considering hydrodynamic attenuation effects. *Nat Commun,* 8**,** 16094.

Russell, L. 2011. Poverty, climate change and health in pacific island countries. Menzies Centre for Health Policy.

Saco, P. M. & Rodríguez, J. F. 2013. Modeling Ecogeomorphic Systems. *In:* SHRODER, J. F. (ed.) *Treatise on Geomorphology.* San Diego: Academic Press.
Saifaleupolu, S. & Elisara, F. M. E. 2013. Biodiversity Audits for the Moata'a Mangrove Wetlands. *In:* (OLSSI), O. L. S. O. O. S. I. (ed.).
Saifaleupolu, S. & Elisara, F. M. E. 2017. Mangrove management plan for the village community of Moata'a. *In:* (OLSSI), O. L. S. O. O. S. I. (ed.).
Sandi, S. G., Rodríguez, J. F., Saintilan, N., Riccardi, G. & Saco, P. M. 2018. Rising tides, rising gates: The complex ecogeomorphic response of coastal wetlands to sea-level rise and human interventions. *Advances in Water Resources,* 114, 135-148.
Schroth, C. L. 1970. *Analysis and prediction of the properties of Western Samoa soils*, University of Hawai'i at Manoa.
Secretariat of the Pacific Regional Environment Programme (Sprep) & Proe 2011. *Regional wetlands action plan for the Pacific islands, 2011-2013,* Apia, Samoa, SPREP.
Sharma, K. K., Verdon-Kidd, D. C. & Magee, A. D. 2020. Decadal variability of tropical cyclogenesis and decay in the southwest Pacific. *International Journal of Climatology,* 40, 2811-2829.
Solomon, S. M. 1994. *A Review of Coastal Processes and Analysis of Historical Coastal Change in the Vicinity of Apia, Western Samoa*, SOPAC.
Suluvale, E. A. 2001. Environmental change of selected mangrove areas in Samoa. Apia Samoa.
Terry, J. P., Kostaschuk, R. A. & Garimella, S. 2006. Sediment deposition rate in the Falefa River basin, Upolu Island, Samoa. *Journal of Environmental Radioactivity,* 86, 45-63.
Van Den Elsen, E., Eeman, S., Stolte, J. & Ritsema, C. Measuring precipitation, infiltration and water discharge on a catchment scale for soil erosion modeling in the south pacific region. 13th Int. Soil Conservation Organisation Conf., ISCO 2004, 2004.
Vilaysane, B., Takara, K., Luo, P., Akkharath, I. & Duan, W. 2015. Hydrological Stream Flow Modelling for Calibration and Uncertainty Analysis Using SWAT Model in the Xedone River Basin, Lao PDR. *Procedia Environmental Sciences,* 28, 380-390.
Villarini, G. & Denniston, R. F. 2016. Contribution of tropical cyclones to extreme rainfall in Australia. *International Journal of Climatology,* 36, 1019-1025.
Williams, J. R. & Berndt, H. D. 1977. Sediment Yield Prediction Based on Watershed Hydrology. *Transactions of the ASAE,* 20, 1100-1104.
Williams, S., Griffiths, J., Miville, B., Romeo, E., Leiofi, M., O'driscoll, M., Iakopo, M., Mulitalo, S., Ting, J. C., Paulik, R. & Elley, G. 2021. An Impacts-Based Flood Decision Support System for a Tropical Pacific Island Catchment with Short Warnings Lead Time. *Water,* 13, 3371.
World Meteorological Organization, European Union, United Nations Educational Scientific and Cultural Organization & Secretariat of the Pacific Community - Applied Geoscience and Technology Division 2012. Catalogue of Rivers for Pacific Islands.
Yeo, S. W. 2001. *A Review of Flooding in Apia, Samoa, April 2001*, South Pacific Applied Geoscience Commission.